

2008
Annual Report

No. 20

The NOVARTIS Foundation(Japan)
for the Promotion of Science

Introduction

“Toward a new organization”

Akimichi Kaneko, Chairman of the Board of Trustees

Novartis Foundation (Japan) for the Promotion of Science held a memorial gathering on March 14th this year to commemorate the 20th anniversary of its establishment, to which about 160 people attended. On this occasion, those who received the Novartis Research Grant in 2006 presented the results of their research work and we saw at first hand their successful achievement. It was really good that we had an opportunity to closely talk with each of them in person. We received various comments and advice on our future operation from our guests and we found the meeting quite informative in this respect.

At the juncture to mark the 20th anniversary, we have faced a major change as the government tries to reform the Public Interest Corporation System in Japan. As you know, the purpose of this reform is to let the private sector play a more active role in promoting the public interest in our social and economic system and to fundamentally review the current Public Interest Corporation System in order to properly address problems seen in the system.

In the introductory note of last year's Annual Report, I wrote "the raison d'etre of the Foundation" and the objectives of the Foundation will remain unchanged even under a new system. We are currently preparing to make a move to a new system with the intention to maintain and even expand the Foundation's objectives. Although our governing structure, such as the Board of Trustees and the Board of Councilors, will change, we intend to keep our current business including the provision of research grants. We would like to change ourselves into a new Foundation which would make this possible.

This report includes essays written by the 2007 grantees. From these essays, you can vividly feel their passion and seriousness in pursuing research activities. They are really wonderful essays. Until recently I was engaged in research work just like them and, therefore, I perfectly understand their passion and seriousness towards scientific research. The amount of our research grant is not particularly large but we think we can achieve our objectives if we can encourage these researchers to pursue their work through our grants. Let's step forward together by uniting our strength!

Background to Establishment

The NOVARTIS Foundation (Japan) for the Promotion of Science was established on September 3rd, 1987 under the authorization of the Ministry of Education by following the process below.

Started Preliminary Investigation (Aug. 1985)

It was decided that the first fundamental research laboratory in Japan shall be established as the part of the Ciba-Geigy Group. Along with the establishment, an exclusive project team was formed to investigate the current situation of Japanese science and what role the established organization must play for the Japanese science by visiting prominent figures in the target fields or other company laboratories. The original purpose of this investigation was to make a plan for the establishment. However, as the investigation progressed, the team members realized the importance of juridical foundations because they were greatly contributing to Japanese science. This is how the Ciba-Geigy Group established a new juridical foundation in Japan. Since then, the team had investigated a number of Japanese research aid foundations for about one year.

Started Preparation for Establishing Foundation (Sept. 1986)

Ciba-Geigy Limited and Nihon Ciba-Geigy K.K. decided to establish a new juridical foundation in Japan to respond anticipated tremendous benefits from Japanese society when the new research laboratory would be completed. At that moment the Ciba-Geigy Group had already established Friedrich Miescher Institute (FMI) in Switzerland and Ciba Foundation in London, so the new foundation would be the third one.

The project team started the preparations for establishing the new foundation and the new research laboratory simultaneously. First they created a charter for the new foundation. The charter was stating three main points; the importance of creative research in Japan, the necessity of international exchange of researchers, and the Group's strong decision to establish a research aid foundation in Japan as the part of the Ciba-Geigy Group. The considerably broad range of target fields including bioscience, chemistry and polymer science was set up. Also the team members asked the selected persons for being the founders, trustees or councilors of the new foundation.

Holding Explanatory Meeting for Establishing Foundation (Jan. 1987)

The team invited major founders to Nihon Ciba-Geigy K.K. to explain them the progress and the purpose of the establishment.

Visited Scientific Research Aid Division of the Research Promotion Bureau, Ministry of Education (Feb. 1987)

The team asked the Ministry of Education (present Ministry of Education, Culture, Sports, Science and Technology) in Japan for administration because the new foundation would cover such a wide range of fields and its main purpose was to support mainly fundamental researches. Although there were somewhat exceptional factors as it was the first foreign-financed foundation in Japan, the Ministry of Education gave the team flexible responses and detailed advices appropriately.

Receiving Donation from Ciba-Geigy Limited as Basic Fund (Mar. 1987)

Ciba-Geigy Limited proposed for donation to the new foundation; 1,000,000,000 yen as its basic fund and 50,000,000 yen every year as its operating fund.

Holding Founders' Meeting (June 1987)

The Founders' Meeting was held on June 3rd. The founders were Drs. Yuichi Yamamura, Saburo Fukui, Hitoshi Nozaki, Hiroshi Mikawa, Morio Ikehara, Yoshiro Okami and Ryo Sato, and additionally, Messrs. Paul Dudler, Toshiaki Simizu, Peter Baumann and Max. M. Burger from Ciba-Geigy Limited. In that meeting Dr. Saburo Fukui was elected for the representative of the founders. Other necessary issues such as the content of the charter were also decided in this meeting.

- Quoted from the 1st issue of the Annual Report

Contents

Part I :

Reports from the Recipients of Novartis Research Grants (Fiscal Year 2006)

1) Biological Sciences

1-1) Molecular Biology

Analysis of DNA repair mechanisms through monoubiquitination of FancD2 protein

Minoru Takata

Radiation Biology Center, Kyoto University

mtakata@house.rbc.kyoto-u.ac.jp

Development for the program of lipid metabolism by anti-metabolic syndrome factor TFE3

Yoshimi Nakagawa

Graduate School of Comprehensive Human Sciences, University of Tsukuba

yosshy@md.tsukuba.ac.jp

Drug discovery using the novel antibiotic-modification enzyme that reduces the toxicity of streptothrinacin

Yoshimitsu Hamano, Ph.D.

Faculty of Bioscience, Fukui Prefectural University

hamano@fpu.ac.jp

The Role of Slits in Migration of Neuroblasts to the Olfactory Bulb.

Kazunobu Sawamoto

Nagoya City University Graduate School of Medical Sciences

sawamoto@med.nagoya-cu.ac.jp

Mechanisms for the control of the size of an organism in the nematode

Yasumi Ohshima

Sojo University

ohshima@life.sojou.ac.jp

Investigation of molecular mechanisms involved in 46,XY disorders of sex development caused by CXorf6 mutation

Maki Fukami, Tsutomu Ogata and Yuka Wada

National Research Institute for Child Health and Development

mfukami@nch.go.jp

Analyses of group III secreted phospholipase A₂ gene-manipulated mice

Makoto Murakami

The Tokyo Metropolitan Institute of Medical Science

mako@rinsoken.or.jp

Role of Osterix in regulation of differentiation program of mesenchymal stem cell

Riko Nishimura

Osaka University Graduate School of Dentistry

rikonisi@dent.osaka-u.ac.jp

1-2) Struktural Biology

Role of Apolipoprotein E Structure in Disorders of Cholesterol Metabolism in Brain

Hiroyuki Saito

Kobe Pharmaceutical University

saito@kobepharma-u.ac.jp

Desensitization Mechanism of G-protein Coupled Receptor and Self-Association at Physiological Concentrations

Yasushi Imamoto

Kyoto University

imamoto@rh.biophys.kyoto-u.ac.jp

1-3) Cell Biology

Molecular Basis of Left-Right Asymmetry Determination in Plants

Takashi Hashimoto

Nara Institute of Science and Technology, Graduate School of Biological Sciences

hasimoto@bs.naist.jp

Elucidation of mechanism for cell polarity formation in cell migration

Yuichi Mazaki

Leading Graduate School System, Kumamoto University

mazaki@kumamoto-u.ac.jp

Mechanism of NF-κB-dependent protection from cell death

Hiroyasu Nakano

Juntendo University School of Medicine

hnakano@med.juntendo.ac.jp

Regulatory pathway that mediates calorie restriction-mediated longevity.

Akira Matsuura

Graduate School of Advanced Integration Science, Chiba University

amatsuur@faculty.chiba-u.jp

Molecular mechanism of meiosis-specific endocytosis

Taro Nakamura

Osaka City University

taronaka@sci.osaka-cu.ac.jp

Identification and functional analysis of proteins that regulate endoplasmic reticulum stress response

Akihiro Tomida

Japanese Foundation for Cancer Research

akihiro.tomida@jfcr.or.jp

Regulation of apoptosis by Bcl-rambo in mitochondria

Takao Kataoka

Kyoto Institute of Technology

takao.kataoka@kit.ac.jp

1-4) Developmental Biology

Elucidation of the role of sugar chain in cartilage formation using mice with abnormal sugar chain

Toshihisa Komori

Department of Cell Biology, Unit of Basic Medical Sciences, Nagasaki University

Graduate School of Biomedical Sciences

komorit@nagasaki-u.ac.jp

The functional analyses of semaphorin in the neural network formation

Masahiko Taniguchi

Department of Biochemistry, Cancer Research Institute, Sapporo Medical University

School of Medicine

taniguti@sapmed.ac.jp

Progressing reproductive biology by analysis of intratesticular oocytes

Kon Yasuhiro

Laboratory of Anatomy, Department of Biomedical Sciences, Graduate School of Veterinary Medicine, Hokkaido University

y-kon@vetmed.hokudai.ac.jp

1-5) Physiology

Physiological relevance of aquaporins in brain

Masato Yasui

Keio University School of Medicine Department of Pharmacology

myasui@sc.itc.keio.ac.jp

Selective estrogen receptor modulator (SERM) in herbs as a potential medicinal seed

Tetsushi Furukawa

Tokyo Medical & Dental University, Medical Research Institute

t_furukawa.bip@mri.tmd.ac.jp

Elucidation of molecular mechanisms for the modulation of learning abilities by emotion

Toshiya Manabe

Institute of Medical Science, University of Tokyo

tmanabe-tky@umin.ac.jp

Regulation of cellular event by activator of G-protein signaling 8 induced by myocardial ischemia

Motohiko Sato

Cardiovascular Research Institute, Yokohama City University School of Medicine

motosato@yokohama-cu.ac.jp

1-6) Pharmacology

Postgenomic approach to identify novel bacterial antibiotic resistome

Kunihiko Nishino

Institute of Scientific and Industrial Research, Osaka University

nishino@sanken.osaka-u.ac.jp

1-7) Plant Biology

Molecular mechanism of the C-to-U RNA editing unique to land plant organelles

Junichi Obokata

Center for Gene Research, Nagoya University

obokata@gene.nagoya-u.ac.jp

The Analysis of The SUMO Posttranslational Modification in Plant

Katsunori Tanaka

Department of Bioscience, School of Science and Technology, Kwansei Gakuin University

katsunori@kwansei.ac.jp

Jasmonic Acid Signaling and Abscisic Acid Signaling in Guard Cells

Yoshiyuki Murata

Okayama University

muta@cc.okayama-u.ac.jp

1-9) Others

Molecular biological analysis of novel hybrid type polyketide synthase from *Dictyostelium*

Tamao Saito

Department of Biological Sciences, Faculty of Science, Hokkaido University
tasaito@sci.hokudai.ac.jp

2) Medical Sciences

2-1) Immune System

Molecular mechanism of immunological tolerance by cytokines

Akihiko Yoshimura

Medical Institute of Bioregulation, Kyushu University
yakihiko@bioreg.kyushu-u.ac.jp

Investigation on the role of CD100 in differentiation of Th17 cells

Atsushi Kumanogoh

Research Institute for Microbial Diseases, Osaka Univ.
kumanogo@ragtime.biken.osaka-u.ac.jp

Mechanisms for Regulation of Inflammatory Responses via Inducible Transcriptional Regulatory Factors

Tatsushi Muta

Tohoku University
tmuta@biology.tohoku.ac.jp

2-2) Central Nervous System

Analysis of genes specifically expressed in primate neocortical areas

Tetsuo Yamamori

National Institute for Basic Biology
yamamori@nibb.ac.jp

2-5) Cardiovascular/Metabolic/Endocrine

Analysis of the molecular mechanisms of the development of non-alcoholic steatohepatitis (NASH)

Terauchi Yasuo

Department of Endocrinology and Metabolism, Yokohama City University Graduate School of Medicine

terauchi@yokohama-cu.ac.jp

Global functional analysis of microRNAs in cardiomyocyte differentiation

Jun K. Yamashita

Institute for Frontier Medical Sciences, Kyoto University

juny@frontier.kyoto-u.ac.jp

Genetic analysis of zebrafish cardiac regeneration

Shinji Makino

Department of Regenerative Medicine and Advanced Cardiac Therapeutics Keio University School of Medicine

koshinji@sc.itc.keio.ac.jp

2-6) Gastro-intestinal

Gene expression profiling and comparative analysis of normal esophagus stem/progenitor cells and esophagus cancer-derived cells

Atsushi Suzuki

Kyushu University

suzukicks@bioreg.kyushu-u.ac.jp

Roles of host immune responses in the development of *Helicobacter*-induced gastritis

Norihiko Watanabe

Kyoto University

norihiro@kuhp.kyoto-u.ac.jp

2-12) Hematology

Regulation of self-renewal capacity of leukemic stem cells by hematopoietic transcription factors

Hideaki Nakajima

Keio University School of Medicine

hnakajim@sc.itc.keio.ac.jp

3) Chemical Sciences

3-1) Organic Chemistry

Preparation of Chiral Boron Reagents for Efficient Synthesis of Biologically Active Substances

Toshimichi Ohmura

Graduate School of Engineering, Kyoto University

ohmura@sbchem.kyoto-u.ac.jp

Development of the Novel Artificial Nucleoside Derivatives for the Control of the Gene Expression in Cells

Fumi Nagatsugi

Institute of Multidisciplinary Research for Advanced Materials Tohoku University

nagatugi@tagen.tohoku.ac.jp

Design of nano-foldamer having chiral centers at the helical surface and its application to chiral molecular recognition

Masakazu Tanaka

Graduate School of Pharmaceutical Sciences, Kyushu University

mtanaka@phar.kyushu-u.ac.jp

Development of Effective Synthetic Method for Oxindoles based on a Claisen Rearrangement

Atsuo Nakazaki

Tokyo University of Science

nakazaki@rs.noda.tus.ac.jp

Synthesis of polycyclic natural products including heteroatom

Kan Toshiyuki

School of Pharmaceutical Sciences, University of Shizuoka

kant@u-shizuoka-ken.ac.jp

Part II :

Reports from the Recipients of Garants for International Meeting
(Fiscal Year 2006)

The 2007 Molecular Biology Society of Japan (MBSJ) Spring Symposium

on “Biology -Old Codes and New Molecules-”

(The 7th the MBSJ spring symposium)

The 5th International Symposium on Molecular Breeding of Forage and Turf
(MBFT2007)

International Congress on Plant Mitochondrial Biology (ICPMB2007)

The 5th International Symposium on Receptor Mechanisms, Signal Transduction
and Drug Effects

-Development of Novel Therapy to Specific Diseases in Organ-

Part I

Reports from the Recipients of Novartis
Research Grants (Fiscal Year 2006)

1) Biological Sciences
1-1) Molecular Biology

Analysis of DNA repair mechanisms through monoubiquitination of FancD2 protein

Minoru Takata

Radiation Biology Center, Kyoto University

mtakata@house.rbc.kyoto-u.ac.jp

Introduction

Fanconi anemia (FA) is a rare hereditary disorder characterized by progressive bone marrow failure, compromised genome stability, and increased incidence of cancer. FA is caused by genetic defects in altogether 13 genes but this number may increase in the future. These include components of the FA core complex (FancA/B/C/E/F/G/L/M), a key factor FancD2, breast cancer susceptibility protein BRCA2/FancD1, BRIP1/FancJ helicase, and just recently identified FANCI. In the DNA damage response, FancD2 is targeted to chromatin and forms nuclear foci following its monoubiquitination, a process likely catalyzed by the FA core complex. This monoubiquitination is critical for regulating nuclear dynamics of FancD2 as well as DNA repair through homologous recombination.

Results

(1) We have previously shown that a putative monoubiquitin-binding protein is required for FANCD2 to be loaded onto chromatin. To identify this protein, we sought an interacting partner of FANCD2 using yeast two-hybrid screen or mass spectrometry of FANCD2 immunoprecipitates, however, we have not yet successfully identified this monoubiquitin receptor. We will surely continue our effort to clarify the mechanisms of FANCD2 chromatin loading.

(2) Instead of the ubiquitin receptor, we have identified KIAA1794 protein as an interactor of FANCD2 by mass spectrometry. Then it was reported that KIAA1794 is actually FANCI protein (Cell. 2007 Apr 20;129(2):289-301). They identified FANCI through a proteomic screen for possible ATM/ATR substrates, combined with a functional screen for MMC sensitivity in siRNA-transfected cells.

Surprisingly, FANCI has weak homology with FANCD2 (we did not notice this), interacts with FANCD2 (called ID complex), monoubiquitinated probably by the core complex, and forms foci colocalized with FANCD2. Furthermore, monoubiquitination of FANCD2 or FANCI depends on monoubiquitination of the other, indicating that ID complex is the substrate for the core complex. Since FANCI has a number of S/TQ sites, FANCI could be a long-sought turn on switch on FA

pathway upon DNA damage.

To test this possibility, we expressed FANCI mutant in which SQ/TQ sites were mutated in various combinations in FANCI-deficient cells that we have created, and tested monoubiquitination of FANCD2 and FANCI following MMC stimulation, and cisplatin sensitivity.

We found that, in chicken DT40 cell system, simultaneous six alanine-substitution mutations in conserved and clustered S/TQ motifs of FancI (termed Ax6 in Figure 1) largely abrogated monoubiquitination as well as foci formation of both FancD2 and FancI. The cells expressing Ax6 mutant FANCI were exquisitely sensitive to cisplatin treatment, nearly as sensitive to FANCI-deficient cells. Thus, the mutation resulted in loss of DNA repair function.

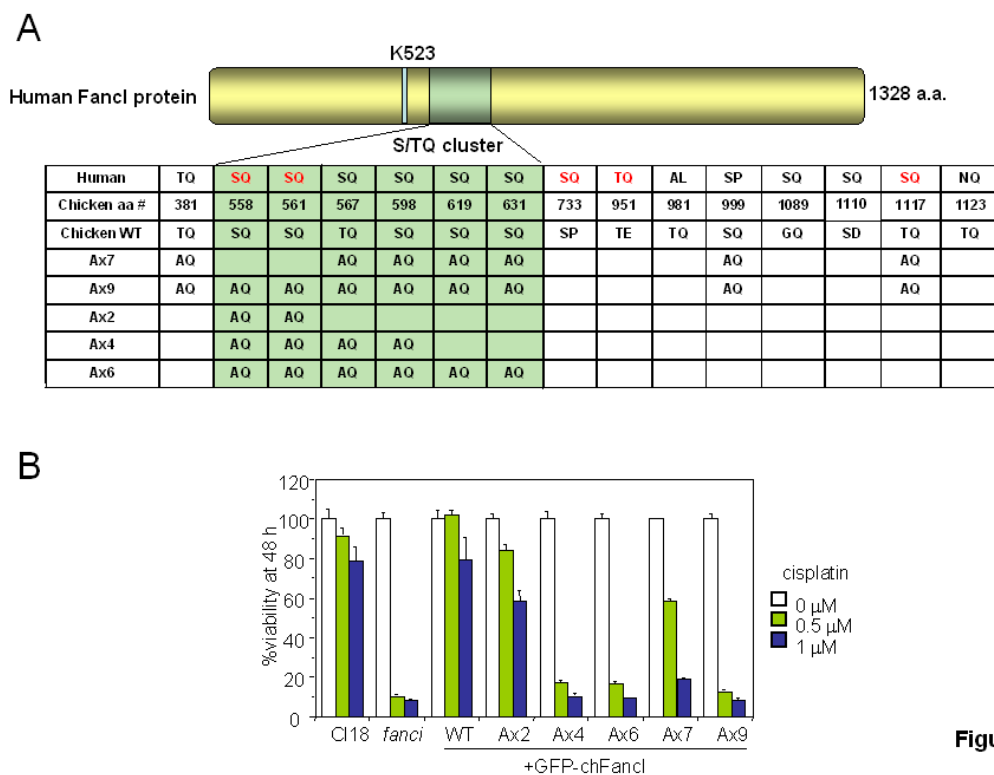
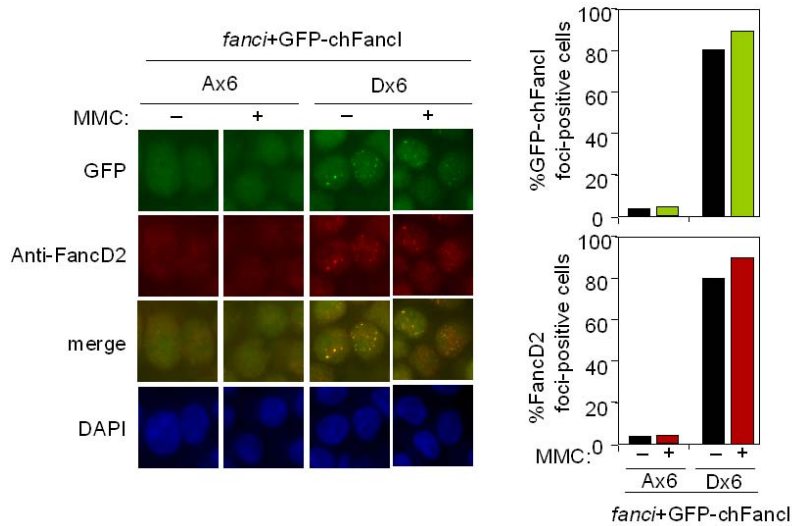


Figure 1

Conversely, FancI protein carrying phospho-mimic mutations to aspartic acid on the same six residues (Dx6 in Figure 2) induced constitutive monoubiquitination and foci formation of FancI and FancD2, and protects against cell killing and chromosome breakage by DNA interstrand crosslinks (ICLs).

**Figure 2**

We have also shown that FANCI phosphorylation actually occurs in residues mutated in Ax6 or Dx6 mutant, which was sensitive to high-dose treatment with ATM/ATR kinase inhibitor wortmannin (100 μ M), using Phos-tag technology. In addition, FancI monoubiquitination does not seem to be absolutely critical for the function of the FA pathway in DT40 cells, although the monoubiquitination site on FancI is conserved through evolution.

Discussion & Summary

These data clearly indicate that multiple phosphorylation is functionally very important for monoubiquitination of ID complex and DNA repair. Based on the data using the phosho-mimic mutant, we propose that the multiple phosphorylation of FancI serves as a molecular switch in activation of the FA pathway. Our data provide a basis for further elucidation of the mechanistic detail of the FA pathway, which should aid development of more rational therapeutics for FA and related conditions.

References

1. Ishiai M et al. FANCI phosphorylation functions as a molecular switch to turn on the Fanconi anemia pathway. Submitted.
2. Kitao H et al. FancJ/Brip1 helicase protects against loss of immunoglobulin heavy chain during gene conversion. Submitted.

1) Biological Sciences
1-1) Molecular Biology

Development for the program of lipid metabolism by anti-metabolic syndrome factor TFE3

Yoshimi Nakagawa

Graduate School of Comprehensive Human Sciences, University of Tsukuba

yosshy@md.tsukuba.ac.jp

Introduction

More than 20 million Japanese either are obese or have the metabolic syndrome. Metabolic syndrome including hypertension, hyperlipidemia, diabetes and obesity impairs the quality of life of patients and leads to increased health-care costs. This is the personal and social problem in the modern society. It is important to study the molecular mechanism for metabolic syndrome and lead to establishment of the new therapy for metabolic syndrome.

Our purpose is to study the molecular mechanism for energy homeostasis via regulation of gene expression by anti-metabolic syndrome factor, TFE3.

Results

Obesity is a major risk factor for type 2 diabetes and is closely associated with the metabolic syndrome—a cluster of disorders linked to insulin resistance and central obesity, including impaired glucose tolerance, circulating lipid abnormalities and fatty liver, hypertension and increased risk of cardiovascular disease. We reported that TFE3 was a novel bHLH transcription factor that strongly activates various insulin signaling molecules in the liver, protecting against the development of insulin resistance and the metabolic syndrome¹). We next analyzed the function of TFE3 in adipose. Moreover, to understand the effects of TFE3 on lipid homeostasis, we studied the function of TFE3 in adipocytes in vitro and in vivo. We examined the TFE3 gene expression in white adipose tissue (WAT) during energy states. Refeeding compared with fasting increased TFE3 gene expression in wild-type mice. And TFE3 was also increased in WAT from ob/ob mice compared to wild type mice. TFE3 gene expression was increased in WAT from diet-induced obesity (DIO) mice compared to wild type mice. These results suggested that TFE3 mRNA was increased in the hypernutrition condition in WAT from mice, relating to the nutrition states. Next, we analyzed the function of TFE3 in vitro using 3T3-L1 fibroblasts, which were differentiated into adipocytes. To characterize TFE3 in 3T3-L1 cells, we measured its expression during adipogenesis by northern blotting analysis. TFE3 mRNA was increased during adipocyte

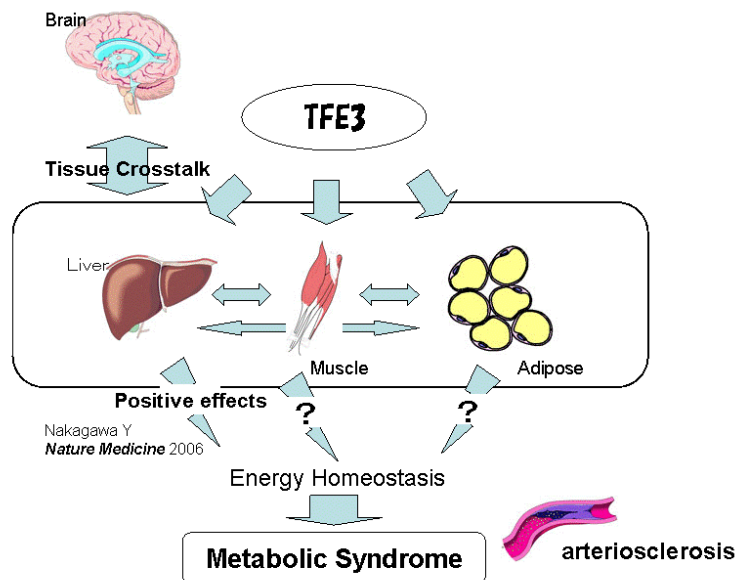
differentiation in 3T3-L1 cells. TFE3 expression was regulated during adipogenesis. To determine the effects of TFE3 on adipocyte differentiation, the adenovirus encoding TFE3 or TFE3 RNAi was infected into 3T3-L1 cells. The cells were subjected to differentiation using a hormonal induction medium. Oil Red O staining showed a decreased lipid accumulation in differentiated TFE3 infected cells during differentiation compared to control. We investigated whether TFE3 affected the gene expression of adipocyte differentiation, aP2, C/EBPa, PPARg, et al. aP2, C/EBPa and PPARg were the important gene to terminally differentiate adipocytes. TFE3 impaired the expression of these genes. These results showed that TFE3 has a role in adipogenesis by affecting the expression of adipogenesis genes including aP2, C/EBPa and PPARg.. Absence of TFE3 in 3T3-L1 cells by RNAi-knockdown led to induction of adipocyte differentiation by showing Oil Red O staining. Reduction of TFE3 was accompanied by induction of C/EBPa and PPARg, transcription factors involved in adipocyte differentiation. In summary, reduction of TFE3 increases adipocyte differentiation. To find the TFE3 target gene in adipogenesis, we focused on Hypoxia-induced factor-1a, HIF-1a. It was reported that HIF-1a suppressed adipogenesis2). Overexpression of TFE3 increased HIF-1a gene expression in 3T3-L1 cells. Reversely, absence of TFE3 decreased HIF-1a gene expression. To characterize whether HIF-1a was a direct target gene for TFE3, we performed the luciferase assay using HIF-1a promoter region. There was a target sequence bound to TFE3, E box in the promoter region. TFE3 directly bound to HIF-1a promoter via E box in its promoter using the luciferase assay. The results suggested that TFE3 activated HIF-1 gene expression, led to reduction of adipogenesis.

Discussion & Summary

TFE3 is a transcription factor to regulate insulin response genes resulting in anti-metabolic syndrome actions in the liver. In this study, we identified a role for TFE3 during adipogenesis. HIF-1a is reported to be a response gene to hypoxia and to suppress adipogenesis by inhibiting PPARg gene expression. TFE3 activated HIF-1a and inactivated PPARg and C/EBPa. We proposed that HIF-1a was upregulated by TFE3, led to suppression of adipogenesis induced gene expression. TFE3 is an inhibitory factor of the adipocyte differentiation process leading from preadipocytes to fully mature adipocytes and could be implicated in obesity. We speculated that TFE3 was connected with the formation of obesity leading to metabolic syndrome. This research also provides insight about new targets for the treatment or prevention of this disease.

Figures & Tables

The study for the effects of TFE3 on energy



References

1. Nakagawa Y, et al. TFE3 transcriptionally activates hepatic IRS-2, participates in insulin signaling and ameliorates diabetes. *Nature Medicine* 2006 Jan;12(1):107-13.
2. Yun Z, et al. Inhibition of PPAR gamma 2 gene expression by the HIF-1-regulated gene DEC1/Stra13: a mechanism for regulation of adipogenesis by hypoxia. *Dev Cell.* 2002 Mar;2(3):331-41.

1) Biological Sciences
1-1) Molecular Biology

Drug discovery using the novel antibiotic-modification enzyme that reduces the toxicity of streptothricin

Yoshimitsu Hamano, Ph.D.

Faculty of Bioscience, Fukui Prefectural University

hamano@fpu.ac.jp

Introduction

Streptothricins (STs) are broad-spectrum antibiotics in prokaryotes and eukaryotes. STs consist of a carbamoylated D-gulosamine to which the β -lysine homopolymer (1 to 7 residues) and streptolidine lactam are attached (Fig. 1). Recently, we have identified an antibiotic-modification enzyme SttH¹⁻², which catalyses the hydrolysis of the streptolidine lactam of STs. Interestingly, the selective toxicity of ST-D possessing the 3 \times β -lysine residues was altered from broad-spectrum to bacterial-specific by the hydrolysis of the streptolidine lactam, although ST-F (1 \times β -lysine) was detoxified by SttH in both prokaryotes and eukaryotes. Therefore, we hypothesized that the hydrolyzed forms of STs possessing longer β -lysine polymers would be potent antibiotics with no toxicity against eukaryotes.

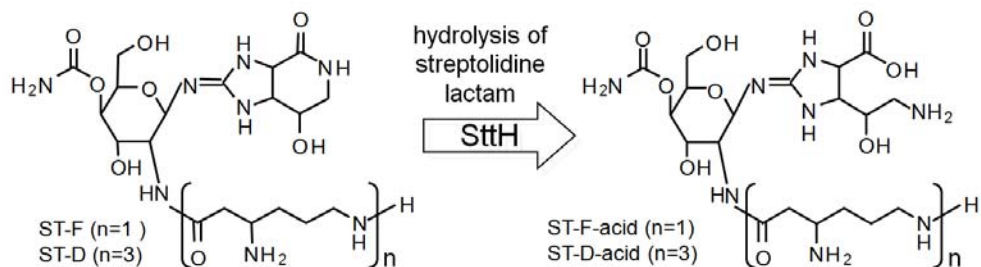


Fig. 1 Chemical structure of streptothricins (STs) and the function of SttH

Results

As described above, we reported that ST-D-acid, which was the hydrolyzed form of ST-D, was detoxified in eukaryotes (yeasts). In this study, we further investigated the biological activity of ST-D-acid against mammalian cells. Cell culture assays using HEK-293 cells revealed no detectable toxicity of ST-D-acid against mammalian cells but the high toxicity of ST-D (Fig. 2). This result further encouraged us to investigate the biological activities of ST-acids possessing longer β -lysine polymers, which would presumably show a higher antibacterial activity with no or low toxicity against eukaryotes.

Although ST-F and ST-D are now commercially available, STs possessing longer β -lysine polymers such as ST-C ($4 \times \beta$ -lysine), ST-B ($5 \times \beta$ -lysine), ST-A ($6 \times \beta$ -lysine), and ST-X ($7 \times \beta$ -lysine), must be purified from the culture broth of the ST-producer *Streptomyces rochei*. However, their yields were found to be extremely low. We therefore decided to clone the ST biosynthetic genes in order to discover a biosynthetic mechanism for construction of strains producing STs with longer β -lysine polymers.

In many cases, antibiotic biosynthetic genes cloned from *Streptomyces* strains are clustered in the genomic DNA region with their own antibiotic-self resistant genes. Therefore, we first cloned the *sttR* gene, which is involved in self-resistance in the ST producers, to clone the ST biosynthetic genes. Based on the highly conserved amino acid sequences of the *sttR* gene products from the ST producers, we designed PCR primers and carried out PCR using *S. rochei* chromosomal DNA as a template. A band with an expected size of approximately 0.5-kbp was readily amplified. The PCR product was cloned, and six randomly selected clones were sequenced. All six clones yielded an identical sequence (except differences resulting from primer utilization), which showed high homology to the *sttR* gene products reported so far. The PCR product was then used as a probe to screen an *S. rochei* cosmid library. From 7 positive clones, one cosmid clone containing a 1.2-kb *Bam*H I hybridizing fragment was selected. Sequence analysis of this fragment was carried out, and frame analysis with the codon usage for *Streptomyces* strains revealed one complete ORF. A database search with BLAST showed that the deduced amino acid sequence of this ORF has a significant similarity to those of the *sttR* gene products from the ST-producing *Streptomyces* strains. To confirm that the cloned *sttR* gene encodes a functional ST-acetyltransferase, the enzyme activity of the recombinant SttR (rSttR) of *S. rochei*, which was overexpressed in *E. coli* and purified to near homogeneity, was assayed *in vitro*. The activity of rSttR was specifically detected with STs as substrates (ST-F and ST-D), demonstrating that the cloned *sttR* gene is indeed the self-resistance gene.

To find the ST biosynthetic genes, we further analyzed the flanking region of the *sttR* gene. By the sequence analysis of the 34-kbp DNA fragment cloned in the cosmid, 24 ORFs were found. Some of the ORFs were expected to encode non-ribosomal peptide synthases by the database search with BLAST, indicating that these ORFs are involved in the ST biosynthesis. To address this, the cosmid was introduced into a heterologous host, *Streptomyces lividans* TK23, and metabolites produced

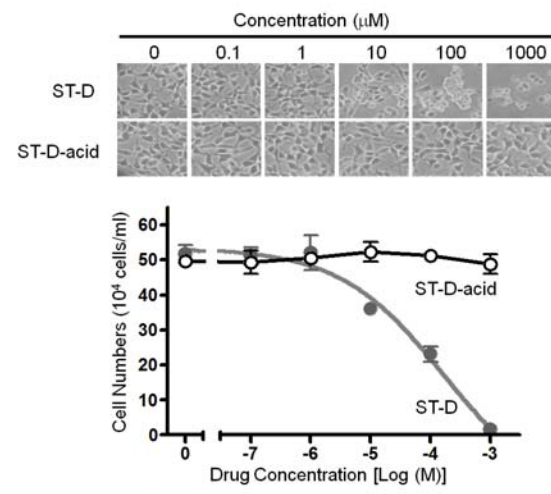


Fig. 2 Cytotoxicity of ST-D-acid in HEK-293 cells

were investigated. LCMS analysis revealed that the *S. lividans* TK23 strain harboring the cosmid produced ST-C ($4\times\beta$ -lysine). Thus, our biosynthetic gene engineering successfully yielded a *Streptomyces* strain producing an ST possessing longer β -lysine polymers. In addition, the ST biosynthetic gene cluster was also identified in the 34-kbp DNA fragment.

We purified ST-C from the culture broth to investigate whether SttH accepts ST-C as a substrate. *In vitro* analysis showed that partially purified ST-C was found to be converted to ST-C-acid by SttH. Otherwise, the biological activities of ST-C and ST-C-acid have not yet been investigated because we have not developed procedures for purifying ST-C and ST-C-acid from culture broth. After we purify these compounds, we plan to investigate their biological activities in pathogenic bacteria and eukaryotes including mammalian cells.

Discussion & Summary

Recently, we demonstrated that the selective toxicity of ST-D possessing the $3\times\beta$ -lysine residues was altered from broad-spectrum to bacterial-specific by the hydrolysis of streptolidine lactam by SttH¹⁻²⁾ (Fig. 1). In this study, we further investigated the biological activity of ST-D-acid against mammalian cells. Cell culture assays using HEK-293 cells revealed no detectable toxicity of ST-D-acid but a high toxicity of ST-D (Fig. 2). This result therefore encouraged us to investigate the biological activities of ST-acids possessing longer β -lysine polymers, which presumably would show a higher antibacterial activity with no or low toxicity against eukaryotes.

STs possessing longer β -lysine polymers must be purified from the culture broth of the ST-producer *Streptomyces rochei*. However, their yields were extremely low. We therefore decided to clone the ST biosynthetic genes in order to discover a biosynthetic mechanism for construction of strains producing STs with longer β -lysine polymers. We successfully cloned the ST biosynthetic genes, and they were introduced into the heterologous host, *S. lividans* TK23. LCMS analysis revealed that the resulting strain produced ST-C ($4\times\beta$ -lysine). Thus, biosynthetic gene engineering successfully yielded a *Streptomyces* strain producing an ST with a longer β -lysine polymer. In addition, ST-C was found to be converted to ST-C-acid by SttH. We are now trying to purify ST-C and ST-C-acid from culture broth.

References

- 1) Yoshimitsu Hamano, Nobuyasu Matsuura, Miwa Kitamura, and Hiroshi Takagi. A novel enzyme conferring streptothrinic resistance alters the toxicity of streptothrinic D from broad-spectrum to bacterial-specific. *J. Biol. Chem.*, **281**, 16842-16848 (2006).
- 2) Yoshimitsu Hamano, Chitose Maruyama, and Hisashi Kimoto. Construction of a knockout mutant of the streptothrinic-resistance gene in *Streptomyces albulus* by electroporation. *Actinomycetologica*, **20**, 35-41 (2006).

1) Biological Sciences
1-1) Molecular Biology

The Role of Slits in Migration of Neuroblasts to the Olfactory Bulb.

Kazunobu Sawamoto

Nagoya City University Graduate School of Medical Sciences
sawamoto@med.nagoya-cu.ac.jp

Introduction

Neuroblasts are continuously generated by stem cells in the subventricular zone (SVZ) and migrate toward the olfactory bulb (OB) through the rostral migratory stream (RMS) throughout life. Neuroblasts migrate in elongated cell aggregates referred as “chains” surrounded by astrocytic processes forming glial tubes¹. Mechanisms regulating the directional neuroblast migration and the role of the surrounding astrocytes are largely unknown.

Slit1 is a secreted protein that binds to its receptor Robo and functions as a chemorepellent in axon guidance and cell migration in the embryonic brain. In the adult brain, Slit1 is expressed in the neuroblasts in the RMS as well as in the septum², while Slit2 is secreted by the choroid plexus into the lateral ventricle and reach the adjacent SVZ, in which they are involved in the control of directional migration of neuroblasts³. These observations suggest their cell-autonomous and non-cell autonomous functions in cell migration. However, the precise role of Slits and the functional difference between Slit1 and Slit2 in the postnatal/adult neuroblast migration remain largely unknown.

Results

To investigate the role of Slit-Robo signaling in migration of neuroblasts in the RMS, we used Slit1/2 knockout ($S1^{-/-}S2^{+/+}$, $S1^{-/-}S2^{+/-}$) mice.

Histological analyses revealed about 10% and 30% reduction in OB volume in $S1^{-/-}S2^{+/+}$ and $S1^{-/-}S2^{+/-}$ mice, respectively (Figure 1a), and enlarged RMS in neonatal and adult $S1^{-/-}S2^{+/+}$ and $S1^{-/-}S2^{+/-}$ mice (Figure 1b), suggesting an impaired neuroblast migration toward the OB in these mice.

Consistent with the previous study², Slit1 was expressed in the neuroblasts in the SVZ, RMS

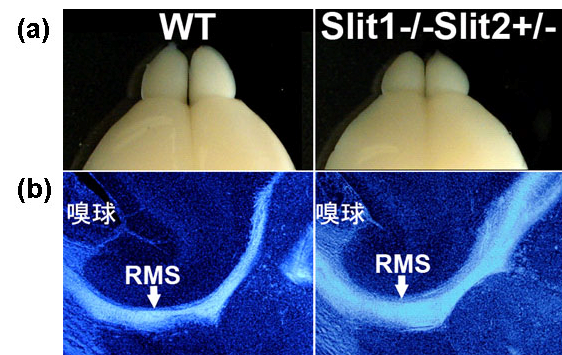


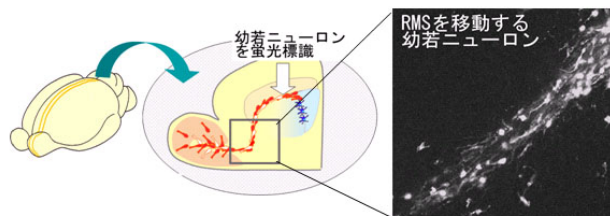
Figure 1

and the OB. Slit2 was expressed in the medial septum, but not in cells in the SVZ, RMS or the OB. Slit receptor Robo2 was strongly detectable along the RMS, suggesting that neuroblasts-derived-Slit1 could transmit physiological signaling mediated by Robo2.

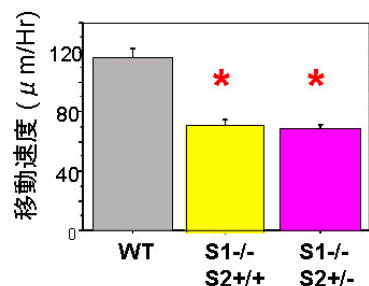
To clarify the migration defect in S1^{-/-}S2^{+/+} and S1^{-/-}S2^{+-/-} mice, we observed the migration behavior of the neuroblasts in the RMS in the cultured brain slice of these mice (Figure 2a). Time-lapse recording of neuroblasts labeled with fluorescence dye showed an approximately 40% reduction in their migration speed (Figure 2b). Similar migration defects were found in wild-type neuroblasts transplanted in the RMS of the S1^{-/-}S2^{+/+} and S1^{-/-}S2^{+-/-} brain slice, and S1^{-/-} neuroblasts transplanted in the wild-type RMS.

These results suggest that Slit-Robo signaling regulates migration of neuroblasts in the RMS in both cell-autonomous and non-cell-autonomous manner.

(a) 脳スライス培養法によるニューロblastの移動の観察



(b) スライス培養上のニューロblastの移動速度



Discussion & Summary

In the RMS, neuroblasts migrate in chain ensheathed by “glial tube” constituted by astrocytes. It seems that the interaction between neuroblasts themselves and that between neuroblasts and their microenvironment should be important for the fast migration.

In this study, We show that Slit1 and Robo2 are expressed in the RMS, and control the migration of neuroblasts. Though further studies are needed, it is possible that Slit-Robo signaling may mediate the cell-cell interactions for normal chain migration.

References

1. Alvarez-Buylla, A. & Garcia-Verdugo, J. M.: J Neurosci, 22: 629-34, (2002)
2. Nguyen-Ba-Charvet, K. T. et al.: J Neurosci, 24: 1497-506, (2004)
3. Sawamoto, K. et al.: Science, 311: 629-32, (2006)

1) Biological Sciences
1-1) Molecular Biology

Mechanisms for the control of the size of an organism in the nematode

Yasumi Ohshima
Sojo University
ohshima@life.sj-u.ac.jp

Introduction

The size of an organism is an important characteristic in animals and plants. However, the mechanisms for the determination or control of the size remain mostly unsolved. The researcher of this research worked to elucidate the mechanisms in the nematode *C. elegans*. Namely, he isolated big mutants, identified the gene responsible for several of them (*egl-4* encoding a G kinase), identified the gene for a small mutant *sma-5* (encoding a MAP kinase), and so on.

Results

On the basis of the results obtained before, research has been done to get the following results.

1. By using yeast two-hybrid screen, six kinds of molecules, including a Ras homolog (DRN-1) and a 7 transmembrane protein (C52B9.4), were identified to interact with EGL-4.
2. These proteins bind to the region near the N-terminus of EGL-4 in the yeast.
3. The mutants of *drn-1* and C52B9.4 showed smaller body size than wild type, suggesting that these genes play a role in the control of the body size.
4. Egl-4, its various fragments and the isolated interacting proteins are expressed in *E. coli*, and are being tested in vitro to verify direct interaction between them.
5. Expression of EGL-4 in yeast *S. cerevisiae* is successful, and EGL-4 is being purified to examine its kinase activity.
6. Yeast two-hybrid screen also resulted in the identification of four proteins interacting with EGL-4, such as vitellogenin and ribosomal protein L22 homologs.
7. For the isolation of new big mutants, the plan has been changed to one using insertion of Mos1 transposon, to facilitate the gene cloning. This method has been tested to isolate other mutants successfully.

Discussion & Summary

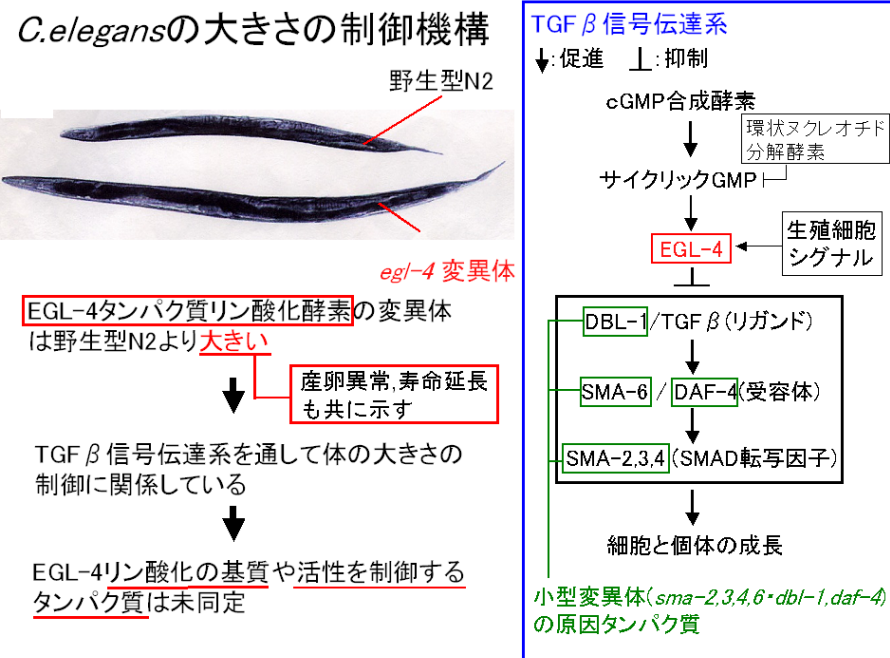
From now on, the following research will follow.

1. Mutants of the interacting proteins, other than DRN-1 and C52B9.4, are obtained and

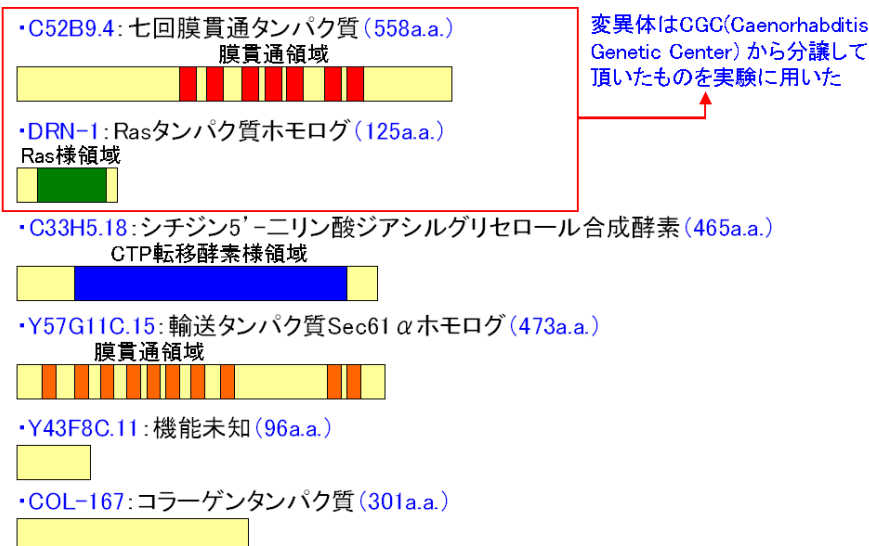
characterized to determine their roles in the control of body size.

2. The sites and developmental stages, in which the identified genes are expressed, are determined.
3. Phosphorylation of the proteins identified in the two-hybrid screen by EGL-4 or SMA-5 are examined.

Figures & Tables



酵母ツーハイブリッドスクリーニングで得られたEGL-4結合タンパク質



References

- T. Hirose, Y. Ohshima et al. : Cyclic GMP-dependent protein kinase EGL-4 controls body size size and lifespan in *C. elegans*. **Development** 130, 1089-1099 (2003).
- N. Watanabe, Y. Nagamatsu, K. Gengyo-Ando, S. Mitani and Y. Ohshima: Control of body CCs size by SMA-5, a homolog of MAP kinase BMK1/ERK5, in *C. elegans*. **Development** 132, D31 3175-3184 (2005).
- N. Watanabe, T. Ishihara and Y. Ohshima: Mutants carrying two *sma* mutations are super sm small in the nematode *C. elegans*. **Genes to Cells** 12, 603-609 (2007).

1) Biological Sciences
1-1) Molecular Biology

Investigation of molecular mechanisms involved in 46,XY disorders of sex development caused by CXorf6 mutation

Maki Fukami, Tsutomu Ogata and Yuka Wada
National Research Institute for Child Health and Development
mfukami@nch.go.jp

Introduction

Chromosome X open reading frame 6 (*CXorf6*) has recently been shown to be a causative gene for 46,XY disorders of sex development (46,XY DSD) (Ref.1). The notion is primarily based on the identification of nonsense mutations in four boys with hypospadias. Since the mouse homolog is transiently expressed in the fetal testis around the critical period for sex development, it is likely that the *CXorf6* mutations cause hypospadias primarily because of testicular dysfunction and resultant compromised testosterone production (1). However, the molecular function of CXorf6 remains unknown.

Results

Structural analysis of CXorf6 protein

To clarify the molecular function of CXorf6, we first searched databases using the CXorf6 protein sequence as bait. CXorf6 had homology to mastermind-like 2 (MAML2) that functions as a co-activator in canonical Notch signaling. In particular, a unique amino acid sequence, which we designate mastermind-like (MAML) motif, was well conserved among MAML2 and CXorf6 orthologs identified in frog, bird, and mammals. In addition, a serine-rich domain was identified in CXorf6, in addition to glutamine- and proline-rich domains.

In vitro functional analysis of the wildtype CXorf6 protein

Transactivation analysis using murine Leydig tumor cells was performed for wildtype CXorf6 protein by luciferase reporter assays (Fig.1). The results demonstrated that

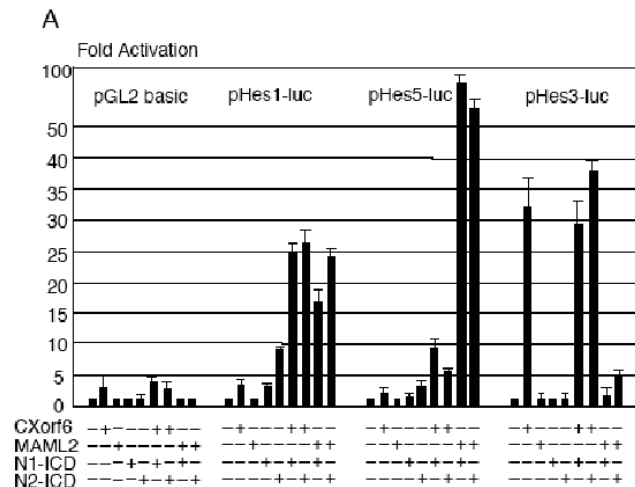


Fig.1

CXorf6 significantly increase the promoter activity of a non-canonical Notch target gene hairy/enhancer of split 3 (Hes3). By contrast, unlike to MAML2, CXorf6 was incapable of enhancing the function of Notch intra-cellular domain on the promoter activities of the canonical Notch target Hes1 and Hes5. Electrophoretic mobility shift assays (EMSA) showed no evidence for binding of CXorf6 to Hes3 promoter sequences. These results argue that CXorf6 exerts its transactivation activity independently of recombination signal binding protein-J (RBP-J) binding sites. Consistent with this, CXorf6 was incapable of enhancing the N-ICD-induced transactivation of pTP-luc which possesses an iterated enhancer element with a RBP-J binding site.

Functional analysis of the mutant CXorf6 proteins

We next analyzed transactivating activities of the previously identified three apparently pathologic nonsense mutants (E124X, Q197X and R653X) and three apparently non-pathologic missense variants (P286S, Q507R, and N589S) of CXorf6. The E124X and Q197X proteins had no transactivation function for Hes3 promoter, whereas the R653X protein as well as the three variant proteins retained a nearly normal transactivating activity. Subcellular localization analysis using green fluorescent protein (GFP)-tagged proteins revealed that wildtype and R653X proteins co-localized with MAML2 protein in the PML bodies of the nucleus, whereas E124X and Q197X proteins were diffusely distributed in the nucleus and were incapable of localizing to PML bodies (Fig.2). Thus, further studies were performed for R653X using lymphoblastoid cell lines of the patients with R653X and the heterozygous mother, revealing the occurrence of nonsense mediated mRNA decay *in vivo*.

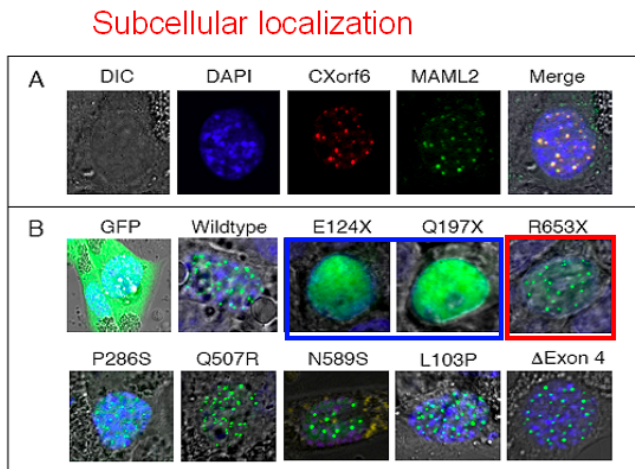


Fig.2

Expression analysis of HES3 and CXorf6

PCR-based screening on the human cDNA library revealed that CXorf6 is expressed in all the examined tissues including fetal testis and that HES3 is expressed in a range of tissues, including fetal testis and adult ovary.

SF-1 target sequence in CXorf6

We found a putative binding sites of steroidogenic factor 1 (SF-1/Ad4BP), which regulates multiple genes involved in sex development, in the upstream of the CXorf6 coding region. EMSA showed that SF-1 bound to this sequence. Moreover, luciferase assays using a luciferase reporter

containing this sequence revealed a significant transactivation activity of SF-1.

Knockdown analysis for mouse CXorf6 homolog

Transient knockdown assays of murine CXorf6 homolog were performed on the murine Leydig tumor cells using two small interfering RNAs (siRNAs). The results showed that transient down regulation of CXorf6 results in significant inhibition of androgen synthesis of the Leydig cells.

Discussion & Summary

These present study provides the first clue for the elucidation of a biological role of *CXorf6*. The results indicate that MAML2 and CXorf6 may be distantly related molecules derived from a common ancestor, and that MAML2 has evolved as a co-activator for the RBP-J dependent canonical Notch signaling whereas CXorf6 has evolved as a co-activator for the transcription of non-canonical Notch target *Hes3*. Furthermore, there may be an interaction among *SF-1*, *CXorf6*, and *HES3* in the fetal testis. Since hypospadias occurs in patients with *CXorf6* mutations, such an interaction may play an important role in the fetal testicular function including testosterone production. We designate CXorf6 as MAMLD1 (mastermind-like domain containing 1) based on its characteristic structure.

References

1. Fukami M, Wada Y, Miyabayashi K, Nishino I, Hasegawa T, Camerino G, Kretz C, Buj-Bello A, Laporte J, Yamada G, Morohashi K, Ogata T. CXorf6 is a causative gene for hypospadias. *Nature Genetics* 38(12):1369–1371, 2006.

1) Biological Sciences
1-1) Molecular Biology

Analyses of group III secreted phospholipase A₂ gene-manipulated mice

Makoto Murakami

The Tokyo Metropolitan Institute of Medical Science

mako@rinshoken.or.jp

Introduction

More than 20 phsopholipase A₂ (PLA₂) enzymes have been identified in mammals. Of these, the secreted PLA₂ (sPLA₂) family consists of 10 isozymes, which exhibit distinct tissue and cellular localizations. To elucidate the pathophysiological roles of sPLA₂ enzymes, we herein analyzed transgenic (Tg) and knockout (KO) mice for group III sPLA₂ (sPLA₂-III), an atypical sPLA₂ isoform whose functions have yet been unresolved.

Results

(1) Atherosclerosis and metabolic syndrome

In sPLA₂-III Tg mice, phospholipids in plasma lipoproteins (LDL and HDL) were hydrolyzed to generate atherogenic lipoprotein particles that facilitate macrophage foam cell formation. sPLA₂-III Tg mice crossed with *apoE*^{-/-} mice had increased aortic atherosclerotic lesion over control *apoE*^{-/-} mice following a high-cholesterol diet.¹⁾ In addition, sPLA₂-III Tg mice fed a high-fat diet displayed obesity and hepatic steatosis, with increased plasma levels of leptin, cholesterol, glucose and lysophosphatidylcholine (LPC) as well as elevated hepatic expression of a panel of genes related to lipid synthesis and uptake. Conversely, sPLA₂-III KO mice showed resistance to high-fat diet-induced obesity and hepatic steatosis, accompanied by amelioration of plasma insulin, leptin, glucose, cholesterol and LPC levels. Expression of the adipocyte differentiation markers PPAR γ and aP2 were significantly reduced in adipose tissue of sPLA₂-III KO mice. Moreover, there were a decrease of phospholipids pools containing docosahexaenoic acid (DHA), an obesity-protective fatty acid, and an increase of LPC, an obsesity-promoting lysolipid, in adipose tissue of sPLA₂-III Tg mice, whereas the adipose LPC level was markedly decreased in sPLA₂-III KO mice. Endogenous sPLA₂-III expression was elevated in adipose tissue of high-fat-fed wild-type mice. These results suggest the relationship of sPLA₂-III and metabolic syndromes.

(2) Allergy

sPLA₂-III KO mice were highly insensitive to IgE/antigen- or compound 48/80-induced passive

cutaneous anaphylactic (PCA) reaction. Bone marrow-derived mast cells (BMMC) from sPLA₂-III KO mice produced less eicosanoids than did wild-type mice following IgE/antigen activation *ex vivo*. Conversely, PCA reaction *in vivo* as well as mast cell production of eicosanoids *ex vivo* was significantly elevated in sPLA₂-III Tg mice. Although PCA reaction was restored in mast cell-deficient W/W^v mice after transplantation of wild-type BMMC, replicate W/W^v mice that received transplantation of sPLA₂-III-null BMMC still remained unresponsive to IgE/antigen, indicating that the impaired allergic response of sPLA₂-III KO mice is ascribed to a defect in mast cells. Considering that bee venom PLA₂, a homolog of sPLA₂-III, is a strong allergy inducer, our results suggest that sPLA₂-III may represent an endogenous regulator of mast cell-dependent allergic/anaphylactic response.

(3) Asthenozoospermia

Male sPLA₂-III KO mice were found to be infertile. Epididymal sperms prepared from sPLA₂-III KO mice showed impaired motility and thereby reduced fertilization capacity with oocytes *ex vivo*. Ultrastructural morphology of sPLA₂-III KO sperms was abnormal. In wild-type mice, sPLA₂-III was highly expressed in the duct epithelium of the initial segment and caput in the epididymis, where functional maturation of spermatozoa occurs. Microarray gene profiling of the epididymis revealed marked decreases in a subset of genes related to sperm motility in sPLA₂-III KO mice. These results suggest that sPLA₂-III plays a role in the maturation of sperm in the restricted portion of the epididymis.

(4) Neuronal extension and survival ²⁾

sPLA₂-III was expressed in several neuronal cells. Adenoviral expression of sPLA₂-III in neuronal cells facilitated neurite outgrowth, whereas that of sPLA₂-III-directed siRNA or a catalytically inactive sPLA₂-III mutant reduced NGF-induced neuritogenesis. sPLA₂-III also suppressed neuronal death induced by NGF deprivation. These results suggest the potential contribution of sPLA₂-III to neuronal differentiation and function under certain conditions.

(5) Inhibition of adenocirus infection ³⁾

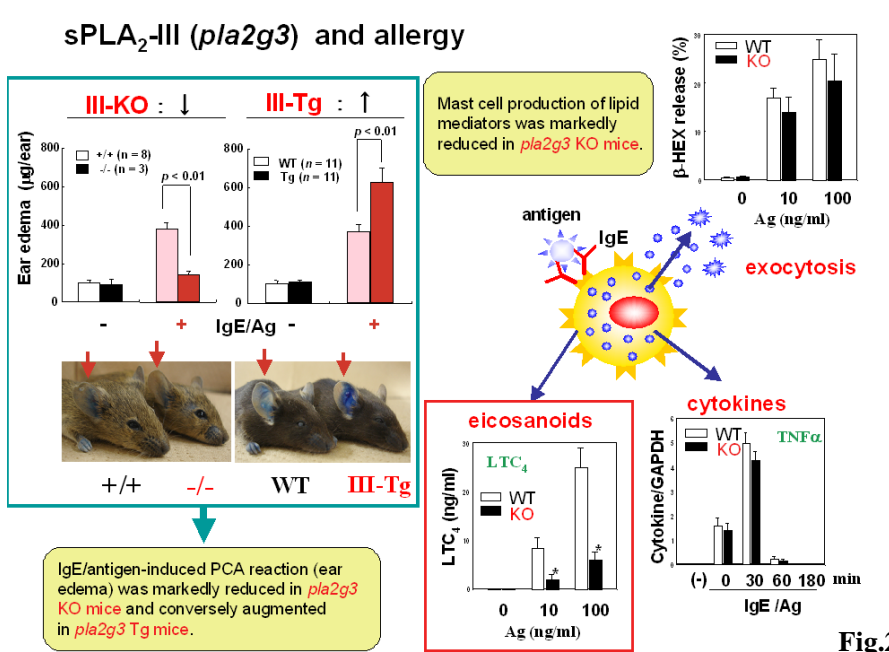
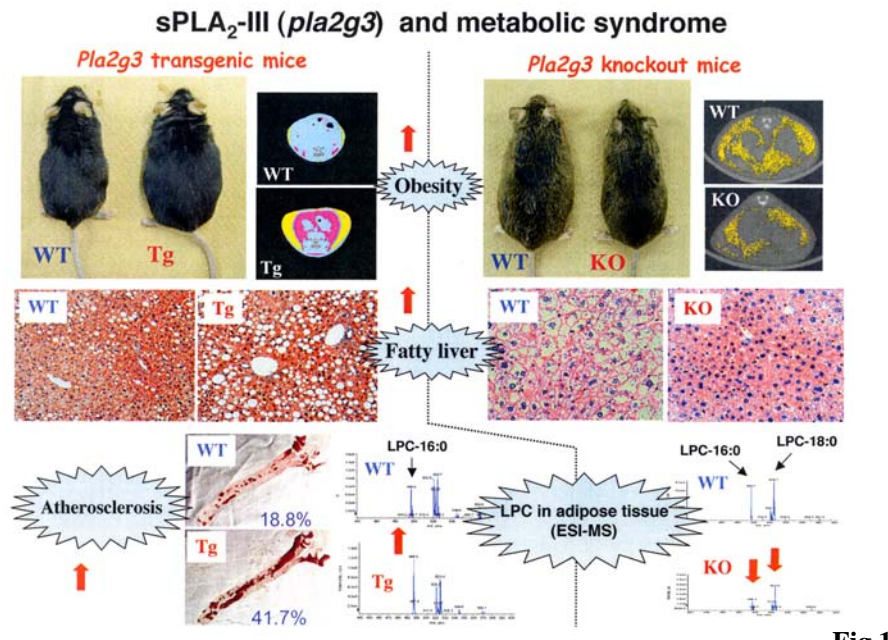
sPLA₂-III has the capacity to inhibit adenovirus infection into host cells possibly through the production of LPC in host cell membranes.

Discussion & Summary

sPLA₂-III Tg mice displayed atherosclerotic and metabolic syndrome-like phenotypes after western diet and were hypersensitive to allergic reaction after sensitization with IgE and exposure to a cognate antigen. On the other hand, sPLA₂-III KO mice were refractory to metabolic syndromes and allergy. These observations point to sPLA₂-III as a potential target for the development of a novel anti-atherosclerotic, diabetic and allergic drug. However, considering the asthenzoospermia phenotype of sPLA₂-III KO mice, the use of the anti-sPLA₂-III drug would need caution since it

might cause male infertility as an adverse effect. Molecular mechanisms underlying these *in vivo* actions of sPLA₂-III need further elucidation. Also, physiological relevance of the neuritogenic and antiviral actions of sPLA₂-III should be clarified by future studies using using sPLA₂-III Tg and KO mice.

Figures & Tables



References

- 1) Sato, S., Kato, R., Isogai, Y., Saka, G., Ohtsuki, M., Taketomi, Y., Yamamoto, K., Miki, Y., Tsutsumi, K., Yamada, J., Arata, S., Masuda, S., Ishikawa, Y., Ishii, T., Kobayashi, T., Ikeda, K., Taguchi, R., Hatakeyama, S., Hara, S., Kudo, I., Itabe, H., and Murakami, M. (2008) Analysis of human group III secreted phospholipase A₂ transgenic mice reveals its potential participation in plasma lipoprotein modification, macrophage foam cell formation, and atherosclerosis. *submitted*.
- 2) Masuda, S., Yamamoto, K., Hirabayashi, T., Ishikawa, Y., Ishii, T., Kudo, I., and Murakami, M. (2008) Human group III secreted phospholipase A₂ promotes neuronal outgrowth and survival. *Biochem. J.* 409, 429-438
- 3) Mitsuishi, M., Masuda, S., Kudo, I., and Murakami, M. (2007) Human Group III Phospholipase A₂s suppresses adenovirus infection into host cells: evidence that group III, V and X phospholipase A₂s act on distinct cellular phospholipids molecular species. *Biochim. Biophys. Acta*, 1771, 1389-1396

- 1) Biological Sciences
- 1-1) Molecular Biology

Role of Osterix in regulation of differentiation program of mesenchymal stem cell

Riko Nishimura

Osaka University Graduate School of Dentistry

rikonisi@dent.osaka-u.ac.jp

Introduction

Osterix/Sp7, a member of the Sp1 transcription factor family, plays an essential role in bone formation and osteoblastogenesis. Although Osterix has been shown to be induced by BMP2 in a mesenchymal cell line, the molecular basis of the regulation, expression and function of Osterix during osteoblast differentiation is not fully understood. Thus we examined the role of BMP2 signaling in the regulation of Osterix using the mesenchymal cell lines C3H10T1/2 and C2C12.

Results

Regulation of Osterix expression by Runx2

To address whether Runx2 is involved in the regulation of Osterix expression, we examined Osterix expression in the mesenchymal cell line C2C12 using RT-PCR. Consistent with that previous study, Osterix was induced by BMP2 treatment in a dose-dependent manner. Runx2 overexpression also induced Osterix expression. These effects of BMP2 and Runx2 were confirmed by real-time PCR analysis.

Osteoblastogenic action of Osterix

To understand the functional role of Osterix in osteoblast differentiation, we examined the effect of Osterix overexpression in C2C12 cells. Osterix overexpression induced ALP activity and osteocalcin expression in C2C12 cells. Similar to BMP2 treatment or Runx2 overexpression, Osterix overexpression also induced ALP activity in C3H10T1/2 cells. In contrast to BMP2 treatment, Osterix had very little effect on the expression of Coll1a1 or collagen synthesis, suggesting that other transcription factors, which would be controlled by BMP2, might be involved in the regulation of Coll1a1 expression and maturation. Furthermore, Osterix overexpression in mouse primary osteoblasts clearly stimulated calcification of the cells. These findings indicate that Osterix has osteoblastogenic activity. Interestingly, we observed that the osteoblastogenic activity of Osterix differed from that of Runx2, suggesting that Osterix and Runx2 have distinct and separate roles during osteoblast differentiation. To verify this possibility, we compared the target genes of Runx2

and Osterix by performing microarray analyses. Several genes, including Wnt4, Bglap1 and BMP7, were similarly induced by Runx2 or Osterix. However, we found that there were two groups of genes that were induced by either Runx2 or Osterix but not both.

Regulation of Osterix expression independently of Runx2

As described above, Osterix has distinct roles during osteoblast differentiation. Therefore we examined whether Runx2 is necessary for induction of Osterix expression using mesenchymal cells isolated from Runx2 deficient mice. These cells were able to differentiate into ALP positive osteoblastic cells upon BMP2 treatment or Runx2 overexpression within 3 days. Although the cells had some ability to differentiate into chondrocytic cells, real-time PCR analyses indicated that the cells preferentially differentiated into osteoblastic cells. As expected, Runx2 induced Osterix expression in these cells. Surprisingly, BMP2 treatment induced Osterix expression in the Runx2 deficient mesenchymal cells. These results suggest that Osterix expression is regulated by BMP2 through both Runx2-dependent and -independent mechanisms.

Regulation of Osterix expression by Smad and Msx2 signaling

To understand the molecular mechanism by which BMP2 induces Osterix expression in Runx2 deficient cells, we first examined whether Smad signaling is implicated in the regulation of Osterix expression, since Smad signaling plays a central role in BMP2-regulated osteoblast differentiation. Overexpression of Smad1 and Smad4 stimulated BMP2-induced ALP activity in Runx2 deficient mesenchymal cells. Moreover, overexpression of Smad1 and Smad4 enhanced Osterix expression by BMP2 in these cells. To confirm the involvement of Smad signaling in Runx2-independent Osterix expression, we next examined the effect of Smad6 on Runx2 deficient cells. We found that overexpression of Smad6 abolished induction of Osterix and ALP activity by BMP2 in Runx2 deficient cells. Collectively, these results indicate that Smad signaling is necessary for Osterix expression in Runx2 deficient mesenchymal cells, and subsequent osteoblastic differentiation.

Because we previously reported that Msx2 regulates osteoblast differentiation via a Runx2-independent mechanism, we hypothesized that Msx2 may function as upstream of Osterix. First, we determined whether Msx2 is induced by BMP2 treatment in Runx2 deficient mesenchymal cells. BMP2 clearly upregulated Msx2 expression even in the absence of the Runx2 gene. Importantly, Msx2 overexpression induced Osterix expression in the Runx2 deficient mesenchymal cells. Moreover, knockdown of Msx2 clearly inhibited induction of Osterix by BMP2 in the Runx2 deficient mesenchymal cells. Our findings indicate that Msx2, which is regulated by BMP2, controls Osterix expression via a Runx2-independent mechanism.

Osteoblastogenic activity of Osterix in Runx2 deficient mesenchymal cells

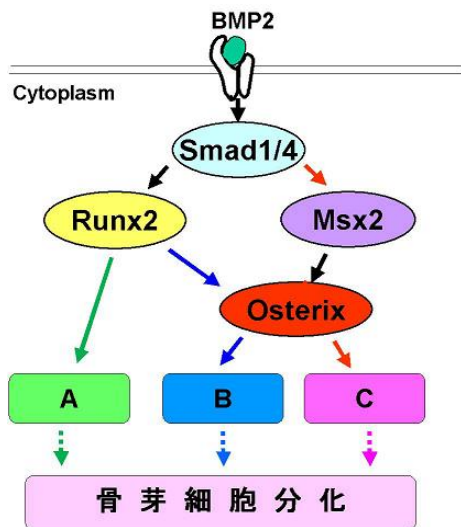
We next examined whether Osterix was able to promote osteoblast differentiation in Runx2 deficient mesenchymal cells. We exogenously introduced Osterix into Runx2 deficient mesenchymal cells, and found that Osterix induced ALP activity in these cells. In addition, Osterix significantly

stimulated osteocalcin and Bsp expression. These results suggest that Osterix itself has osteoblastogenic activity.

Discussion & Summary

Although a previous genetic study raised the possibility that Osterix functions as downstream of Runx2 (13), the mechanism by which BMP2 regulates Osterix expression during osteoblast differentiation has been unclear. In this study, we demonstrated that Osterix expression is regulated by both Runx2-dependent and -independent mechanisms. Other researchers and we have previously demonstrated that BMP2 upregulates Runx2 expression during osteoblast differentiation (10,11,24) and thus it is likely that BMP2 controls Osterix expression through Runx2. We showed here that overexpression of Runx2 induces Osterix expression in mesenchymal cell lines. Notably, we demonstrated that BMP2 and Msx2 induced Osterix expression in Runx2 deficient mesenchymal cells. Furthermore, knockdown of Msx2 blocked the induction of Osterix in the Runx2 deficient mesenchymal cells. Thus, these results indicate the novel paradigm that BMP2 controls Osterix expression independently of Runx2 through Msx2.

Figures & Tables



References

- Nakashima, K., Zhou, X., Kunkel, G., Zhang, Z., Deng, J.M., Behringer, R.R., and de Crombrugghe, B.(2002). *Cell* **108**, 17-29
 Nishimura, R., Hata, K., Harris, S.E., Ikeda, F., and Yoneda, T.(2002). *Bone* **31**, 303-312

- 1) Biological Sciences
 1-2) Struktural Biology

Role of Apolipoprotein E Structure in Disorders of Cholesterol Metabolism in Brain

Hiroyuki Saito
 Kobe Pharmaceutical University
 saito@kobepharma-u.ac.jp

Introduction

Apolipoprotein E (apoE) is a key protein regulating lipid transport in the cardiovascular and central nervous systems. In humans, apoE exists in three major isoforms, apoE2, apoE3, and apoE4; each differing by cysteine and arginine at positions 112 and 158. In neuronal repair and remodeling, apoE4 which is known to be a major risk factor for Alzheimer's disease is much less effective than wild type apoE3. To understand the molecular basis for the disorders of cholesterol metabolism in brain by apoE4, we compared physicochemical and biological properties of apoE isoforms.

Results

Cell experiments showed that the levels of apoE4-mediated cholesterol and phospholipid efflux from cultured neurons were about 5-fold less than those by apoE3. The N-terminal 22-kDa domain largely contributed to the apoE-mediated lipid efflux from neurons, in sharp contrast to the situation of macrophages in which the C-terminal lipid-binding domain plays a dominant role in lipid efflux (1). Domain interaction in apoE4 appears to inhibit the C-terminal domain-induced lipid efflux because addition of longer segments of the C-terminal domain to the apoE3 22-kDa fragment additively induced lipid efflux in a length dependent manner, whereas no additive effect was seen in the apoE4 22-kDa. In addition, we found that dimerization of apoE3 through forming a disulfide bond at Cys-112 significantly enhanced the ability to release neuronal lipids.

To understand the molecular basis for such an apoE isoform-dependent lipid efflux, we first examined the effect of progressive truncation of the C-terminal domain in apoE isoforms on their lipid-free structure and lipid binding properties (2). Removal of the C-terminal helical regions spanning residues 273-299 reduced the ability of both isoforms to bind to lipoproteins. Gel filtration chromatography experiments demonstrated that the monomer-tetramer distribution is different for the two isoforms with apoE4 being more monomeric than apoE3 and that removal of the C-terminal helices favors the monomeric state in both isoforms. Consistent with this, fluorescence measurements of Trp-264 in single Trp mutants revealed that the C-terminal domain in apoE4 is less

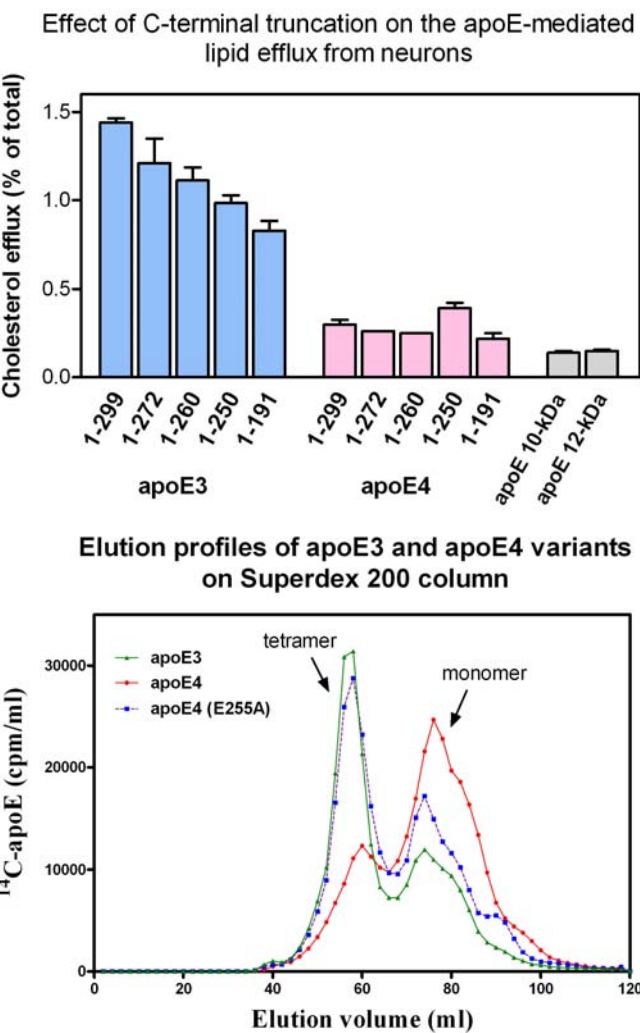
organized and more exposed to the aqueous environment compared to apoE3. In addition, the solubilization of dimyristoyl phosphatidylcholine multilamellar vesicles is more rapid with apoE4 than with apoE3; removal of the C-terminal helices significantly affected solubilization rates with both isoforms.

Binding of apoE to glycosaminoglycans (GAG) is involved in the differential effects of the apoE isoforms on neurite growth, repair, and consequently, the progression of late onset familiar Alzheimer's disease. Using surface plasmon resonance, we previously showed that the binding of apoE to heparin is a two-step process; the initial binding involves fast electrostatic interaction, followed by a slower hydrophobic interaction (3). Here, we examined the contributions of the N- and C-terminal domains to each step of the binding of apoE isoforms to heparan sulfate (HS) and dermatan sulfate (DS). ApoE3 bound to less sulfated HS and DS with a decreased favorable free energy of binding in the first step compared to heparin, indicating that the degree of sulfation has a major effect on the electrostatic interaction of GAG with apoE. Mutation of a key Lys residue in the N-terminal heparin binding site of apoE significantly affected this electrostatic interaction. Progressive truncation of the C-terminal α -helical regions which favors the monomeric form of apoE3 greatly reduced the binding ability of apoE3 to HS, with much reduced favorable free energy of binding of the first step, suggesting that the C-terminal domain contributes to the GAG binding of apoE by the oligomerization effect. Supporting this, dimerization of the apoE3 N-terminal fragment via disulfide linkage restored the electrostatic interaction of apoE with HS. Significantly, apoE4 showed much greater binding amount to HS and DS than apoE2 or apoE3 in both lipid-free and lipidated states, perhaps resulting from enhanced electrostatic interaction through the N-terminal domain.

Discussion & Summary

We found that there are two major factors, intra-molecular domain interaction and inter-molecular dimerization that cause the apoE isoform-dependent lipid efflux from neurons. The domain interaction in apoE4 modulates the organization of the C-terminal domain differently from wild type apoE3 so that apoE4 self-associates less and binds more avidly to lipid compared to apoE3. The dimerization of apoE3 via disulfide linkage enhances the electrostatic interaction of the apoE N-terminal domain with cell-surface GAG through the oligomerization effect. These differences in the conformational organization and interactions with lipid and GAG among apoE isoforms seem to lead to the pathological sequelae for cardiovascular and neurodegenerative diseases.

Figures & Tables



References

- (1) Vedhachalam, C., Narayanaswami, V., Neto, N., Forte, T. M., Phillips, M. C., Lund-Katz, S., Bielicki, J. K. "The C-terminal lipid-binding domain of apolipoprotein E is a highly efficient mediator of ABCA1-dependent cholesterol efflux that promotes the assembly of high-density lipoproteins" *Biochemistry* 46, 2583-2593 (2007)
- (2) Tanaka, M., Vedhachalam, C., Sakamoto, T., Dhanasekaran, P., Phillips, M. C., Lund-Katz, S., Saito, H. "Effect of Carboxyl-Terminal Truncation on Structure and Lipid Interaction of Human Apolipoprotein E4" *Biochemistry* 45, 4240-4247 (2006)
- (3) Futamura, M., Dhanasekaran, P., Handa, T., Phillips, M. C., Lund-Katz, S., Saito, H. "Two-step mechanism of binding of apolipoprotein E to heparin: implications for the kinetics of apolipoprotein E-heparan sulfate proteoglycan complex formation on cell surfaces" *J. Biol. Chem.* 280, 5414-5422. (2005)

- 1) Biological Sciences
- 1-2) Struktural Biology

Desensitization Mechanism of G-protein Coupled Receptor and Self-Association at Physiological Concentrations

Yasushi Imamoto
 Kyoto University
 imamoto@rh.biophys.kyoto-u.ac.jp

Introduction

Rhodopsin is a photoreceptor protein present in animal retina. It is a typical G-protein coupled receptor widely involved in the signal transduction system of the cell. GPCR activated by a stimulus interacts with G-protein. It is then phosphorylated and binds to arrestin, which inactivate GPCR. Arrestin is tetramerized in a concentration-dependent manner at the physiological concentration (40-200 μ M). However, biochemical assay is so far carried out at very low concentration (~nM), in which the effect of tetramerization of arrestin is not taken into consideration. In the present study, the physiological relevance of tetramerization of arrestin is investigated by assaying the interaction between rhodopsin and arrestin at the physiological concentration.

Results

The quaternary structure of arrestin was studied by small-angle X-ray scattering (SAXS). Because rhodopsin is a membrane protein, it should be solubilized by detergent for SAXS measurements. However, detergent micelle significantly scatters X-ray, which overlaps with the scattering from proteins. In the present study, the synthetic peptide corresponding to C-terminal 25 amino acid residues of rhodopsin, which is considered to interact with arrestin, was used to measure the SAXS in detergent-free system.

The 25 amino acid peptide phosphorylated at three serine residues (P-Rh25) as well as non-phosphorylated peptide (Rh25) was synthesized. Arrestin was isolated from fresh bovine retina. The apparent molecular weight of arrestin was estimated by the intensity of forward scattering of X-ray, which is known to be proportional to the product of molecular weight and weight concentration. Arrestin was in ~1:1 mixture of monomer and tetramer at 2 mg/ml (44 μ M). By adding P-Rh25, apparent molecular weight was increased (Figure 1). In the presence of 40-folds molar excess of P-Rh25 (6 mg/ml), arrestin is associated to show the forward scattering intensity equivalent to dodecamer. It implies that the binding of arrestin to rhodopsin induces the association. Thus it is likely that one phosphorylated rhodopsin molecule binds to ~10 molecules of arrestin.

However, Rh25 also induced the association of arrestin, suggesting that phosphate does not directly interact with arrestin but regulates the structure of the C-terminal segment of activated rhodopsin for interaction with arrestin.

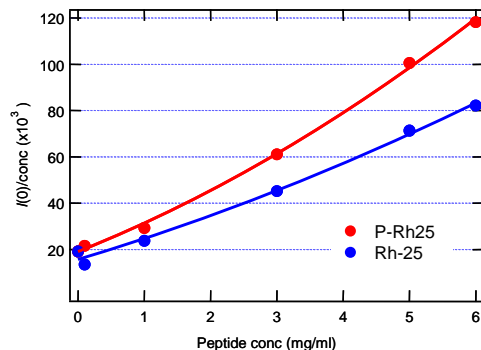


Figure 1: Oligomerization of arrestin in the presence of rhodopsin N-terminus 25-amino acid peptide with and without phosphorylation (P-Rh25 and Rh25, respectively). Note that $I(0)/\text{conc}$ is proportional to the molecular weight of the scatterer. Arrestin monomer gives $I(0)/\text{conc}$ value of 10,000.

Discussion & Summary

This study showed that rhodopsin C-terminus peptide induces the oligomerization of arrestin. It suggests that the activation of G-protein by rhodopsin is completely suppressed by covering the cytoplasmic surface of rhodopsin by a cluster of arrestin (Figure 2). It is consistent with the previous finding that rhodopsin C-terminus peptide enhances the binding of arrestin to rhodopsin. Although arrestin specifically binds to photoactivated and phosphorylated rhodopsin, Rh25 and P-Rh25 similarly interact with arrestin. Therefore, it is likely that the phosphorylation of rhodopsin alters the structure of the C-terminal segment of rhodopsin, which results in higher affinity to arrestin.

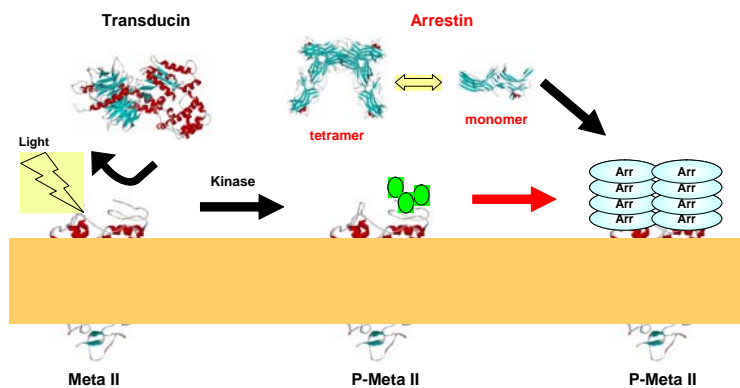


Figure 2: Schematic drawing of inactivation mechanism of metarhodopsin II by arrestin.

References

- Imamoto, Y., Tamura, C., Kamikubo, H., and Kataoka, M. (2003) Concentration-dependent tetramerization of bovine visual arrestin. *Biophys J.* **85**, 1186-1195.

1) Biological Sciences
1-3) Cell Biology

Molecular Basis of Left-Right Asymmetry Determination in Plants

Takashi Hashimoto

Nara Institute of Science and Technology, Graduate School of Biological Sciences
hasimoto@bs.naist.jp

Introduction

Rapidly expanding cells in the roots and the etiolated hypocotyls grow longitudinally to form highly elongated, cylindrical cells, and possess arrays of cortical microtubules that are arranged largely perpendicular to the cell's long axis. The importance of transverse arrays for straight growth has been indicated by pharmacological studies and experiments with helical growth mutants of *Arabidopsis thaliana*. Previous results indicate that dysfunctional cortical microtubules can arrange in helical arrays, rather than normal transverse arrays, and affect the direction of growth of expanding cells.

Here, we identified 32 *Arabidopsis* twisting tubulin mutants which provide new insights into how conserved tubulin residues contribute to microtubule dynamics, and how dynamic microtubules attribute to the growth pattern of the root.

Results

We screened mutagenized M2 seedlings in the presence of 3 μ M propyzamide for mutants that displayed root growth distinct from the wild type. Candidate mutants were then tested for skewed root growth phenotypes in the absence of the drug. After genetic loci for root twisting were mapped with respect to the tubulin loci, closely linked tubulin genes were sequenced. Finally, we obtained 40 tubulin mutant plants that showed either right- or left-handed helical growth in the root and other rapidly elongating organs. Since the same mutations were found independently in several isolates, the total number of tubulin mutations was 32. The majority of tubulin mutants were semi-dominant.

We next examined whether mutant tubulin proteins are incorporated into the microtubule and produce dominant-negative effects. Most mutations were individually introduced into the *Arabidopsis* TUA6 tagged with a Myc epitope at the C-terminus, or into the *Arabidopsis* TUB4 tagged with a multimerized Myc epitope at the N-terminus. When wild-type myc-tagged tubulin proteins were expressed in *Arabidopsis*, they were incorporated into the microtubule but did not affect seedling growth or morphology. In contrast, ectopically expressed mutant tubulins

reproduced the twisting phenotypes upon co-polymerization with wild-type tubulins into microtubule polymers.

Close inspection of the three-dimensional structure of the $\alpha\beta$ -tubulin heterodimer and the microtubule protofilament shows that mutations are classified into five categories. Tubulin mutations are described here as a combination of the tubulin isoform and the exchanged amino acids. Three left-handed helical growth mutants ($tua4^{S178\Delta}$, $tub4^{L250F}$, and $tub4^{S351F}$) had mutations at the intradimer interface between α - and β -tubulins. Mutations at the longitudinal interface between the $\alpha\beta$ -tubulin subunits resulted in either right-handed helical growth (TUA6 P325S , TUB1 S95F , TUB4 S95F , TUB4 G96D , and TUB4 P220S) or left-handed helical growth (TUA2 T349I , TUA4 T349I , TUB4 T178I , and TUB1 A394T). Mutations at the lateral contact regions led mostly to right-handed helical growth (TUA4 S277F , TUA6 S277F , TUA6 A281T , TUA2 E284K , TUB2 P287L , TUB3 P287L , TUB4 P287L , TUA2 T56I , TUA4 T56I , TUA6 T56I , and TUA4 V62I) but also to left-handed helical growth in one case (TUB4 E288K). One right-handed mutant had a TUA5 D251N mutation in the critical residue that contacts the guanine nucleotide of β -tubulin during microtubule polymerization, thus activating the inherent GTPase activity in β -tubulin.

Cortical microtubules were examined in the epidermal cells at the root elongation zone. Cortical arrays of tubulin mutants were arranged in shallow helices of distinct handedness. Mean pitch angles of microtubule helices were plotted against the skew angles of seedling roots that were grown on the hard agar surface. A strong correlation (correlation coefficient -0.918) was found between the two parameters; all the right-handed helical growth mutants had left-handed microtubule arrays, whereas all the left-handed mutants had right-handed arrays.

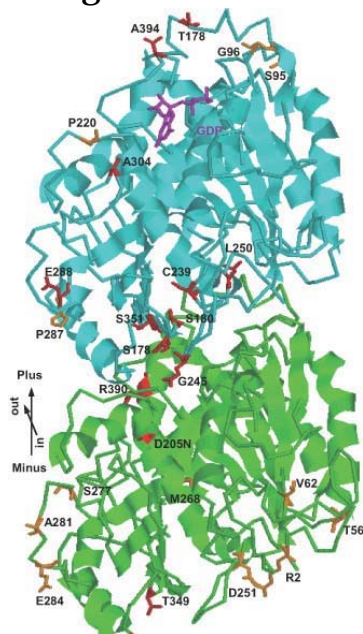
The GFP-TUB6 marker line was used to analyze the dynamic behavior of cortical microtubules in the wild type and two select α -tubulin mutants. The microtubules or bundles of microtubules in $tua5^{D251N}$ were more numerous and tended to align more perpendicular to the growth axis than those in the wild type and $tua4^{S178\Delta}$. The microtubule dynamics in $tua5^{D251N}$ was highly suppressed, as seen by the slower growth and shrinkage. Remarkably, the lagging end of $tua5^{D251N}$ microtubules did not depolymerize appreciably, and was highly stable. In $tua4^{S178\Delta}$ microtubules, the effect was most clearly observed at the leading end, which polymerized more rapidly, resulting in a highly dynamic end. Catastrophe and rescue frequencies of these mutant microtubules were not markedly different from the wild-type frequencies at either end.

GFP-EB1 was next used to probe the mutant microtubules. In the wild type, GFP-EB1 decorated the growing leading-end of microtubules as a comet with a trailing tail. The size of the GFP-EB1 comet was slightly smaller in $tua4^{S178\Delta}$, whereas GFP-EB1 also labeled the entire side wall of $tua5^{D251N}$ microtubules. FRAP showed that the photo-bleached GFP-EB1 signal on the wall of $tua5^{D251N}$ microtubules recovered well before the photo-bleached GFP-TUB6 signal did, indicating that GFP-EB1 in the cytoplasmic pool directly associated with the microtubule wall.

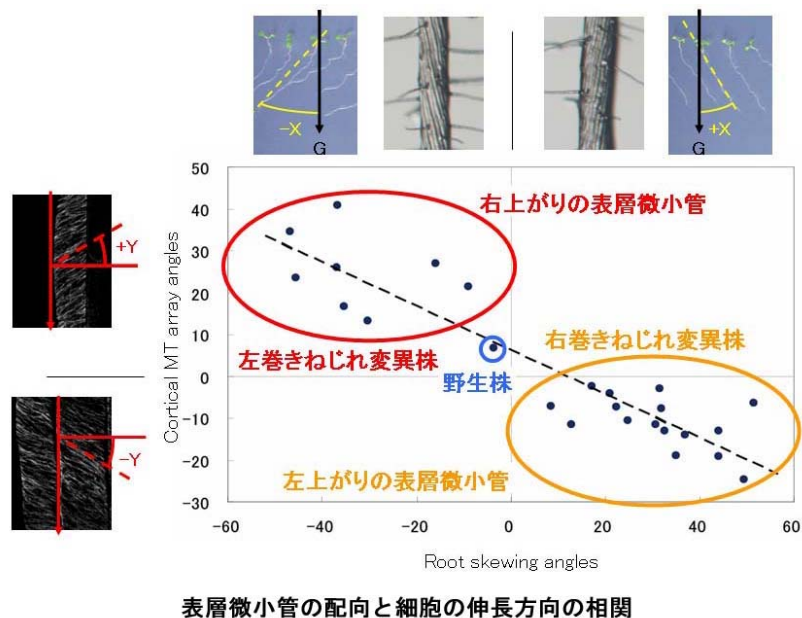
Discussion & Summary

Anisotropic expansion of plant cells requires organized arrays of cortical microtubules. Mutations in microtubule-associated proteins and a particular mutation in α -tubulins were reported to cause abnormal microtubule arrays and result in helical growth in *Arabidopsis thaliana*. However, the way in which these mutations affect the organization of microtubules remains unknown. We here identified 32 new *Arabidopsis* twisting mutants that have either missense or amino acid deletion mutations in α - or β -tubulins. Mutations were mapped to the GTPase-activating domain in α -tubulin, intra- and inter-dimer interfaces of tubulin heterodimers, and lateral contact regions between adjacent protofilaments. These dominant-negative tubulin mutants were incorporated into the microtubule polymer, and formed shallow helical arrays of distinct handedness along the long axis of the root epidermal cells. A striking correlation exists between the direction in which cortical helical arrays are skewed and the growth direction of elongating roots. The GTPase-activating-domain mutant had left-handed helical arrays composed of highly stabilized microtubules, which could be decorated along the entire microtubule lattices with the otherwise tip-localized End Binding 1 protein. A mutation at the intradimer interface, on the other hand, generated highly dynamic microtubules and right-handed helical arrays. Cortical microtubules in wild type and these two tubulin mutants were composed mainly of 13 protofilaments. This comprehensive analysis on tubulin mutations provides new insights into the mechanism by which tubulin structures influence microtubule dynamics and organization.

Figures & Tables



ねじれ表現形を与える
チューブリン変異



表層微小管の配向と細胞の伸長方向の相関

References

- T. Ishida, Y. Kaneko, M. Iwano, and T. Hashimoto (2007) Helical microtubule arrays in a collection of twisting tubulin mutants of *Arabiodpsis thaliana*. *Proc. Natl. Acad. Sci. USA* 104: 8544-8549.
- T. Ishida, S. Thitamadee, and T. Hashimoto (2007) Twisted growth and organization of cortical microtubules. *J. Plant Res.*, 120: 61-70.
- T. Hashimoto, and T. Kato (2006) Cortical control of plant microtubules. *Curr. Opin. Plant Biol.* 9: 5-11.

- 1) Biological Sciences
1-3) Cell Biology

Elucidation of mechanism for cell polarity formation in cell migration

Yuichi Mazaki

Leading Graduate School System, Kumamoto University

mazaki@kumamoto-u.ac.jp

Introduction

Cell migration is a pivotal process in development and maintenance of multicellular organisms. Directional cell migration involves initial recognition of extracellular stimuli followed by the development of a dominant leading lamella directed toward the source of the stimuli. Recently, elucidation of molecular mechanisms in cell migration has been advanced by identification of chemoattractant receptors and studies of regulation of actin polymerization. However, molecular mechanism of polarization in directional cell migration remains unknown.

To approach to this problem, we studied about relationship between ADP ribosylation factors (Arfs) and directional cell migration in neutrophil.

Results

Neutrophils play important roles in innate immunity and in the initiation of an acute response to infection. During such a response neutrophils are activated, move towards the site of inflammation and actively produce antimicrobial agents, including a number of reactive oxygen species.

Most chemoattractants, including bacterial products, complement fragments and chemokines, bind to cell surface receptors linked to the G α i family of heterotrimeric G proteins (G protein-coupled receptors, GPCRs). G β γ subunits, which are released upon activation of heterotrimeric G proteins by GPCR stimulation, bind to p21-activating protein kinase 1 (PAK1), which simultaneously binds to α PIX, a Dbl family Rac and Cdc42 guanine nucleotide exchange factor (GEF); thus a linear complex of G β γ -PAK1- α PIX is formed. This G β γ -PAK1- α PIX complex plays pivotal roles in directional sensing and persistency of GPCR-stimulated neutrophils. PAK1, Rac and Cdc42 also influence actin cytoskeletal organization.

GIT proteins are GTPase-activating proteins (GAPs) that regulate Arf family proteins. GIT1 and GIT2 are structurally conserved. In addition to negatively regulating Arf activity, GIT proteins are thought to play a role in linking the regulation of Arf proteins with other intracellular signaling events. Of note, the Spa2 homology domains of GIT proteins bind to the GIT-binding domain of α PIX.

Arf family proteins are primarily implicated in the membrane and vesicle traffic in mammalian cells. The family includes six isoforms of Arf and the Arf-like proteins. The six Arf isoforms are highly homologous to one another and assigned to class I, II, or III based on sequence similarity. Arf family proteins exist in two forms: GTP bound form and GDP bound form. The interconversion between the two forms of Arfs is promoted by two types of activities: guanine nucleotide exchange factors (GEFs) increase the level of activated Arfs and GAPs speed the intrinsic hydrolysis of the bound GTP.

Previously, we have generated GIT2-deficient mice, and found that GIT2 is essential for neutrophil function *in vivo*. Loss of GIT2 in neutrophils resulted in impaired GPCR-induced chemotactic directional sensing. In addition, we found that expression of GIT2 lacking GAP activity affected fMLP-induced cell migration of neutrophil-like cells, differentiated HL-60 cells. On the other hand, Arf1 became activated in neutrophils after fMLP treatment.

Here, we studied roles of Arf family proteins in chemotaxis of neutrophils. We first examined effects of Brefeldin A (BFA), which inhibits the activities of Arf proteins, on fMLP-induced cell migration. We found that BFA suppressed fMLP-induced cell migration of both neutrophils and differentiated HL-60 cells. On the other hand, free cell migration and adhesion to fibrinogen-coated surfaces was not notably affected with BFA. To understand the mechanism as to how Arf is activated in fMLP stimulation, we attempted to identify Arf GEFs which are involved in fMLP-induced cell migration. There are 15 genes in human encoding proteins bearing the Sec7 domain, a putative Arf GEF domain. We examined mRNA expression of Arf GEF in differentiated HL-60 cells, and found that they express 10 different Arf GEF genes. Among these 10 Arf GEFs, small interfering RNA-mediated knockdown of GBF1 significantly blocked the fMLP-induced cell migration. Moreover, we found that a significant fraction of GBF1 localized to leading edge in migrating cells, whereas GBF1 localized to Golgi apparatus in resting cells.

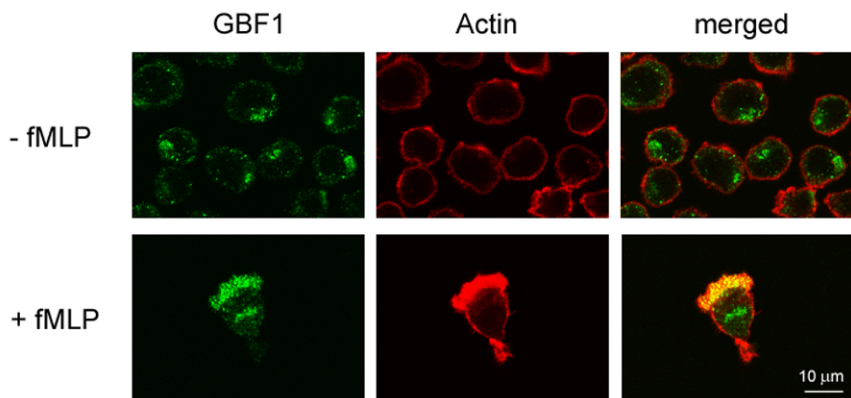
Discussion & Summary

It has been reported that Arf6 are important proteins in cell migration. Until now, however, roles of Arf family proteins in directional cell migration remain unknown. Here, we have shown that BFA suppressed fMLP-induced cell migration of both neutrophils and differentiated HL-60 cells, whereas BFA did not block their free cell migration. Our results are consistent with previous reports, because BFA has not blocked Arf6 activation.

GBF1 is a BFA sensitive GEF with for Class I and II Arfs *in vitro*. It has been reported that GBF1 co-localized with well-characterized Golgi markers to perinuclear strictures. We have shown that small interfering RNA-mediated knockdown of GBF1 significantly blocked the fMLP-induced cell migration. In addition, we have shown that a significant fraction of GBF1 localized to leading edge in migrating cells. These results suggested that GBF1 is involved in fMLP-induced cell

migration of differentiated HL-60 cells.

Figures&Tables



Figures legend: Subcellular localization of GBF1 in differentiated HL-60 cells. A significant fraction of GBF1 localized to leading edge in fMLP-induced migration cells, whereas GBF1 localized to Golgi apparatus in resting cells.

References

Morishige, M., Hashimoto, S., Ogawa, E., Toda, Y., Kotani, H., Hirose, M., Wei, S., Hashimoto, A., Yamada, A., Yano, H., Mazaki, Y., Kodama, H., Nio, Y., Manabe, T., Wada, H., Kobayashi, H., Sabe, H.

GEP100 links epidermal growth factor receptor signaling to Arf6 activation to induce breast cancer invasion. *Nat. Cell Biol.* **10**: 85-92 (2008).

- 1) Biological Sciences
 1-3) Cell Biology

Mechanism of NF-κB-dependent protection from cell death

Hiroyasu Nakano
 Juntendo University School of Medicine
 hnakano@med.juntendo.ac.jp

Introduction

NF-κB is a collective term of dimeric transcriptional factors that belong to the Rel family of proteins, and regulates expression of various inflammatory cytokines, chemokines, and adhesion molecules (Ghosh and Karin, 2002). NF-κB is activated by various inflammatory cytokines and cellular stress including tumor necrosis factor (TNF) α , interleukin-1 (IL-1), UV, and γ -irradiation. Moreover, NF-κB, especially the RelA-containing complex, inhibits cell death induced by TNF α , Fas ligand, TRAIL, and genotoxic stress. Currently, the anti-apoptotic functions of NF-κB are supported to be mainly mediated by upregulation of anti-apoptotic genes (Karin and Lin, 2002). However, the detailed molecular mechanisms are not completely understood.

Results

Here we show that cellular FLICE-inhibitory protein (c-FLIP) is rapidly lost in NF-κB activation-deficient, but not wild-type fibroblasts upon TNF α stimulation, indicating that NF-κB normally maintains the cellular levels of c-FLIP. The ectopic expression of the long form of c-FLIP (c-FLIP_L) inhibits TNF α -induced prolonged JNK activation and ROS accumulation in NF-κB activation-deficient fibroblasts. Conversely, TNF α induces prolonged JNK activation and ROS accumulation in *c-Flip*^{-/-} fibroblasts. Moreover, c-FLIP_L directly interacts with a JNK activator, MKK7 in a TNF α -dependent fashion and inhibits the interactions of MKK7 with MEKK1, ASK1, and TAK1. This stimuli-dependent interaction of c-FLIP_L with MKK7 might selectively suppress the prolonged phase of JNK activation. Taken that ROS promote JNK activation and activation of the JNK pathway may promote ROS accumulation, c-FLIP_L might block this positive feed back loop, thereby suppressing ROS accumulation.

To apply this observation to tumor therapy, we knocked down c-FLIP by RNA interference in various tumor cells. Consistent with the results using *c-Flip*^{-/-} MEFs, we found that TNF α stimulation induced caspase-dependent prolonged JNK activation and ROS accumulation, followed by apoptotic and necrotic cell death in various tumor cells. Furthermore, TNF α and Fas induced the

cleavage of mitogen-activated protein kinase/ERK kinase kinase (MEKK)1, resulting in generation of a constitutive active form of MEKK1 leading to JNK activation in c-FLIP knockdown cells. Given that ROS accumulation and necrotic cell death enhance inflammation followed by compensatory proliferation of tumor cells, selective suppression of caspase-dependent ROS accumulation will be an alternative strategy to protect cells from ROS-dependent DNA damage and compensatory tumor progression.

Discussion & Summary

Upregulation of c-FLIP_L has been shown to be correlated with resistance to Fas-induced apoptosis *in vitro* in certain tumor cell lines and also associated with autoimmune diseases. One of the strategies to treat these pathological conditions is to block the c-FLIP_L-mediated suppression of caspase activation, thereby promoting apoptosis of tumor cells and autoreactive T cells. In addition, blocking the suppressive function of c-FLIP_L on JNK activation might be an alternative strategy to treat these diseases, resulting in prolonged JNK activation-induced cell death. In this respect, the interaction of c-FLIP_L with MKK7 might be an attractive target to develop new drugs to treat various diseases such as cancers and autoimmune diseases.

Figures & Tables

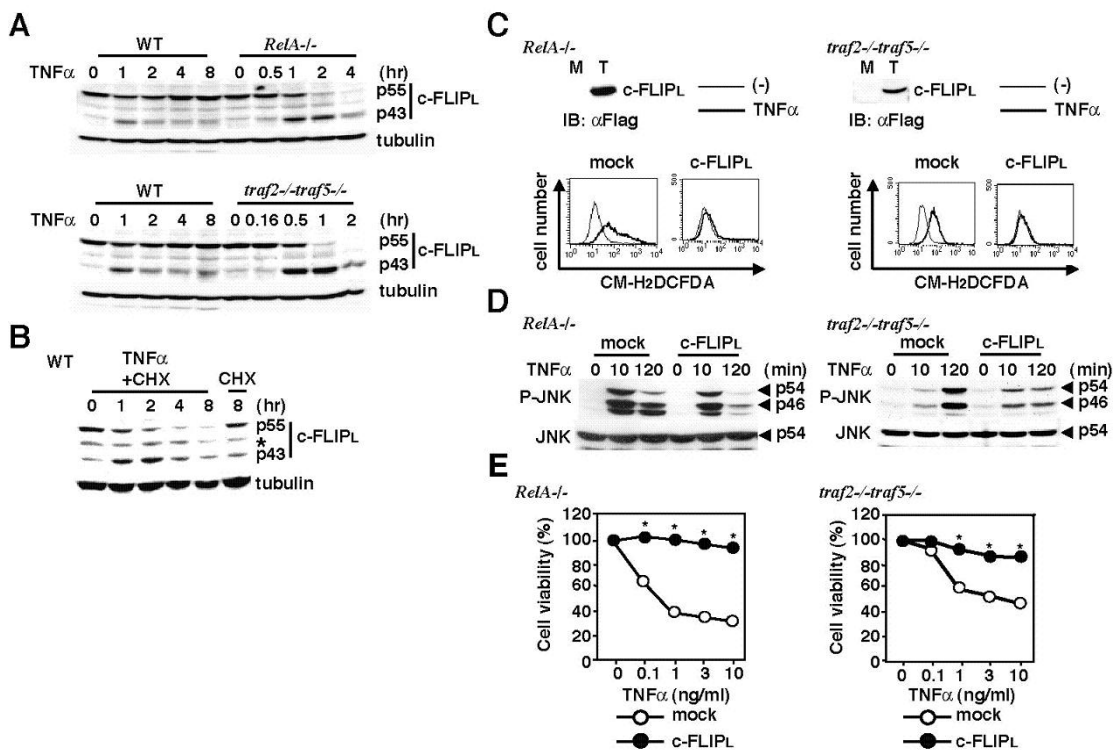


Figure1

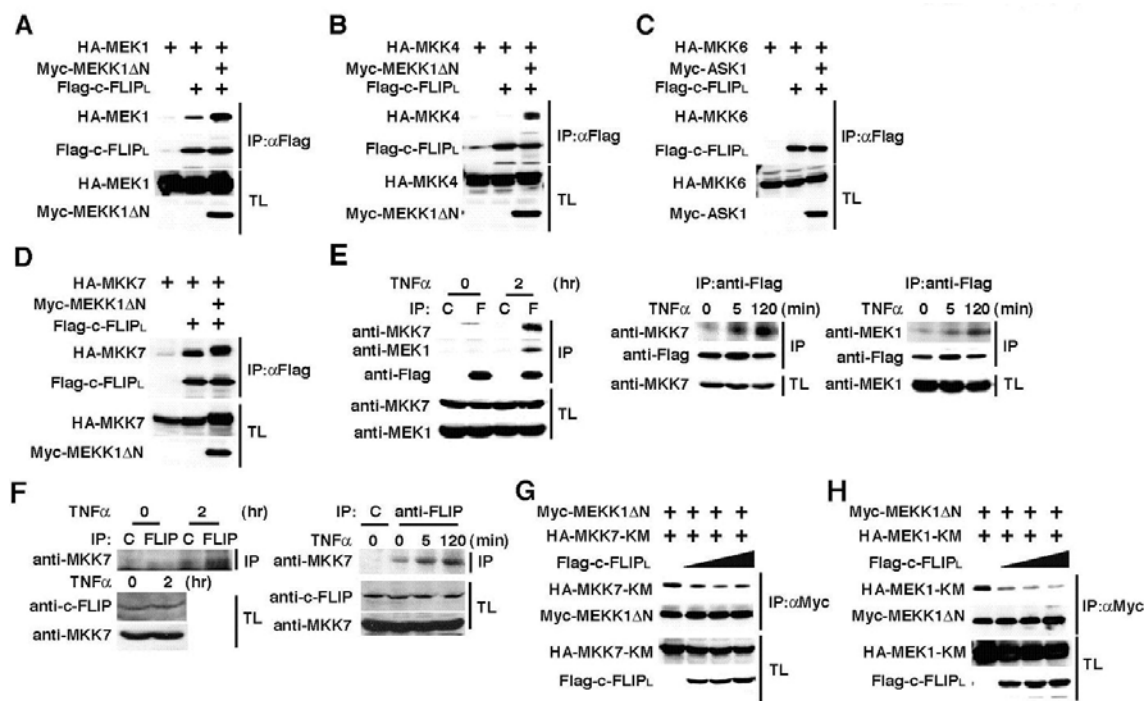


Figure2

References

1. Ghosh, S. and Karin, M. (2002) Missing pieces in the NF- κ B puzzle. *Cell*, **109 Suppl**, S81-96.
2. Karin, M. and Lin, A. (2002) NF- κ B at the crossroads of life and death. *Nat Immunol*, **3**, 221-227.

- 1) Biological Sciences
 1-3) Cell Biology

Regulatory pathway that mediates calorie restriction-mediated longevity

Akira Matsuura

Graduate School of Advanced Integration Science, Chiba University
amatsuur@faculty.chiba-u.jp

Introduction

Plant-derived polyphenols such as resveratrol have been reported to extend lifespan in yeast, fruit fly, and worm. The mechanism on which resveratrol regulates the lifespan involves a similar pathway to dietary restriction-mediated longevity, by regulating evolutionarily conserved Sirtuin family. To gain insight into the mechanism that determines organismal lifespan by chemical genetic approach, we screened for novel compounds that possessed anti-ageing activity on yeast.

Results

A food-derived compound library enriched in those with anti-oxidative activity was screened for factors possessing anti-ageing activity on yeast. Consequently, we identified tetrahydrocurcumin (THU) as a novel compound that has activity to extend replicative lifespan of yeast strains. Resveratrol, a previously identified polyphenol, has been implicated in regulation of lifespan by stimulating Sir2, a yeast sirtuin family protein. We observed that resveratrol did not extend the lifespan of *sir2* mutant, nor did THU. Thus, these compounds require Sir2 protein to fulfill this activity. Although in vitro assay showed that Sir2 deacetylase activity was directly up-regulated by resveratrol as reported previously, THU did not stimulate the activity. Moreover, THU did not affect expression of *SIR2* itself as manifested by RT-PCR analysis. These data suggest that THU does not directly target Sir2. Microarray analysis showed that tetrahydrocurcumin affected lifespan through alleviated expression of *UTH1*, a longevity-related gene. Consistent with the reduced *UTH1* expression by THU treatment in wild-type cells, administration of THU did not extend further the lifespan of *uth1* mutant. Therefore, the effect of THU on yeast lifespan is apparently mediated through regulation of *UTH1* expression. At the same time, we investigated genetic interaction between *SIR2* and *UTH1* by comparing lifespan of *sir2 uth1* double mutant with that of wild type and each of single mutants. The mean lifespan of *sir2* mutant and *sir2 uth1* double mutant was reduced comparably. These results suggest that the extension of yeast lifespan by *uth1* deletion requires normal Sir2 function. Collectively, a plausible model for the action of THU on yeast life

span extension is that the compound reduces the *UTH1* mRNA level, which in turn appears to regulate the Sir2-dependent mechanism.

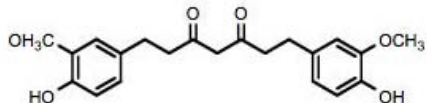
To further investigate the mechanism how THU targets *UTH1* gene, we conducted a promoter assay using lacZ gene fusing as long as 700 bp sequences which located at the upstream of the *UTH1* gene. The promoter has been predicted to contain the binding sites of several transcription factors including Mot3 and Skn7, which are involved in cellular response to oxidative stress. The β -galactosidase activity in *mot3* mutant yeast strain was significantly decreased by THU, but THU did not affect the activity in *skn7* mutant yeast strain. This result suggests that Skn7 is a target of THU effect on *UTH1* gene expression. Promoter assay suggested that repression of *UTH1* was mediated by an oxidative stress-responsive transcription factor Skn7, and this possibility was supported genetically by the fact that *UTH1* was not repressed by THU in the *skn7* mutant.

We found that THU extended lifespan of fruit fly as well. Genetic experiments showed that the effect of tetrahydrocurcumin on fruit fly required factors involved in the insulin-like growth factor signaling pathway, and was mediated through Sir2 and a forkhead transcription factor FOXO.

Discussion & Summary

Our data suggest that genetic pathway(s) regulating longevity is conserved, and that polyphenols cause extension of lifespan by targeting several molecules including Sir2. Lines of evidence suggest that targets of food-derived compounds *in vivo* may be diverse, and that several genetic pathways affected by the compounds may act multiply or in parallel to regulate organismal lifespan. It was reported that tetrahydrocurcumin significantly lengthened average life span of mice. Therefore, tetrahydrocurcumin can regulate lifespan of metazoan commonly, on the mechanism that might be different from that of resveratrol. Nonetheless, our results highlight a prominent responsibility of the Sir2 family proteins for lifespan regulation, since polyphenols, even if not directly activate, require *SIR2* to lengthen the lifespan.

Figures & Tables



Structure of tetrahydrocurcumin

References

1. **Howitz, K.T. et al.** Small molecule activators of sirtuins extend *Saccharomyces cerevisiae* lifespan. *Nature* **425**, 191-6 (2003).
2. **Wood, J. G. et al.** Sirtuin activators mimic caloric restriction and delay ageing in metazoans. *Nature* **430**, 686-9 (2004).
3. **Baur, J. A. et al.** Resveratrol improves health and survival of mice on a high-calorie diet. *Nature* **444**, 337-342 (2006).
4. **Osawa, T., Sugiyama, Y., Inayoshi, M. & Kawakishi, S.** Antioxidative activity of Tetrahydrocurcumin. *Biosci. Biotechnol. Biochem.* **59**, 1609-1612 (1995).
5. Kaeberlein, M., MeVey, M., Guarente, L. **The SIR2/3/4 complex and SIR2 alone promote longevity in *Saccharomyces cerevisiae* by two different mechanisms.** *Genes Dev.* **13**, 2570-17045 (1999).
6. **Tissenbaum, H. A. & Grarente, L.** Increase dosage of a Sir-2 gene extends lifespan in *caenorhabditis elegans*, *Nature* **410**, 227-230 (2001)
7. **Rogina, B. & Helfand, S. L.** Sir2 mediates longevity in the fly through a pathway related to calorie restriction. *Proc. Natl. Acad. Sci. U.S.A.* **101**, 15998-16003 (2004).

1) Biological Sciences
1-3) Cell Biology

Molecular mechanism of meiosis-specific endocytosis

Taro Nakamura
Osaka City University
taronaka@sci.osaka-cu.ac.jp

Introduction

Syntaxin is a component of t-SNARE complex, which is responsible for the specific fusion between membrane vesicle and its target membrane. The fission yeast syntaxin 1 Psy1 is essential for both vegetative growth and sporulation. Psy1 localizes to the plasma membrane in vegetative growth and early meiosis. Interestingly, after meiosis I, Psy1 dynamically relocates from the plasma membrane to the forespore membrane, which becomes spore plasma membrane. This relocation is regulated by an endocytosis. The aim of this study is to dissect this meiosis-specific endocytosis.

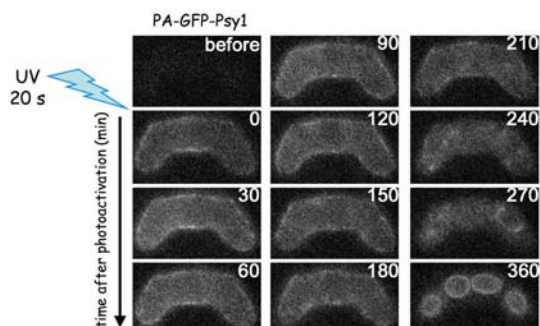
Results

To determine whether relocalization of Psy1 in meiosis is translocation from the plasma membrane to forespore membrane, Psy1 was labeled with photoactivatable-GFP (PA-GFP). In meiosis I, most of Psy1 signal was observed in the plasma membrane of zygote. Psy1 in meiosis was photoactivated and was observed behavior of PA-GFP-Psy1. Psy1 signal on the plasma membrane was disappeared after completion of meiosis I and reappeared on the forespore membrane (Fig. 1). These data indicate that Psy1 translocates from the plasma membrane to the forespore membrane.

As described above, relocalization of Psy1 is regulated by meiosis-specific endocytosis. We examined the behavior of various plasma membrane-resident proteins. Pma1, a P-type ATPase, persisted on the plasma membrane even meiosis II began (Fig. 2). On the other hand, a putative hexose transpoter, Ght6, relocalized to the forespore membrane, albeit substantial part persisted on the plasma membrane. These data suggest that selective mechanism exists in meiotic endocytosis.

Addition of Breferdin A, which inhibits the membrane transport from ER

Psy1 translocates from the plasma membrane to the forespore membrane.

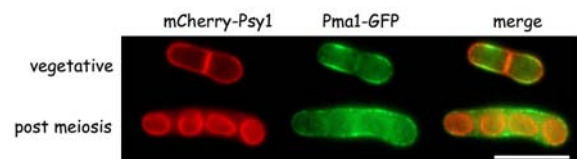


After the photoactivation by UV, Psy1 signal was observed every 30 minutes.

and/or Golgi, cannot inhibit the translocation of Psy1, suggesting that translocation of Psy1 is mainly regulated by endocytosis.

Translocation of Psy1 was inhibited by the mutations in *fim1⁺* and *adf1⁺*, which are actin-related proteins and regulated general endocytosis, suggesting that actin-dependent endocytosis is involved in the meiosis-specific endocytosis.

Some plasma membrane proteins persist on the plasma membrane in meiosis II.



In meiosis II, while Psy1 translocates to the forespore membrane, another plasma membrane protein Pma1 persisted on the plasma membrane.

Discussion & Summary

- 1, Psy1 translocates from the plasma membrane to the forespore membrane in meiosis.
- 2, Meiosis-specific endocytosis has a selective mechanism of its target proteins.
- 3, Actin-related proteins are involved in the meiosis-specific endocytosis.

References

Yukiko Nakase, Michiko Nakamura-Kubo, Yanfang Ye, Aiko Hirata, Chikashi Shimoda, and Taro Nakamura. Meiotic spindle pole bodies acquire the ability to assemble the spore plasma membrane by sequential recruitment of sporulation-specific components in fission yeast. Molecular Biology of the Cell. Vol19, in press

1) Biological Sciences
1-3) Cell Biology

Identification and functional analysis of proteins that regulate
endoplasmic reticulum stress response

Akihiro Tomida
Japanese Foundation for Cancer Research
akihiro.tomida@jfcr.or.jp

Introduction

The functions of endoplasmic reticulum (ER) are often affected by such pathophysiological conditions as nutrient starvation. To cope with ER stress, cells activate a signal transduction pathway, which is called the unfolded protein response (UPR). The adaptive response is initiated by ER-transmembrane sensor proteins, ATF6, PKR-like ER kinase (PERK) and inositol-requiring 1 (IRE1). However, the regulatory mechanisms of these sensor proteins are not fully understood. In this study, we focused on NUCB1, one of ER stress-inducible genes that we identified using a cDNA microarray system, and found that NUCB1 suppresses ATF6 activation during ER stress.

Results

NUCB1, an ER stress-responsive gene

We conducted a microarray analysis of gene expression to identify novel genes induced by glucose starvation, one of the physiological ER stress conditions. As a result, NUCB1 was identified as a glucose starvation-inducible gene. To validate the finding, we analyzed mRNA expression of NUCB1 by RT-PCR. Enhanced NUCB1 expression, as well as GRP78 expression, was seen in cells starved of glucose for 18 h. NUCB1 was also induced by treatment with 2-deoxyglucose (2DG) and tunicamycin, representative chemical ER stressors. Immunoblot analysis revealed that NUCB1 protein was also upregulated by glucose withdrawal or 2DG treatment.

Subcellular localization of NUCB1

Immunostaining demonstrated that NUCB1 localized at the Golgi apparatus. However, NUCB1 was also reported as a secretory protein. In fact, NUCB1 was detected in the culture medium under both normal and stress conditions, and the secretion was increased by the chemical stressors within 3 h. At that time point, GRP78 induction was marginal, suggesting that the increased NUCB1 secretion occurred at a relatively early phase of the UPR. These results indicate that NUCB1 can be Golgi-resident inside the cells and can be secreted outside the cells.

ER stress-responsive elements in NUCB1 promoter

We cloned an approximate 700-bp putative promoter region of the human NUCB1 gene, including the transcriptional initiation site (-584 to +112), into a luciferase reporter vector. The NUCB1 promoter was found to be activated by treating cells with tunicamycin in a dose-dependent manner. We also found that co-transfection of pATF6act or pXBP1sp, the active forms of UPR transcription factors ATF6 and XBP1, respectively, resulted in a strong activation of NUCB1 promoter activity. Examination of the NUCB1 promoter region revealed one ERSE II (-124-114, inverted) and one unfolded protein response element (UPRE)-like sequence (-152-144) as potential ER stress-responsive cis-elements. Mutational analysis revealed that both ERSE II and UPRE-like regions mediate NUCB1 promoter activation during ER stress.

NUCB1 represses UPR with inhibiting ATF6 activation

We found that co-transfection of NUCB1 and a GRP78 promoter reporter plasmid significantly attenuated GRP78 promoter activity induced by chemical stressors. Consistently, NUCB1 overexpression significantly attenuated induction of endogenous UPR target proteins under stress conditions. We also found that the production of processed ATF6 was decreased by co-transfection of NUCB1. Conversely, siRNA-mediated NUCB1 knockdown enhanced the processed form production during ER stress. These results indicate that NUCB1 can negatively regulate ATF6 processing for its activation during ER stress.

NUCB1 represses ATF6 activation in the Golgi apparatus

We examined whether or not NUCB1 overexpression influenced the subcellular localization of ATF6. Upon ER stress, ATF6 was concentrated in Golgi-like structures either with or without NUCB1 overexpression. However, the nucleus translocation of ATF6 was repressed by NUCB1 overexpression at the Golgi apparatus.

Impairment of interaction between ATF6 and S1P by NUCB1

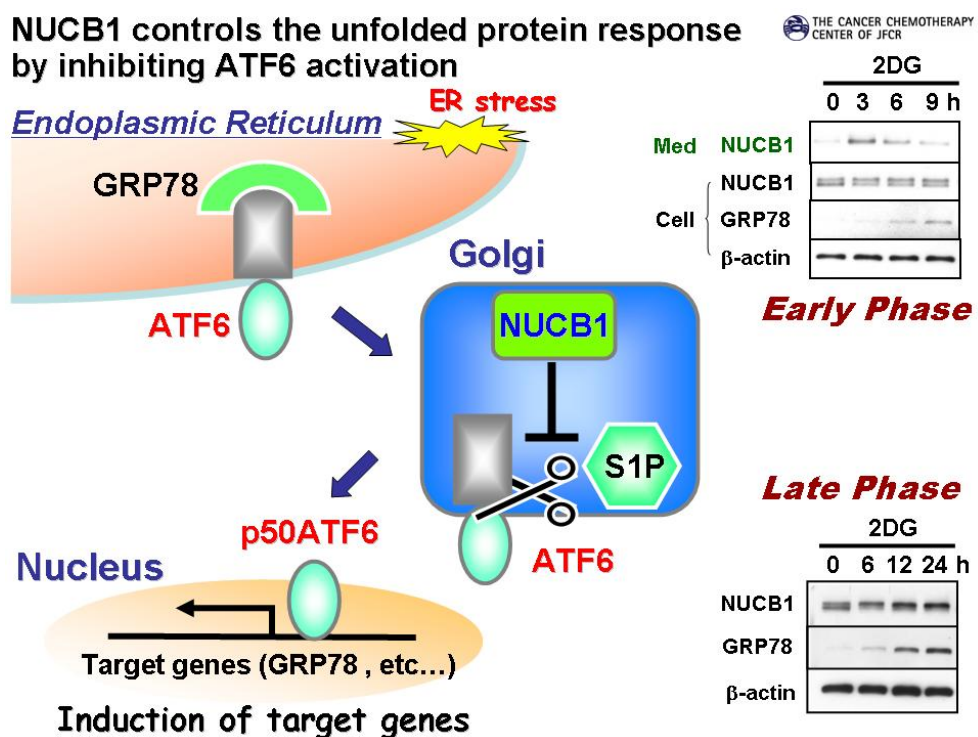
We found that interaction between ATF6 and S1P was detected during ER stress by a co-immunoprecipitation assay. Interestingly, ER stress-induced interaction between ATF6 and S1P was clearly diminished by NUCB1 overexpression. At the same time, NUCB1 overexpression inhibited production of the active form of ATF6. Thus, NUCB1 prevented the interaction between ATF6 and S1P leading to ATF6 cleavage during ER stress.

Discussion & Summary

In this study, we identified NUCB1 as a novel UPR negative regulatory protein that suppresses the S1P-mediated cleavage activation of ATF6 in the Golgi apparatus. NUCB1 is an ER stress-inducible gene with the promoter region having functional *cis*-elements for transcriptional activation by ATF6. Overexpression of NUCB1 inhibits S1P-mediated ATF6 cleavage without affecting ER-to-Golgi transport of ATF6, whereas knock-down of NUCB1 by siRNA accelerated

ATF6 cleavage during ER stress. NUCB1 protein localizes in the Golgi apparatus, and disruption of the Golgi localization results in loss of the ATF6-inhibitory activity. Consistent with these observations, NUCB1 can suppress physical interaction of S1P-ATF6 during ER stress. These results demonstrate that NUCB1 is the first-identified, Golgi-localized negative feedback regulator in the ATF6-mediated branch of the UPR. We also found that enhanced NUCB1 secretion occurs during ER stress. This may also be intriguing, as increased NUCB1 secretion has reportedly been associated with induction of autoimmunity in murine models of lupus. Thus, our findings could offer information for studying the relationship between the UPR and autoimmune response, as well as other UPR-associated pathophysiological states.

Figures & Tables



1) Biological Sciences
1-3) Cell Biology

Regulation of apoptosis by Bcl-rambo in mitochondria

Takao Kataoka
Kyoto Institute of Technology
takao.kataoka@kit.ac.jp

Introduction

The Bcl-2 family of proteins plays a key role in regulation of apoptosis. The Bcl-2 homologue Bcl-rambo has been identified to be a protein of 485 amino acids containing N-terminal Bcl-2 homology (BH) domain, BHNo (No BH motif) domain, and C-terminal transmembrane domain (Fig. 1) (Kataoka et al., 2001). Recently, it has been suggested that Bcl-rambo is a prognostic factor in childhood acute lymphoblastic leukemia (Holleman et al., 2006). In this study, we investigated the physiological function of Bcl-rambo in mitochondria-dependent apoptosis.



Fig. 1 Structure of Bcl-rambo

Results

Bcl-rambo protein is ubiquitously expressed in human cell lines

Bcl-rambo has been shown to be localized to mitochondria (Kataoka et al., 2001). The expression of Bcl-rambo in various human cell lines was examined by Western blotting (Fig. 2). As previously shown, Bcl-rambo was expressed ubiquitously in all human cell lines tested (A549, HepG2, HEK293, HeLa, HT-1080, Jurkat, K-562, Kym-1, MCF-7, Raji, THP-1, U-251, U-937). Among them, Bcl-rambo was most abundantly expressed in human chronic myelogenous leukemia K-562 cells and human rhabdomyosarcoma Kym-1 cells. Therefore, it seems that Bcl-rambo may

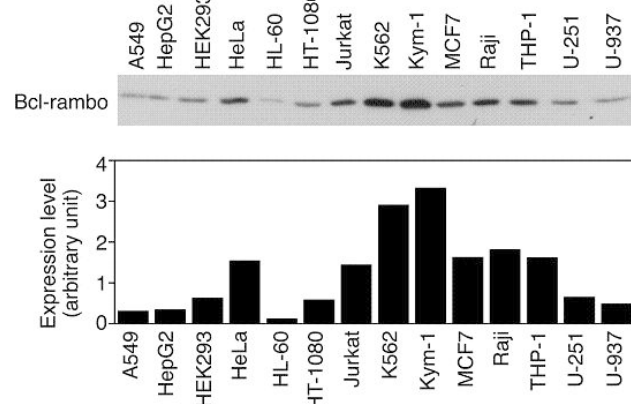


Fig. 2 Expression of Bcl-rambo in human cell lines

have more important roles in proliferation and apoptosis in these cell lines. To address the physiological function of Bcl-rambo, small interfering RNA (siRNA)-mediated knock down of Bcl-rambo was performed. Bcl-rambo was efficiently and reproducibly knocked down by several different siRNA in K562 cells, whereas these siRNA were quite ineffective to knock down Bcl-rambo in Kym-1 cells. Hence, K562 cells were used for further experiments.

Bcl-rambo may amplify mitochondria-dependent apoptosis

K-562 cells were exposed to the protein kinase inhibitor staurosporine and the protein synthesis inhibitor acetoxycycloheximide (Kadohara et al., 2005). Staurosporine induced the release of cytochrome *c* into the cytosol, as well as processing of caspase-3 into active fragments within 3 h, whereas the cytochrome *c* release and caspase-3 activation were slightly decreased in Bcl-rambo-knocked down cells. In addition, acetoxycycloheximide induced caspase-3 activation and the cytochrome *c* in mock-transfected K562 cells, while these apoptotic phenotypic changes were reduced in K562 cells transfected with Bcl-rambo siRNA. It should be noted that Bcl-rambo protein is relatively short-lived, because acetoxycycloheximide greatly decreased the cellular amount of Bcl-rambo within 6 h. These data suggest that Bcl-rambo may amplify mitochondria-dependent apoptosis.

Identification of Bcl-rambo binding proteins

Due to the fact that Bcl-rambo is devoid of known enzymatic activities, Bcl-rambo binding proteins may be better clues to predict the physiological function of Bcl-rambo. To identify the Bcl-rambo binding proteins, stable transfectants expressing FLAG-tagged Bcl-rambo were established. HEK293 cells were transfected with the FLAG-Bcl-rambo gene by electroporation, and neomycin-resistant clones were subsequently isolated and tested for the expression of Bcl-rambo by Western blotting using anti-FLAG antibody. In one of the FLAG-Bcl-rambo transfectants, Bcl-rambo has been shown to be present mostly in mitochondria but not the cytosol. The mitochondria fraction was prepared from the Bcl-rambo-transfected cells, and subjected to the immunoprecipitation using anti-FLAG antibody. The immunoprecipitates were analyzed by SDS-PAGE and the silver staining. Some protein bands have been identified to be present in the immunoprecipitates from the Bcl-rambo-transfected cells, but not the mock-transfected cells.

Discussion & Summary

The Bcl-2 family members containing all four BH motifs, such as Bcl-2 and Bcl-x_L, exert anti-apoptotic activity. Although Bcl-rambo is predicted to be anti-apoptotic due to the presence of all four BH motifs (BH1, BH2, BH3, BH4), overexpression of Bcl-rambo is able to induce apoptosis dependent on its unique BHNo domain (Kataoka et al., 2001). Therefore, the function of Bcl-rambo under the physiologic conditions has yet to be understood. In this study, we have shown that Bcl-rambo is ubiquitously expressed in human cancer cell lines and may play a role in the

amplification of mitochondria-dependent apoptosis. Since it has been shown that Bcl-rambo is a prognostic factor in childhood acute lymphoblastic leukemia (Holleman et al., 2006), the clarification of the physiological function of Bcl-rambo is expected to be important for its therapeutic intervention.

References

- Kataoka, T., Holler, N., Micheau, O., Martinon, F., Tinel, A., Hofmann, K., and Tschopp, J. (2001) Bcl-rambo, a novel Bcl-2 homologue that induces apoptosis via its unique C-terminal extension. *J. Biol. Chem.*, 276, 19548-19554
- Holleman, A., den Boer, M. L., de Menezes, R. X., Cheok, M. H., Cheng, C., Kazemier, K. M., Janka-Schaub, G. E., Göbel, U., Graubner, U. B., Evans, W. E., and Pieters, R. (2006) The expression of 70 apoptosis genes in relation to lineage, genetic subtype, cellular drug resistance, and outcome in childhood acute lymphoblastic leukemia. *Blood*, 107, 769-776
- Kadohara, K., Tsukumo, Y., Sugimoto, H., Igarashi, M., Nagai, K., and Kataoka, T. (2005) Acetoxycycloheximide (E-73) rapidly induces apoptosis mediated by the release of cytochrome *c* via activation of c-Jun N-terminal kinase. *Biochem. Pharmacol.*, 69, 551-560

1) Biological Sciences
1-4) Developmental Biology

Elucidation of the role of sugar chain in cartilage formation using
mice with abnormal sugar chain

Toshihisa Komori

Department of Cell Biology, Unit of Basic Medical Sciences, Nagasaki University Graduate School
of Biomedical Sciences
komorit@nagasaki-u.ac.jp

Introduction

Proteoglycan was shown to play important roles in the localization of growth factors and their binding to each receptor in cartilage (1). However there is no report about mucin-type sugar chains in cartilage. To clarify the function of mucin-type sugar chains in cartilage, we analyzed the expression of pp-GalNAc-Ts in cartilage and generated chondrocyte-specific pp-GalNAc-T3 transgenic mice.

Results

We examined the expression of 16 isoforms of pp-GalNAc-Ts in cartilage by real-time RT-PCR, and detected the expression of the 13 isoforms of pp-GalNAc-Ts in cartilage. Further, we examined whether the expression of these isoforms can be induced by Runx2, which is an important transcription factor for chondrocyte maturation. The expressions of pp-GalNAc-T3 and pp-GalNAc-T6 were induced by Runx2. To examine the function of pp-GalNAc-T3, we generated pp-GalNAc-T3 transgenic mice under the control of Col2a1 promoter, because knockout mice of pp-GalNAc-T1,4,5,13 showed no phenotypes, suggesting the functional redundancies among the isoforms. pp-GalNAc-T3 transgenic mice were lethal and showed severe dwarfism. Cartilage matrix was reduced and chondrocytes were more condensed compared with wild-type mice. The frequencies of BrdU labeling and TUNEL staining were increased, and chondrocytes maturation was retarded in pp-GalNAc-T3 transgenic mice compared with wild-type mice. The levels of staining with Safranin O, Tluidin blue, and Alcian blue in pp-GalNAc-T3 transgenic mice were much weaker than those in wild-type mice, whereas the level of staining with PAS was more intense in pp-GalNAc-T3 transgenic mice compared with wild-type mice. The content of chondroitin sulfate was severely reduced in pp-GalNAc-T3 transgenic mice compared with wild-type mice.

Discussion & Summary

The phenotypes of pp-GalNAc-T3 transgenic mice showed that proteoglycan was reduced but mucin-type sugar chains were increased in the cartilage. As pp-GalNAc-Ts and xylose transferase add GalNAc and xylose, respectively, to serine or threonin, overexpression of pp-GalNAc-T3 may inhibit the activity of xylose transferase (Figure 1). Preliminary data showed that growth factors differentially affected both the growth of cartilage and chondrocyte maturation in pp-GalNAc-T3 transgenic mice as compared with wild-type mice. Therefore, pp-GalNAc-T3 transgenic mice are useful for the functional analysis of proteoglycan as well as mucin-type sugar chains in cartilage.

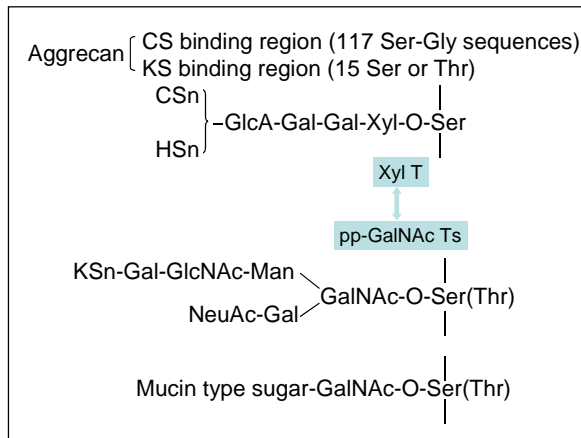


Figure 1

References

1. Hardingham T. E. and Fosang A. J. Proteoglycans: many forms and many functions FASB J. 6:861-870, 1992.

- 1) Biological Sciences
- 1-4) Developmental Biology

The functional analyses of semaphorin in the neural network formation

Masahiko Taniguchi

Department of Biochemistry, Cancer Research Institute, Sapporo Medical University

School of Medicine

taniguti@sapmed.ac.jp

Introduction

During embryogenesis, axons reach their specific targets correctly to form the complex neural network found in the mature functional nervous system. Several groups of axon guidance molecules such as semaphorins, ephrins, netrins, and slits have been reported to repel or attract growing axons that express their cognate receptors. Semaphorin gene family contains a large number of secreted and transmembrane proteins, and some of them function as the repulsive and attractive cues of axon guidance during development.

Results

Zebrafish (*Danio rerio*) is an excellent model organism to investigate vertebrate nervous system development and functions because transparent embryos and Morpholino Oligo techniques facilitate *in vivo* function analyses of the interesting genes. Previously, I cloned a novel member of class 6 semaphorin gene, *semaphorin 6D (sema6D)* in mouse. *Sema6D* is expressed predominantly in the nervous system in mammals. As an initial step to investigate how Sema6D regulates nervous circuit formation through molecular genetic approaches in zebrafish, I cloned a zebrafish orthologue of mammalian *sema6D*. By 24 hpf *sema6D* expression was detected in the lens, otic capsule, telencephalon and rhombomere. *Sema6D* expression was detected in the lens, dorsal thalamus, posterior tuberculum, tectum opticum, otic ganglion, rhombic lip and medulla oblongata at 48 hpf, and in the lens, dorsal thalamus, posterior tuberculum, tectum opticum and medulla oblongata at 72 hpf. Plexins are known to be semaphorin receptors. I found that Sema6D binds Plexin-A1 *in vitro*, but not other Plexins. I estimated the binding affinity of Sema6D-alkaline phosphatase (AP) fusion proteins to cells expressing Plexin-A1 in equilibrium binding experiments. The estimated Kd was 8.6 ± 1.3 nM. I performed a repulsive assay using chick dorsal root ganglion (DRG) and sympathetic neurons to examine whether Sema6D exhibits significant biological activity. Sema6D induces the repulsion of DRG axons, but not sympathetic axons.

I also cloned a novel secreted type of mouse semaphorin gene and termed *semaphorin 3G* (*sema3G*). *Sema3G* is mainly expressed in the lung and kidney, and a little in the brain. Interestingly, in the adult rodent brain *sema3G* is expressed only in the granular layer of the cerebellum. I also found that Sema3G binds Neuropilin-2 (NP-2), but not Neuropilin-1. We estimated the binding affinity of Sema3G-AP fusion proteins to cells expressing NP-2 in equilibrium binding experiments. The estimated Kd was 58 ± 17 pM. Sema3G induces the repulsion of sympathetic axons, but not DRG axons.

Discussion & Summary

I identified and cloned zebrafish *sema6D* cDNA. Characteristic expressions of *sema6D* are in the lens and rhombomeres. Sema6D might function in retinal ganglion cell axons as a guidance molecule. Rhombomeres are segmental units of the developing vertebrate hindbrain. Zebrafish Sema6D might function in the rhombomere boundary formation. I found that Sema6D binds Plexin-A1. Sema6D exhibits chemorepellent activity for DRG axons expressing Plexin-A1. These results suggest that Sema6D might use Plexin-A1 as a receptor to execute chemorepulsion. Taken together, Sema6D might function in the axon guidance as a repulsive guidance cue in the nervous system.

I identified and cloned a novel mouse *sema3G* cDNA. We found that Sema3G can bind NP-2, but not NP-1. Sema3G exhibits chemorepellent activity for sympathetic axons expressing NP-1 and NP-2, but not DRG axons. These results suggest that Sema3G may utilize NP-2 as a receptor to exert chemorepulsion for sympathetic axons.

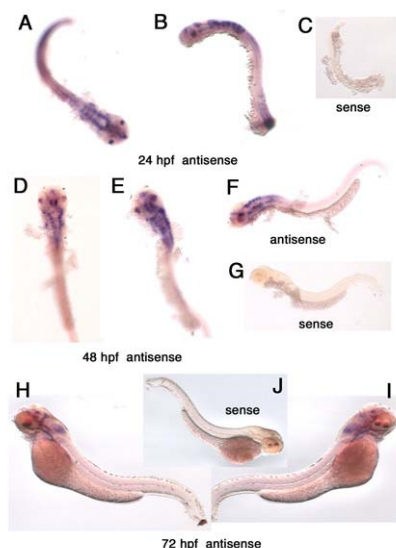


Figure 1. Zebrafish Sema6D expression pattern of embryos at 24, 48 and 72 hpf by whole mount *in situ* hybridization.
(A-C) 24 hpf (D-G) 48 hpf (H-J) 72 hpf zebrafish embryos.
(A,D,E) Dorsal view (B,C,F,G,H,I,J) Lateral view

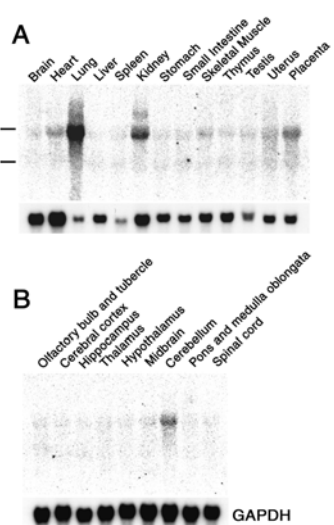


Figure 2. Analysis of Sema3G expression by Northern blotting.
(A) The distribution of Sema3G in adult mouse tissues.
(B) Regional distribution of Sema3G in adult rat brain.
The lines show the location of murine 28S and 18S ribosomal RNAs.

References

Kimura M, Taniguchi M, Mikami Y, Masuda T, Yoshida T, Mishina M, Shimizu T. Identification and characterization of zebrafish semaphorin 6D. Biochem Biophys Res Commun 363: 762-768, 2007.

1) Biological Sciences
1-4) Developmental Biology

Progressing reproductive biology by analysis of intratesticular oocytes

Kon Yasuhiro

Laboratory of Anatomy, Department of Biomedical Sciences, Graduate School of Veterinary Medicine, Hokkaido University
y-kon@vetmed.hokudai.ac.jp

Introduction

It has been generally believed that in mammals, males produce only sperm, and oocytes are only produced in females. It is also known that vertebrates born as either males or females never change their sex during their lifetimes. Although some genetic abnormalities of sexual differentiation in mammals can cause the appearance of oocytes in the testes or the development of ovotestis, it has never been reported that apparently healthy and fertile male animals can produce oocytes during spermatogenesis (1). We found oocytes in the seminiferous tubules of newborn MRL/MpJ male mice, and report here some characteristics of these testicular oocytes.

Results

Testicular oocytes were found in testes obtained from *lpr* mice, and in testes from M+ mice aged 0 to 30 days after birth. They coexisted with gonocytes and spermatogonia in the seminiferous tubules, mostly in the neighborhood of the rete testis. Because of their unique size, 50-70 µm in diameter, they were easily distinguishable from somatic cells and sperm-producing cells. Each oocyte had an abundant cytoplasm and a large nucleus with one or two distinct nucleoli, and each oocyte was surrounded by a zona pellucida-like structure, which was observed between the oocyte and follicular epithelial-like cells. Follicular epithelial-like cells were clearly distinguishable at days 14-30. Each of these follicular epithelial-like cells had a nucleus with an irregular shape containing distinct nucleoli similar to those in Sertoli cells. Although the follicular epithelial-like cells formed a multilayer similar to that observed in early stage secondary follicles, they never formed follicular antrum or a polar body-like structure.

Ultrastructurally, the oocyte extended numerous microvilli through about half the thickness of the zona pellucida, and the follicular epithelial-like cells attached to the cell membrane of the oocyte with slender cytoplasmic processes penetrating the zona pellucida-like structure. In the cytoplasm of the testicular oocyte, a round, highly dense matrix bound by a single smooth membrane was found just beneath the cell membrane; these appeared similar to the cortical granules found in ovarian

oocytes. These cortical granules were divided into two types by their diameters. They were located mainly in two regions. The smaller granules appeared to be synthesized in the juxta-nuclear region, and the larger granules appeared to be synthesized near the cell membrane. The testicular oocytes contained Golgi complexes observed as multiple aggregates of small vesicles, and flattened tubules similar to those involved in the synthesis and formation of cortical granules in ovarian oocytes.

The oocytes were detected in about half of the mice examined (65 of 124), and the maximum number of oocytes detected in one testis was twelve. The appearance of oocytes in the testis peaked on day 14 after birth with an oocyte score of approximately 1.2. No oocyte was observed on days 40 and 50 after birth. The testes of other inbred strains and F1 mice age matched to *lpr* mice with the highest oocyte score (14 days old) were examined. We found no oocytes in these other inbred strains of mice and in MRLB6F1 mice. However, F1 progeny from female B6 mice mated to male MRL mice were shown to have testicular oocytes with a lesser oocyte score than that of the MRL strains.

The zona pellucida-like structures showed a positive reaction to the PAS stain. They were observed as discontinuous lines on days 0 and 4 after birth, and then as continuous lines on day 8 much like ovarian oocytes of the same age. Additionally, zona pellucida-like structures were shown to express ZP3 by immunostaining, and at the same level as that in ovarian oocytes. However, the follicular epithelial-like cells of testicular oocytes were not immunostained with FOXL2, while the follicular epithelium in ovaries were stained.

The expression of oocyte-specific genes in MRL testes was examined by RT-PCR and compared to the expression in B6 testes. The *lpr* testes expressed all of the oocyte-specific genes examined in the present study; however, the intensities of expression were weaker than that found in the ovaries. Expression of the oocyte-specific genes became stronger on day 13 in comparison to day 4. The testicular expression of *Zp1* and *Omt2a* was detected only in *lpr* mice, whereas the expression of *Zp2* and *Zp3* was also observed in testes from B6 mice, and these results were confirmed by sequencing.

Discussion & Summary

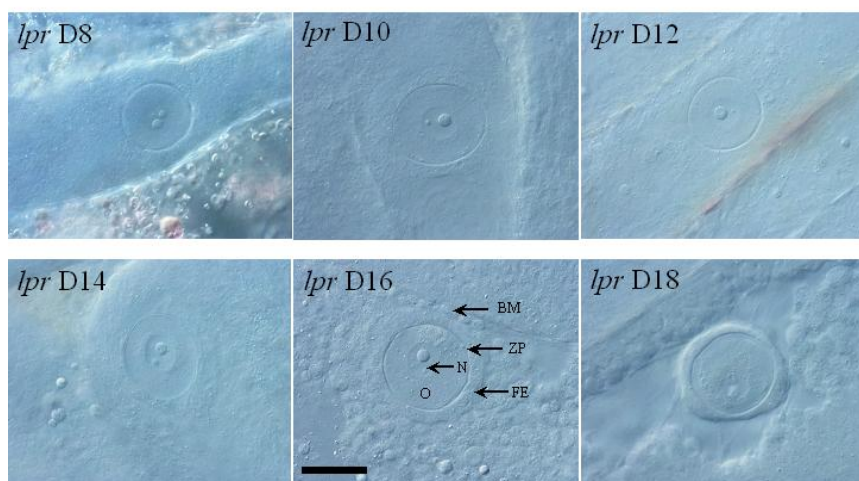
This is the first report of the appearance of testicular oocytes in XY fertile males (2). The existence of binuclear oocytes and the lack of FOXL2 in the follicular cells indicated that the follicular cells do not have abilities to regulate oocyte growth (3). The expression of the *Zp* genes and *Omt2a* indicated that testicular oocytes have the ability to fuse with sperm (4). The observation in F1 mice suggested that this phenotype was dominant as long as the Y chromosome derived from the MRL background in part.

The testicular oocytes in MRL can provide more clues such as the mechanisms of sex differentiation, sex-specific methylation patterns of germ cells, and the mechanism that prevents

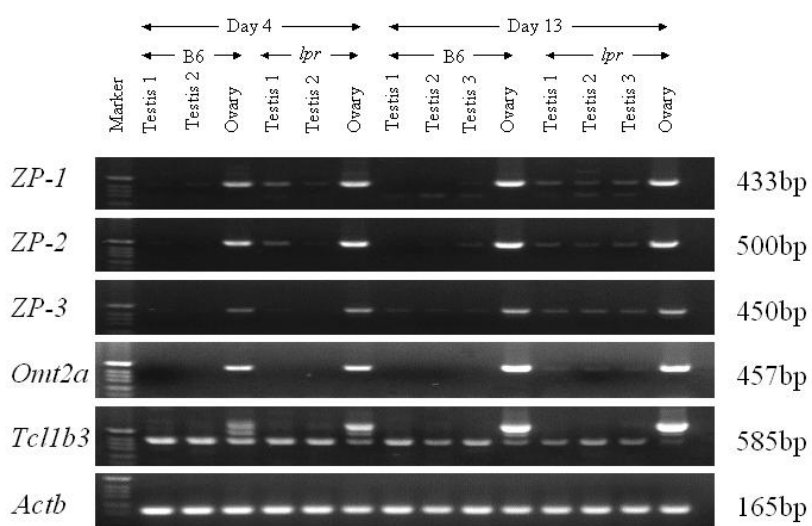
entry into meiosis in male embryos. If the testicular oocytes can be made to mature *in vitro*, it is possible to obtain an embryo with a genome derived entirely from male mice by *in vitro* fertilization and intrafallopian transfer techniques. If we obtain testicular oocytes from one side of the testes and sperm from the other side, an embryo with a genome derived from only one male will be produced, meaning "Eve from Adam". Thus, testicular oocytes in MRL can establish a new concept in reproductive biology.

Figures & Tables

Testicular oocytes in whole-mount testes of *lpr* mice aged 8-18 days. Scale bar = 50 μ m.
All images are of the same magnification. BM, basement membrane; FE, follicular epithelial-like cell; N, nucleus; O, oocyte; ZP, zona pellucida-like structure.



Oocyte-specific gene expression in *lpr* mouse testes. RT-PCR products of testes and ovaries of *lpr* and B6 mice from days 4 and 13 for *Zp1-Zp3*, *Omt2a*, and *Actb* as an internal control.



References

1. Isotani A, Nakanishi T, Kobayashi S, Lee J, Chuma S, Nakatsuji N, Ishino F, Okabe M. Genomic imprinting of XX spermatogonia and XX oocytes recovered from XX↔XY chimeric testes. Proc Natl Acad Sci USA 2005; 102: 4039-4044.
2. Otsuka S, Konno A, Hashimoto Y, Sasaki N, Endoh D, Kon Y. Oocytes in Newborn MRL Mouse Testes. BOR Papers in Press. Published on March 19, 2008 as DOI:10.1095/biolreprod.107.064519.
3. Uhlenhaut NH, Treier M. Foxl2 function in ovarian development. Mol Genet Metab 2006; 88: 225-234.
4. Wassarman PM, Jovine L, Litscher ES. Mouse zona pellucida genes and glycoproteins. Cytogenet Genome Res 2004; 105: 228-234.

1) Biological Sciences
1-5) Physiology

Physiological relevance of aquaporins in brain

Masato Yasui

Keio University School of Medicine Department of Pharmacology

myasui@sc.itc.keio.ac.jp

Introduction

Mercurials inhibit aquaporins (AQPs), and site-directed mutagenesis has identified Cys189 as a site of the mercurial inhibition of AQP1. On the other hand, AQP4 has been considered a mercury-insensitive water channel because it does not have the reactive cysteine residue corresponding to Cys189 of AQP1. Indeed, the osmotic water permeability of AQP4 expressed in various types of cell, including *Xenopus* oocytes, is not inhibited by HgCl₂. To examine the direct effects of mercurials on AQP4 in proteoliposome reconstitution system, His-tagged rat AQP4 M23 was expressed in *Saccharomyces cerevisiae*, purified with a Ni²⁺-nitrilotriacetate affinity column, and reconstituted into liposomes with the dilution method.

Results

The osmotic water permeability of 10His-ratAQP4 M23 reconstituted proteoliposomes (AQP4-proteoliposomes) with or without HgCl₂ was measured with the carboxyfluorescein quenching method with a stopped-flow apparatus. The osmotic water permeability was significantly higher in the AQP4-proteoliposomes [$P_f = 112 \pm 11$ (S.D.) μm/s, n = 8] than in control liposomes (1.47 ± 0.48 μm/s, n = 6; Figure 1). Surprisingly, application of 300 μM HgCl₂ markedly decreased the osmotic water permeability of the AQP4-proteoliposomes to 34.5 ± 6.8 μm/s (n = 4). This inhibition was reversed by the addition of 3 mM β-mercaptoethanol (β-ME). These data indicate that AQP4 is a mercurial-sensitive water channel when reconstituted into proteoliposomes. The

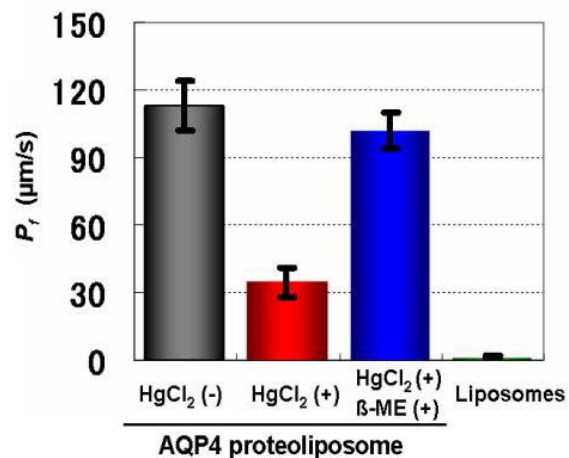


Figure 1| The osmotic water permeability of rAQP4-proteoliposomes is down-regulated by HgCl₂. Figure shown are the calculated osmotic water permeabilities (P_f) in AQP4-proteoliposomes, AQP4-proteoliposomes treated with 300 μM HgCl₂, AQP4-proteoliposomes treated with 300 μM HgCl₂ and 3 mM β-ME, and control liposomes.

osmotic water permeability of AQP4 was not significantly inhibited by 300 μM HgCl₂ when expressed in oocytes.

To investigate the dose- and time-dependent effects of mercurial inhibition, AQP4- and AQP1-proteoliposomes were pretreated with HgCl₂. Proteoliposomes were preincubated for 5 min with different concentrations of HgCl₂, to examine the dose-dependent effects. HgCl₂ at 5 μM inhibited AQP4 by 50%, whereas an HgCl₂ concentration greater than 100 μM was required to inhibit AQP1 by 50%. The time-dependent effects of mercurial inhibition were examined with 300 μM HgCl₂. Fifty-percent inhibition of AQP4 occurred within 30 seconds, while 50% inhibition of AQP1 did not occur until 5 min, suggesting that the mechanisms of HgCl₂ inhibition differ between AQP1 and AQP4.

Site-directed mutagenesis was performed to identify a target cysteine residue for mercurial inhibition. There are six cysteine residues in rat AQP4 M23. Each cysteine was individually mutated. All six AQP4 mutant proteoliposomes exhibited increased osmotic water permeability under basal conditions, similar to that of wild-type AQP4, indicating that all mutants were functional proteins. The effects of HgCl₂ on the osmotic water permeability of each AQP4 mutant proteoliposome were examined. The osmotic water permeability of C76S, C87S, C106S, C123S proteoliposomes were significantly inhibited by both 10 and 300 μM HgCl₂ in the same way as that of wild-type AQP4. In contrast, the osmotic water permeability of C178S proteoliposome ($P_f = 127 \pm 7 \mu\text{m/s}$, $n = 3$) was not inhibited by 10 μM HgCl₂ ($P_f = 128 \pm 9 \mu\text{m/s}$, $n = 3$) but was slightly inhibited by 300 μM HgCl₂ ($P_f = 99.9 \pm 7.7 \mu\text{m/s}$, $n = 3$). Note that C178 is localized in cytoplasmic loop D. The C253S mutant ($P_f = 93.8 \pm 6.1 \mu\text{m/s}$, $n = 3$) was inhibited by 10 μM HgCl₂ to the same extent as wild type AQP4 ($P_f = 81.8 \pm 11.6 \mu\text{m/s}$, $n = 3$).

To determine the orientation of AQP4 in the liposome membrane, two antibodies against AQP4 were employed: an anti-human NMO-IgG, which recognizes the extracellular region of AQP4, and a rabbit anti-AQP4, which binds to the rat AQP4 C-terminus intracellular region. AQP4-proteoliposomes, control liposomes, oocytes injected with AQP4 cRNA, or control oocytes were incubated with either NMO-IgG or rabbit anti-AQP4 IgG antibodies without any detergents and were then subjected to SDS-PAGE immunoblot analysis to detect the antibodies bound to AQP4. In AQP4-proteoliposomes, NMO-IgG and rabbit anti-AQP4 IgG antibodies were detected by anti-human IgG and anti-rabbit IgG, respectively. In oocytes, NMO-IgG, but not rabbit anti-AQP4 IgG, was detected. Note that the binding of the rabbit anti-AQP4 IgG to AQP4 M23 expressing in oocytes was confirmed with immunoblot of membrane fraction of control- and AQP4- oocytes using the rabbit anti-AQP4 IgG. These data indicate that AQP4 is reconstituted into liposome membranes in two orientations, whereas AQP4 is configured in a single orientation in oocyte membranes.

Discussion & Summary

AQP4 has been considered a mercurial-insensitive water channel because its osmotic water permeability is not affected by $HgCl_2$ and because AQP4 does not have a cysteine residue at the position corresponding to Cys189 in AQP1 (Figure 2A). However, we have unexpectedly found with the AQP4-proteoliposome that the channel is also inhibited by $HgCl_2$ and identified Cys178 as a target residue for mercurial inhibition of AQP4. Cys178 is localized in cytosolic loop D. We reasoned, therefore, that a difference in the orientation of membrane proteins might explain the difference in mercurial inhibition between AQP4-incorporated oocytes and proteoliposomes. In the AQP4-oocytes, loop D is always on the cytoplasmic side Ref.). On the other hand, in 50% of reconstituted AQP4, loop D may be exposed to the outside of the proteoliposome because AQP4 is incorporated randomly in both orientations in the liposome membranes (Figure 2B). Mercury could hardly be permeated through the membrane - It is considered that a little amount of mercury could be permeated though the membrane since the mercury inhibition for AQP4 was approximately 60%. Mercury could easily approach Cys178 in proteoliposomes but not in oocytes.

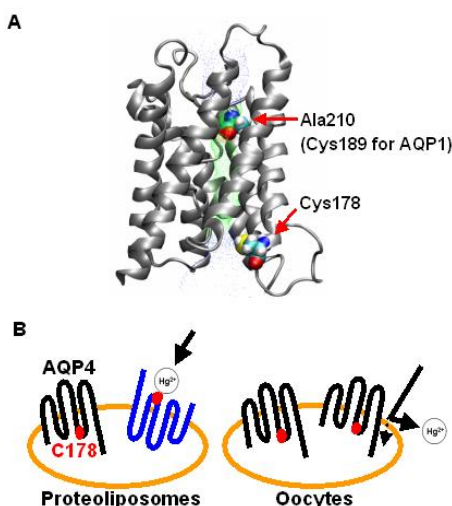


Figure 2| (A) Structural model of AQP4 monomer. This figure was constructed by Visual Molecular Dynamics (VMD). The pore boundaries were illustrated by HOLE. Structure of AQP4 shown in ribbon form and the structures of Cys178 and Ala210 are shown with space-fill models (carbon atoms are light blue, oxygen atoms are red, nitrogen atoms are blue, and sulfur atoms are yellow). (B) Schematic model showing a difference between AQP4-proteoliposomes and AQP4-oocytes, in terms of accessibility of $HgCl_2$.

References

- Hiroaki, Y., Tani, K., Kamegawa, A., Gyobu, N., Nishikawa, K., Suzuki, H., Walz, T., Sasaki, S., Mitsuoka, K., Kimura, K., Mizoguchi, A. and Fujiyoshi, Y. (2006) Implications of the aquaporin-4 structure on array formation and cell adhesion. *J. Mol. Biol.* **355**, 628-63

1) Biological Sciences

1-5) Physiology

Selective estrogen receptor modulator (SERM) in herbs as a potential medicinal seed

Tetsushi Furukawa

Tokyo Medical & Dental University, Medical Research Institute

t_furukawa.bip@mri.tmd.ac.jp

Introduction

Estrogen replacement therapy for rapid development of atherosclerosis, osteoporosis, and other symptoms in post-menopausal women is hampered by increased risk of estrogen-sensitive tumor. Thus, the development of selective estrogen receptor modulators (SERMs) is highly desired. Ginsenoside, a main phytosterol of Panax ginseng, has been successfully used for post-menopausal syndrome in Eastern medicine without increased risk of malignant tumor. Thus, we tried to characterize estrogen-like effects of ginsenoside.

Results

Ginsnoside binds to the estrogen receptor in a dose-dependent manner with a K_d value of 33.8 nM. We examined genomic effects of ginsenoside using proliferation of mammalian cancer-derived cell line, MCF-7. Ginsenoside Re did not induce proliferation of MCF-7 cells, and partially inhibited 17β -estradiol-induced MCF-7 proliferation.

We performed co-factor recruitment assay using a fluorescent resonance energy transfer (FRET) probe, ER-SCCoR. Ginsenoside did not induce co-factor recruitment, and partially inhibited 17β -estradiol-induced co-factor recruitment.

In addition to the canonical genomic action, estrogen exhibits non-genomic action which takes place in a membrane-delimited manner. Ginsenoside induced nitric oxide (NO) production via the non-genomic pathway consisting of membrane-type estrogen receptor, c-Src, PI3-kinase, Akt, and endothelial type NO synthase (eNOS).

Ginsenoside induced protection against Ca^{2+} accumulation during the ischemia-reperfusion insult, which was mediated by NO produced via the non-genomic pathway of estrogen receptor.

Discussion & Summary

Our study demonstrated that ginsenoside, a main phytosterol of panax ginseng, is a selective agonist of non-genomic pathway of estrogen receptor. The lack of genomic action by ginsenoside was due to

the failure of co-factor recruitment, possibly because the presence of bulky side chain in the chemical structure of ginsenoside disrupts the formation of co-factor binding pocket. Since the NO production via the non-genomic action induced protection of cardiac myocytes against ischemia-reperfusion insult, the non-genomic effects of ginsenoside may provide a potential candidate for SERMs.

Figures & Tables

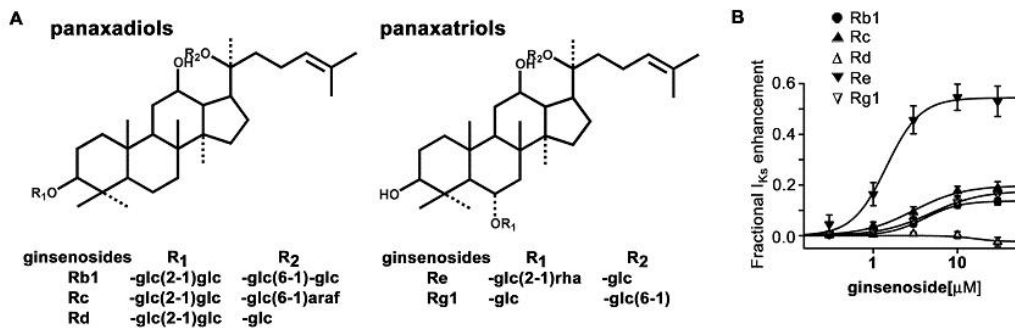


Figure 1

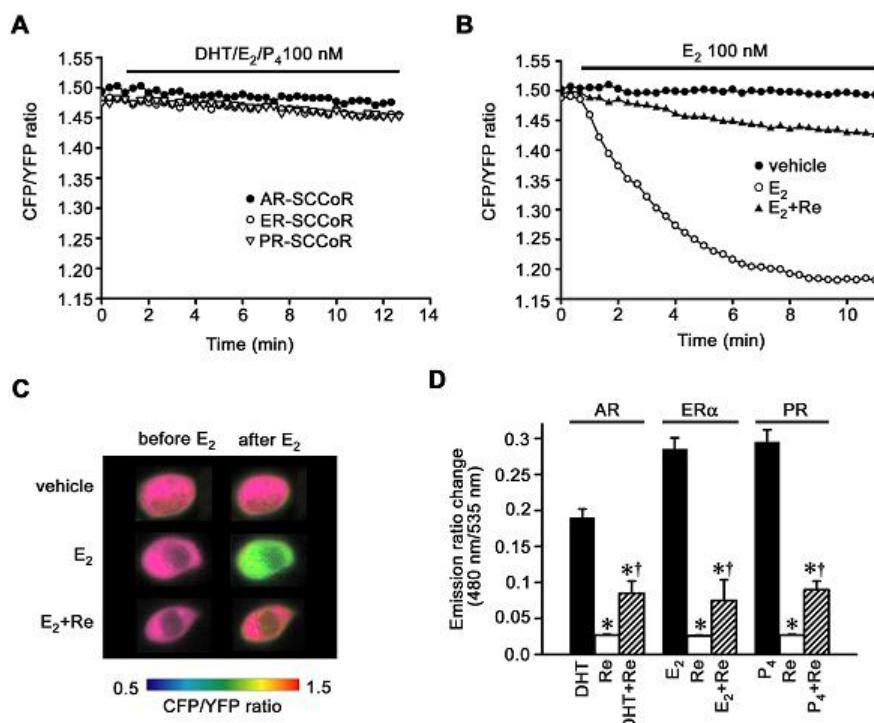


Figure 2

References

- Furukawa T, Bai C-X, Kaihara A, Ozaki E, Kawano T, Nakaya Y, Awai M, Sato M, Umezawa Y, Furukawa T. Ginsenoside Re, a main phytosterol of Panax ginseng, activates cardiac potassium channels via a nongenomic pathway of sex hormones. *Molecular Pharmacology* 2006;70:1916-1924.
- Furukawa T, Kurokawa J. Regulation of cardiac ion channels via non-genomic action of sex steroid hormones: implication for the gender difference in cardiac arrhythmias. *Pharmacology & Therapeutics* 2007;115:106-115.

1) Biological Sciences

1-5) Physiology

Elucidation of molecular mechanisms for the modulation of learning abilities by emotion

Toshiya Manabe

Institute of Medical Science, University of Tokyo

tmanabe-tky@umin.ac.jp

Introduction

The NMDA receptor is composed of the NR1 and NR2 subunits, and switching from the NR2B to NR2A subunit is thought to underlie functional alteration of the receptor during synaptic maturation, and it may result in preferential localization of NR2A subunits on the synaptic site and that of NR2B subunits on the extrasynaptic site in the mature brain. In this study (Miwa et al., J. Physiol., 2008), we have investigated whether NR2B subunit-containing receptors are present and functional at mature synapses in the lateral nucleus of the amygdala (LA) and the CA1 region of the hippocampus, comparing their properties between the two brain regions.

Results

We first examined whether NR2B subunits contributed to NMDA receptor-mediated normal synaptic transmission at thalamo-LA synapses with whole-cell patch-clamp recordings from principal cells in the LA, comparing it with that at Schaffer collateral/commissural-CA1 synapses (CA1 synapses). Ifenprodil, an NR2B subunit-selective antagonist, significantly inhibited NMDA EPSCs in both types of synapses; however, the inhibition at the thalamo-LA synapse was significantly larger than that at CA1 synapses (Figure 1).

The decay time constant of NMDA EPSCs in the LA became much faster when the NR2B subunit was selectively blocked by ifenprodil, compared with that in the control external solution. On the other hand, the decay time constant in the CA1 region was changed only

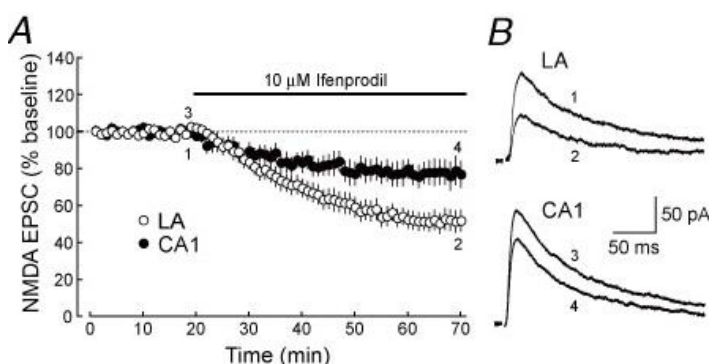


Figure 1

slightly in the presence of ifenprodil, compared with that in the control external solution. These results suggest that the NR2B subunit is a member of the NMDA receptor complex on the synaptic

site and that its contribution is greater in the LA.

We next performed the postembedding immunogold electron-microscopic analysis at excitatory synapses in the LA and the CA1 region. In the two brain regions, both NR2A and NR2B subunits were enriched on the synaptic membrane, which was defined as the membrane associated with the postsynaptic density (PSD). In contrast, these subunits were by far less expressed at the extrasynaptic membrane in the spine. The relative abundance of synaptic NR2B subunits to synaptic NR2A subunits in the LA was significantly greater than in the CA1 region. Taken together, these data indicate that NMDA receptors are highly accumulated on synaptic sites in both brain regions, but the content of NR2B subunits relative to NR2A subunits is higher at the thalamo-LA synapse than at the CA1 synapse.

We next compared the properties of NMDA EPSCs between the two brain regions to test whether the difference in the relative abundance of NR2B subunits affected properties of NMDA EPSCs. The ratio of NMDA to AMPA EPSC amplitudes was significantly larger in the LA than in the CA1 region. In addition, the *I-V* curve in the LA was significantly different from that in the CA1 region at the membrane potentials between 0 and -90 mV. Furthermore, we found that the sensitivity to 1.3 mM Mg²⁺ was significantly lower in the LA than in the CA1 region.

In many types of central synapses, the activation of NMDA receptors is required for synaptic plasticity. We found that LTP in the LA induced by the pairing protocol was completely blocked by D-APV, an NMDA receptor antagonist, indicating that this form of LTP was also dependent on the NMDA receptor. To assess a possible role of the NR2B subunit in LTP induction, we next investigated the effect of the blockade of NR2B subunit-containing NMDA receptors on LTP induction. LTP was reduced in magnitude in both the LA and the CA1 region. However, in the LA, LTP disappeared almost completely in the presence of ifenprodil, whereas LTP was significantly but only partially inhibited in the CA1 region, suggesting that LTP induction in the LA required the activation of NR2B subunit-containing NMDA receptors to a greater extent than in the CA1 region.

Discussion & Summary

In the present study, we have demonstrated that NR2B subunit-containing NMDA receptors contribute substantially to synaptic NMDA receptor-mediated responses, as well as synaptic plasticity, in the LA and the hippocampal CA1 region even in adult mice. In addition, we have found for the first time that the properties and subunit composition of the NMDA receptor are different between the LA and the CA1 region. Since the properties of NR2A and NR2B subunits are differentially regulated by tyrosine phosphorylation, the difference in the ratio of NR2 subunits between the CA1 region and the LA may result in qualitatively different modification of synaptic functions between the brain regions. In fact, the activation of synaptic NR2B subunit-containing NMDA receptors is involved in the induction of LTP more critically in the LA of the adult mouse.

Thus, our results strongly suggest that NR2B subunits are present at mature synapses and play critical roles in the induction of synaptic plasticity in adult animals.

References

- Miwa, H., Fukaya, M., Watabe, A. M., Watanabe, M. and Manabe, T. (2008). Functional contributions of synaptically localized NR2B subunits of the NMDA receptor to synaptic transmission and LTP induction in the adult mouse CNS. *J. Physiol. (London)* 586:2539-2550.

1) Biological Sciences

1-5) Physiology

Regulation of cellular event by activator of G-protein signaling 8 induced by myocardial ischemia

Motohiko Sato

Cardiovascular Research Institute, Yokohama City University School of Medicine

motosato@yokohama-cu.ac.jp

Introduction

Recent study indicates the existence of regulatory protein which regulates the activation status of heterotrimeric G protein independent of receptor (1,2). Such proteins may provide additional checking points for adaptation process of cell and influence on the development of disease (Figure 1). Bearing this mind, we identified Activator of G-protein signaling 8 (AGS8), from rat hearts subjected to repetitive transient ischemia (Figure 2) (3,4). AGS8 mRNA was up-regulated in the ischemic area of the ventricle but not other disease models. AGS8 interacted directly with G_{βγ} and stimulated G_{βγ} signaling in cell. AGS8 would regulate cellular events in adaptation process of myocardium to ischemia, however the nature of this protein has not been well characterized. As an initial approach to identify the physiological role of AGS8, we tried to determine an influence of AGS8 on hypoxia-induced apoptosis of cultured cardiomyocytes.

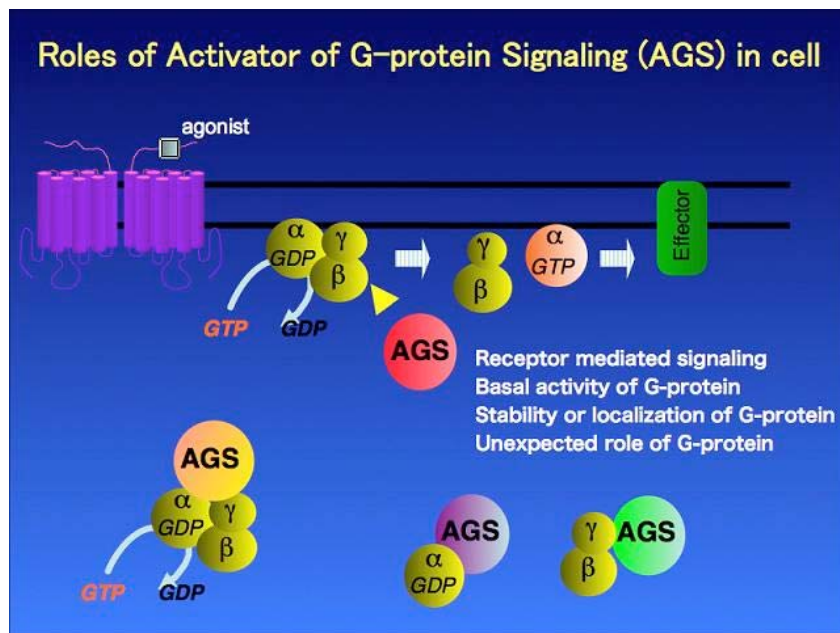
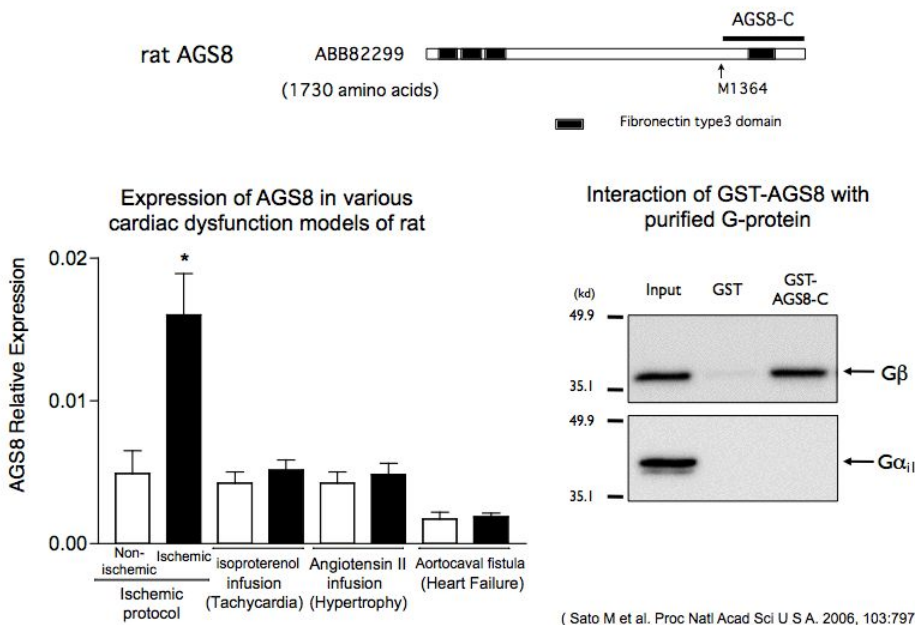


Figure 1

**Figure 2**

Results

Preparation and induction of apoptosis of neonatal cardiomyocyte. Cardiomyocytes were prepared from 1-day old neonatal of SD rats by enzyme digestion. Cultured rat cardiomyocytes were exposed to hypoxia (1% oxygen) following 48 h later of transfection of siRNAs or plasmids.

Introduction of siRNA or plasmid to cells. We applied two siRNAs for AGS8 as well as scrambled oligonucleotides as control. Each of siRNAs was successfully suppressed the level of AGS8 of cardiomyocyte to the 30%. In some experiments, pcDNA3::AGS8 was introduced to cardiomyocyte utilizing virus envelope system to overexpress AGS8.

Suppression of AGS8 reduced apoptosis of cardiomyocytes induced by hypoxia. Neonatal cardiomyocytes were exposed to hypoxia or normoxia for 6 or 24 h following transfection of siRNAs. Cells were immediately applied for TUNEL stain at the end of exposure. Apoptotic cells were increased in the dependent of exposure time in all of control group transfected with universal negative control siRNA or scrambled siRNA. However, interestingly, apoptotic cells were significantly low in cardiomyocytes transfected with siRNAs for AGS8.

Suppression of AGS8 reduced apoptosis induced by hypoxia/reoxygenation. It was well known that reoxygenation following hypoxic period enhanced apoptotic process in cardiomyocytes. An influence of AGS8 on apoptosis of cardiomyocytes induced by hypoxia/reoxygenation was tested. Cultured neonatal cardiomyocytes were sequentially exposed to hypoxia (1% oxygen) for 6 h and normoxia for 18 h following transfection of siRNA for AGS8. Cells were immediately applied to TUNEL stain or the detection of change of mitochondrial membrane potential at the end of exposure.

Again, as observed hypoxia-alone challenge, suppression of AGS8 reduced apoptosis of cardiomyocyte induced by hypoxia/reoxygenation.

Overexpression of AGS8 increased apoptosis following hypoxia/reoxygenation. These data suggested that AGS8 acted as pro-apoptotic factor in the face of hypoxic stress, however this was observed under the suppressed level of AGS8. AGS8 was up-regulated in the ischemic myocardium of repetitive transient ischemia in which AGS8 was originally identified. Thus, we introduced pDNA3::AGS8 to the cardiomyocytes to evaluate an effect of increase of AGS8 on apoptosis. The increase of apoptotic cells following hypoxia(6h)/reoxygenation(18h) was enhanced in the presence of AGS8. Interestingly, AGS8 did not influence on the number of apoptotic cells cultured in the normoxia.

AGS8 was enriched in the plasma membrane of cardiomyocyte. The question was that in which subcellular domain AGS8 is located and operates the cellular events involved in apoptosis. To address this issue, we generated antibody against AGS8 and detected signals in the myocardium as well as cultured cardiomyocyte. The antibody recognized immuno-reactive signal in the plasma membrane of left ventricle as well as cultured cardiomyocytes. Interestingly, the signal was enriched in the cell-cell interface, suggesting possibility of that AGS8 may form protein complex with other proteins in the cellular junction.

AGS8 formed protein complex with connexin 43. Immunoprecipitation of AGS8 indicated connexin 43 was co-immunoprecipitated from the left ventricle. Recent reports indicated that connexin 43 was involved in apoptosis of cardiomyocytes and its reduction was related to enhancement of ischemic injury.

AGS8 regulated the level of connexin 43. We looked if AGS8 influenced on the level of connexin43 in the cultured cardiomyocyte. The level of connexin43 was reduced when AGS8 was overexpressed in cardiomyocyte. Conversely, the suppression of AGS8 by siRNA enhanced the level of connexin 43. The result indicated that AGS8 act to reduce the level of connexin 43 in the cardiomyocytes.

Discussion & Summary

These data indicated 1) AGS8 enhanced apoptosis of cultured cardiomyocytes following exposure of hypoxia and hypoxia/reoxygenation, 2) AGS8, interestingly, did not influence on the population of apoptotic cells in the normoxia, 3) AGS8 was enriched in the plasma membrane of cardiomyocytes including cell-cell interface, 4) AGS8 formed the protein complex with connexin 43, 5) AGS8 decreased the level of connexin 43 when it was expressed in cardiomyocytes.

It was of interesting that AGS8 was involved in the cellular event related to the pathophysiological condition in which AGS8 was originally identified. An effective inhibition of cardiac apoptosis by siRNA for AGS8 suggested a potential of AGS8 as a novel therapeutic target for ischemic heart

disease. The observations also indicated that AGS8 contributed to the hypoxia-induced apoptotic process at least in part via changing status of connexin 43. The regulation of connexin 43 by AGS8 may shed light on a new mechanism and management of ischemic injury of the heart.

References

1. Sato M, Blumer JB, Simon V, Lanier SM. ACCESSORY PROTEINS FOR G-PROTEINS: PARTNERS IN SIGNALING. *Annu Rev Pharmacol Toxicol.* vol 46, 151-87, 2006.
2. Blumer JB, Sato M, Lanier SM. AGS3. UCSD-Nature Molecule Pages (2007). (doi:10.1038/mp.a000228.01).
3. Sato M, Cismowski MJ, Toyota E, Smrcka AV, Lucchesi PA, Chilian WM, Lanier SM. Identification of a receptor-independent activator of G protein signaling (AGS8) in ischemic heart and its interaction with G $\beta\gamma$. *Proc Natl Acad Sci U S A.* vol 103, 797-802, 2006.
4. Yuan C, Sato M, Lanier SM, Smrcka AV. Signaling by a non-dissociated complex of G-protein beta gamma and alpha subunits stimulated by a receptor-independent activator of G protein signaling, AGS8. *J Biol Chem.* 2007;282:19938-47.

- 1) Biological Sciences
 1-6) Pharmacology

Postgenomic approach to identify novel bacterial antibiotic resistome

Kunihiko Nishino

Institute of Scientific and Industrial Research, Osaka University
 nishino@sanken.osaka-u.ac.jp

Introduction

Salmonella enterica is a pathogen that causes a variety of diseases in humans ranging from gastroenteritis to bacteremia and typhoid fever. Multidrug-resistant strains of *Salmonella* are now encountered frequently and the rates of multidrug resistance have increased considerably in recent years. Here, we report that the two-component regulatory system BaeSR increases multidrug and metal resistance in *Salmonella* through induction of drug efflux systems.

Results

Screening of random fragments of genomic DNA for ability to increase β -lactam resistance in *Salmonella enterica* led to the isolation of a plasmid containing *baeR*, which codes for the response regulator of BaeSR. When over-expressed, *baeR* significantly increased the resistance of the *AacrB* strain to oxacillin, cloxacillin and nafcillin. *baeR* over-expression conferred resistance to novobiocin and deoxycholate as well as β -lactams in *Salmonella*. The increase in drug resistance caused by *baeR* over-expression was completely suppressed by deletion of the multifunctional outer membrane channel gene *tolC*. TolC interacts with different drug efflux systems. Among the nine drug efflux systems in *Salmonella*, quantitative real-time PCR analysis showed that BaeR induced the expression of *acrD* and *mdtABC*. Double deletion of these two genes completely suppressed BaeR-mediated multidrug resistance, whereas single deletion of either gene did not. The promoter regions of *acrD* and *mdtABC* harbor binding sites for the response regulator BaeR, which activates *acrD* and *mdtABC* transcription in response to indole, copper and zinc. In addition to their role in multidrug resistance, we found that BaeSR, AcrD and MdtABC contribute to copper and zinc resistance in *Salmonella*.

Discussion & Summary

In this study, we performed a genome-wide search for a regulator of multidrug resistance in *S. enterica* serovar Typhimurium by random shotgun cloning and discovered BaeR, which up-regulates the *mdtABCD* locus and *acrD*, thereby increasing resistance to β -lactams, novobiocin and

deoxycholate (Fig. 1). Sequences resembling the BaeR box were found in the region upstream of the *mdt-bae* operon and *acrD*, and an electrophoretic mobility shift assay showed that the BaeR protein binds to these regions. This indicates that the BaeS/BaeR two-component system generates a positive feedback loop by regulating the *mdt-bae* operon. In this study, we found that the MdtABC, AcrD drug efflux systems and the two-component BaeSR signal transduction system contribute to copper and zinc resistance in *Salmonella*. The MdtABC and AcrD systems may be related to bacterial metal homeostasis by transporting metals directly. This is reminiscent of the copper and silver resistance mechanism by cation efflux of the CusABC system belonging to the RND protein superfamily. Our results suggest a previously uncharacterized physiological role for AcrD and MdtABC in metal resistance.

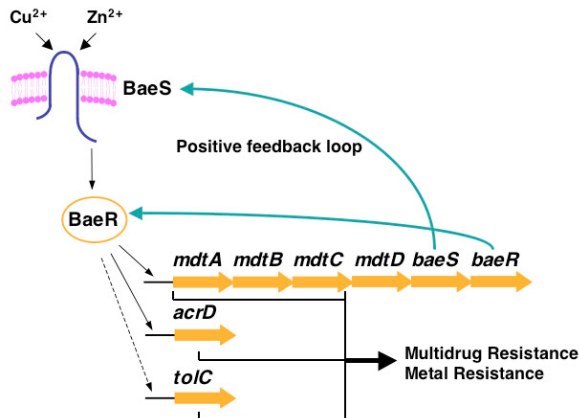


Fig. 1. Model for the control of drug efflux system genes by the two-component BaeS/BaeR regulatory system

References

- Nishino K *et al.* J. Bacteriol. 2007; 189: 9066-9075.
- Nishino K *et al.* J. Infect. Chemother. 2008; 14: 23-29.
- Nishino K *et al.* J. Antibiot. 2008; 61: 120-127.
- Nishino K and Yamauchi A. IUBMB Life 2008; doi: 10.1002/iub.90

1) Biological Sciences
1-7) Plant Biology

Molecular mechanism of the C-to-U RNA editing unique to land plant organelles

Junichi Obokata

Center for Gene Research, Nagoya University
obokata@gene.nagoya-u.ac.jp

Introduction

The chloroplast genome of higher plants contains 20–40 C-to-U RNA editing sites, whose number and locations are diversified among plant species (1,2). Biochemical analyses using *in vitro* RNA editing systems with chloroplast extracts have suggested that there is one-to-one recognition between proteinous site recognition factors and their respective RNA editing sites (3,4,5), but their rigidness and generality are still unsettled. In this study, we addressed this question with the aid of an *in vitro* RNA editing system from tobacco chloroplast extracts and with UV-crosslinking experiments.

Results

The tobacco chloroplast genome is known to have 38 RNA editing sites (Figure 1). In this study, we first examined the RNA editing efficiencies of 36 tobacco editing sites in our *in vitro* RNA editing system from chloroplast extracts, and picked up six editing sites that exhibited relatively high editing efficiency. Next, we carried out UV-crosslinking experiments for these six editing sites using the RNA substrates labeled with ^{32}P , and found that each editing site is bound by specific RNA-binding protein. Among them, proteins specifically binding to the ndhB-9 and ndhF-1 editing sites especially attracted our attention, because their molecular masses appeared to be both 95 kD.

To ensure that the p95s are involved in RNA editing, we examined the correlation between the RNA editing activity and the binding of p95s to their respective RNA editing sites. For this sake, we introduced 5 nt scanning mutations to the –15 to –1 region of the ndhB-9 and ndhF-1 RNA substrates (relative to the editing site as +1), respectively, and then supplemented them to an *in vitro* RNA editing system as competitors. The obtained results showed that RNA editing activity and the binding of p95s to the editing sites were well correlated over the mutations scanning from –15 to –1 for both the ndhB-9 and ndhF-1 editing sites. We also compared the bindings of p95s to the upstream regions (-15 to -1) and to the editing sites (+1). Taken together with these results, we conclude that the p95s are site-specific *trans*-acting factors for the ndhB-9 and ndhF-1 RNA editing sites, and that they are recruited by the upstream *cis*-elements (from –15 to –6) and then interact with the editing

site (+1). However, the relationship between these two p95s that specifically bind to ndhB-9 or ndhF-1 is still unknown.

To clarify whether a given p95 can specifically bind to either or both of the ndhB-9 and ndhF-1 editing sites, we tested the binding specificity of the p95s to these sites by a cross-competition experiment. First, we tested whether the p95 that specifically binds to the ndhB-9 site could also recognize the ndhF-1 site, with the aid of ndhB-9 RNA radiolabeled at +1 as a probe. As was expected, RNA editing activity and the binding of p95 to the ndhB-9 site were both inhibited by the addition of the same RNA as a competitor, but not by the competitors that have mutations on the p95-binding sites. Surprisingly, similar results were obtained when ndhF-1 RNAs were added as competitors: ndhF-1 RNA inhibited both RNA editing and the binding of p95 to the ndhB-9 site, but those with mutations did not. This result indicates that the p95 that specifically binds to the ndhB-9 site can also bind to ndhF-1 in a sequence-specific manner.

Next, we examined the reverse case, using the ndhF-1 RNA as a probe. The obtained results indicate that the p95 that specifically binds to the ndhF-1 site can also recognize the ndhB-9 site.

These complementary results let us conclude that the ndhB-9 and ndhF-1 RNA editing sites are corecognized by the identical *trans*-acting factor, p95.

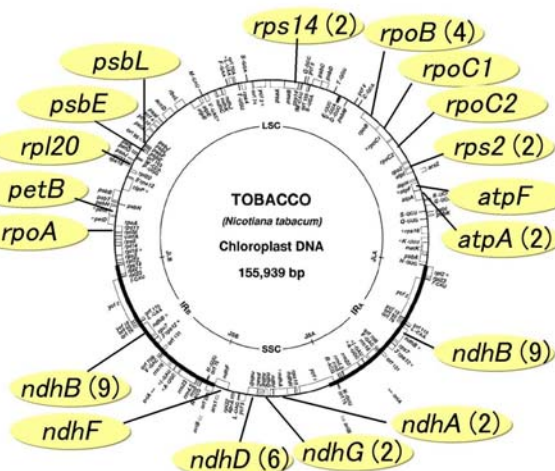


Figure 1. Tobacco chloroplast genome has 38 C-to-U RNA editing sites, which are mapped on the chloroplast DNA map. Names of genes whose transcripts are subjected to RNA editing are indicated, with the number of editing sites shown in parenthesis when indicated gene has more than one editing sites.

Discussion & Summary

This study clearly showed that ndhB-9 and ndhF-1 RNA editing sites of tobacco chloroplasts are both recognized by the identical *trans*-acting factors of 95 kDa. The binding regions of the 95 kDa protein on the ndhB-9 and ndhF-1 transcripts showed 60% identity in nucleotide sequence. This is the first biochemical demonstration that a site recognition factor of plant organellar RNA editing

recognizes plural sites.

On the basis of this finding, we discuss how plant organellar RNA editing sites have diverged during evolution (Figure 2). On condition that preexisting editing sites are recognized by their respective *trans*-acting factors, new T-to-C transitions in the organellar genome are neutral only when their upstream *cis*-sequences are recognized by preexisting *trans*-acting factors, allowing the mutated C to be converted to U at the mRNA level. This study demonstrated that, in the case of *ndhB-9* and *ndhF-1*, 60% sequence identity in the *cis*-region between -15 to -1 is enough for such corecognition to occur. Once such corecognition occurs between preexisting and newborn editing sites, those T-to-C mutations could be stochastically fixed in the organellar genome.

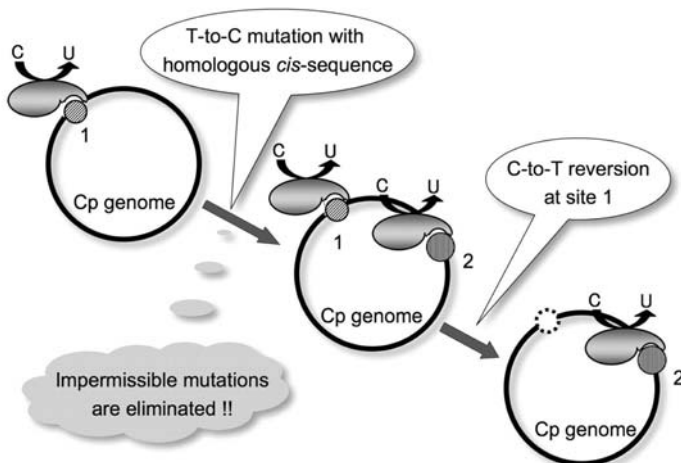


Figure 2. Putative diversification process of chloroplast RNA editing sites during plant evolution. T-to-C transitions are permissible when their upstream sequences are moderately similar to those of preexisting sites.

References

1. Bock, R. (2001) RNA editing in plant mitochondria and chloroplasts. In Bass, B.L. (ed.) *RNA Editing*. Oxford University Press, Oxford, United Kingdom. pp. 38–60
2. Shikanai,T. and Obokata,J. (2008) Machinery of RNA editing in plant organelles. In by Harold C. Smith (ed.) *Frontiers of RNA and DNA Editing*. Wiley Press. pp. 99-119
3. Kotera,E., Tasaka,M. and Shikanai,T. (2005) A pentatricopeptide repeat protein is essential for RNA editing in chloroplasts. *Nature*, 433, 326–330.
4. Miyamoto,T., Obokata,J. and Sugiura,M. (2002) Recognition of RNA editing sites is directed by unique proteins in chloroplasts: biochemical identification of *cis*-acting elements and *trans*-acting factors involved in RNA editing in tobacco and pea chloroplasts. *Mol. Cell. Biol.*, 22, 6726–6734.
5. Miyamoto,T., Obokata,J. and Sugiura,M. (2004) A site-specific factor interacts directly with its cognate RNA editing site in chloroplast transcripts. *Proc. Natl. Acad. Sci. USA*, 101, 48–52.

1) Biological Sciences
1-7) Plant Biology

The Analysis of The SUMO Posttranslational Modification in Plant

Katsunori Tanaka

Department of Bioscience, School of Science and Technology, Kwansei Gakuin University
katsunori@kwansei.ac.jp

Introduction

Small ubiquitin-related modifier (SUMO) modification is a reversible post-translational modification, which is essential for normal cell growth in most organisms. SUMO is expressed as a precursor and is proteolytically processed to expose the C-terminal Gly-Gly motif. Covalently attached SUMO can inhibit or facilitate a protein-protein interaction, as well as inducing the protein conformational change through non-covalent binding with the SUMO interacting motif (SIM) in a target protein. This SUMOylation regulates localization and stability of target proteins, as well as protein-protein interactions, and is involved in multiple cellular processes including cell cycle progression, DNA repair, and transcription.

Results

Diversity of the SUMO post-translational modification system in *Arabidopsis thaliana*

In *Arabidopsis* SUMOs are encoded by a gene family of eight members, AtSUMO1-8. It has been reported that AtSUMO1 and 2 are essential for cell viability, nevertheless, the role of individual SUMO isoforms is still unclear. In order to reveal the possible functional specificity of each SUMO gene, we analyzed their gene expression patterns, the C-terminal processing patterns and the ability of SUMOylation. The result of RT-PCR and the histochemical GUS assay revealed tissue specific expression pattern of each SUMO gene, except for AtSUMO8, whose expression was not detected (Figure). For the C-terminal processing test, AtSUMO1-7 precursors overexpressed and purified from *E. coli* were incubated with plant protein extracts from various organs. The processing of AtSUMO1, 2, and 3 was observed, whereas the other SUMOs were not processed in this system. Furthermore, all the analyzed mature SUMOs, AtSUMO1, 2, 3, 5, 6, and 7, were shown to be able to sumoylate a substrate protein by *in vivo* SUMOylation system in *E. coli*, despite the lack of the C-terminal Gly-Gly motif in AtSUMO4, 6, and 7.

The crosstalk between COP9 signalosome function and SUMOylation

The SUMO gene family in *Arabidopsis* consists of eight members. The relatively large number of

the isoforms comparing to those in other organisms implies the functional specificity of each SUMO gene. In order to test the substrate species of each SUMO molecule, we initially performed the yeast two-hybrid screening for the SUMO target proteins. Through the screening, CSN5a, a subunit of COP9 signalosome, was isolated as an AtSUMO3 interacting protein. CSN5a was shown to bind exclusively to AtSUMO3. Moreover, the mature form of AtSUMO3 with the mutated C terminus was also shown to interact with CSN5a. Since the CSN5a-AtSUMO3 interaction was reproduced in the co-immunoprecipitation experiment using *E. coli*, this interaction was proved to be non-covalent. The identification of the SUMO-interacting motif (SIM) in CSN5a and the SIM-interacting position in AtSUMO3 is currently in progress. Furthermore, we are now investigating the CSN5a-AtSUMO3 interaction in planta.

Discussion & Summary

In this work, we showed that individual SUMO isoforms might acquire their own specific function by the distinctive tissue distribution and the specific processing manner, respectively. Furthermore, we found the possibility of the crosstalk between COP9 signalosome function and SUMOylation. Further analysis will be needed to reveal the crosstalk between Cop9 signalsome function and SUMOylation pathway.

Figures & Tables

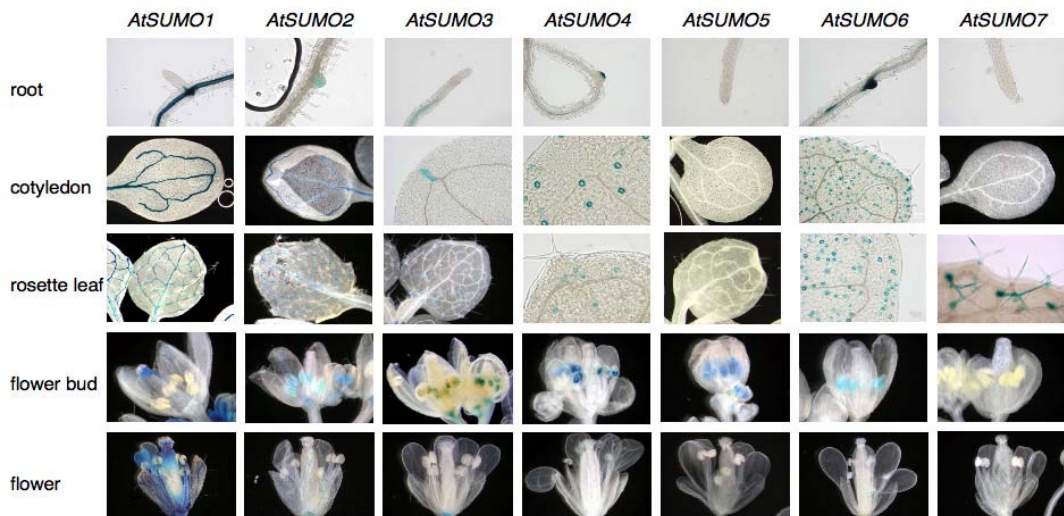


Figure legend:

Gene expression pattern of *AtSUMOs*

AtSUMOs-b-glucuronidase (GUS) reporter genes fusing a 2-kb genomic fragment containing the native *AtSUMOs* promoter to a GUS reporter gene were used to understand the tissue specificities of *AtSUMOs* gene expression.

1) Biological Sciences

1-7) Plant Biology

Jasmonic Acid Signaling and Abscisic Acid Signaling in Guard Cells

Yoshiyuki Murata

Okayama University

muta@cc.okayama-u.ac.jp

Introduction

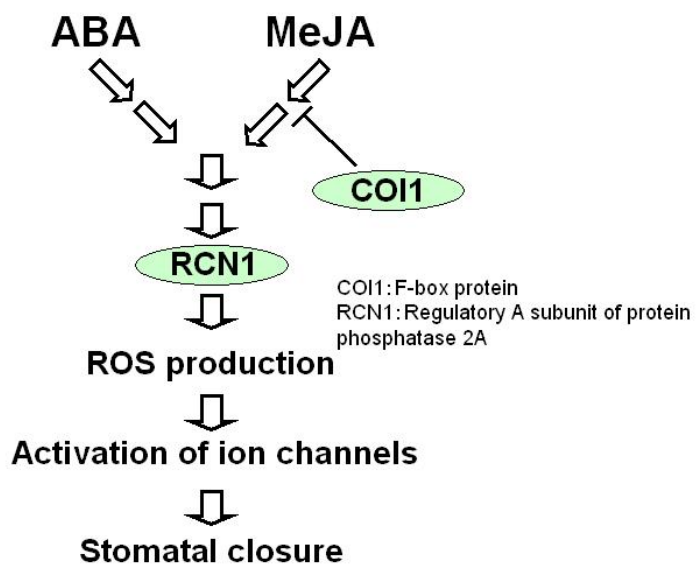
Stomatal pores that are formed by a pair of guard cells respond to various stimuli, including plant hormones and elicitors. Methyl jasmonate (MeJA), which mediates various plant defense responses, has been reported to induce stomatal closure as abscisic acid (ABA). However, MeJA signaling in guard cells remain to be clarified.

Results

MeJA, which belongs to the jasmonate family, elicits stomatal closure as ABA, but MeJA signaling in guard cells remains to be clarified. We investigated roles of MeJA in second messenger production (reactive oxygen species: ROS and nitric oxide: NO) and Ca^{2+} permeable cation channel (IC_a channel) and slow anion channel (S-type anion channel) in *Arabidopsis* guard cells using MeJA-insensitive *Arabidopsis* mutant *coi1*. The *coi1* mutation impaired MeJA-induced stomatal closure but not ABA-induced stomatal closure. MeJA as well as ABA induced the production of ROS and NO in wild-type guard cells whereas MeJA did not induce production of ROS and NO in *coi1* guard cells. The experiments using an inhibitor and scavengers demonstrated that both ROS and NO are involved in MeJA-induced stomatal closing as well as ABA-induced stomatal closing. Not only ABA but also MeJA activated S-type anion channels and IC_a channels in the plasma membrane of wild-type guard cell protoplasts (GCPs). However, in *coi1* GCPs, MeJA did not elicit either S-type anion currents or IC_a currents but ABA activated both types of ion channels. Furthermore in order to elucidate signaling interaction between ABA and MeJA in guard cells, we examined MeJA signaling in ABA-insensitive mutant *abi2-1* whose ABA signal transduction cascade has some disruption downstream of ROS production and NO production. MeJA also did not induce stomatal closing but stimulated production of ROS and NO in *abi2-1*. These results suggest that MeJA triggers stomatal closing via a receptor distinct from the ABA receptor and that the *coi1* mutation disrupts MeJA signaling upstream of the branch point of ABA signaling and MeJA signaling in *Arabidopsis* guard cells.

Discussion & Summary

In summary, MeJA triggers stomatal closing via a receptor distinct from the ABA receptor and that the *coi1* mutation disrupts MeJA signaling upstream of the branch point (Fig. 1). *COI1* encodes one of F-box proteins that function in E3 ubiquitin-ligase complexes, which are involved in the 26S proteasome-mediated protein degradation pathway. In this study, we found that the *coi1* mutation impaired production of second messengers and activation of ion channels induced by MeJA in guard cells, suggesting that the ubiquitin/proteasome pathway could regulate production of second messengers and activation of ion channels in plants.



References

- Munemasa, S., Oda, K., Watanabe-Sugimoto, M., Nakamura, Y., Shimoishi, Y. and **Murata, Y.** (2007) The *coi1* Mutation Reveals the Hormonal Signaling Interaction Between ABA and MeJA in *Arabidopsis* Guard Cells: Specific Impairment of Ion Channel Activation and Second Messenger Production. *Plant Physiol.*, **143**, 1398-1407.

1) Biological Sciences

1-9) Others

Molecular biological analysis of novel hybrid type polyketide synthase from *Dictyostelium*

Tamao Saito

Department of Biological Sciences, Faculty of Science, Hokkaido University

tasaito@sci.hokudai.ac.jp

Introduction

Polyketides are made by polyketide synthases (PKSs) and they can produce an enormous variety of compounds. The structural range of polyketides is being increased by PKS engineering. This type of engineering requires the integration of different domains and modules into a functional whole and is not easily achieved. The discovery of a functional fusion between a type I and a type III PKSs from *Dictyostelium* provides an evolutionary template for integrating these proteins which, if understood, might provide the basis for engineering diverse polyketides. The aim of this work is better understanding of the domain integration in ‘steely’ PKS.

Results

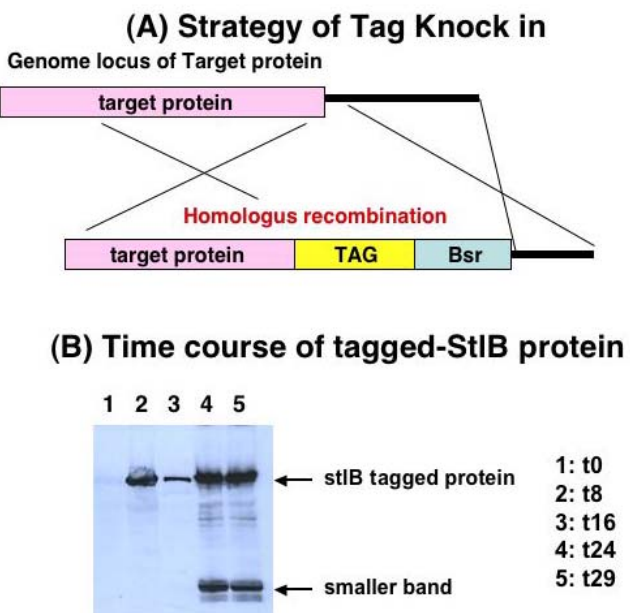
1:Purification and identification of the alternative products (called CCDs) of SteelyB (StlB) polyketide synthase (PKS)

Since the production of CCDs in widely used strain Ax2 was not so good than I expected, I needed to find other strain that can be a good CCDs producer. The work with equilibrium ^{36}Cl - labelling showed that the CCDs are very abundant in fruiting bodies in the different strain, V12M2 – more than 0.1 mM in stalk cells – are stable and can be highly purified by two steps of reverse phase HPLC, using ^{36}Cl radioactivity to track their elution position. I have optimized production and extraction conditions from fruiting bodies of V12M2, and plan to purify these compounds on a milligram scale. I’m expecting to do the MS spectrometry analysis in the near future with purified compounds.

2: Structural and Functional analysis of SteelyB enzyme

One key strategic decision is to base most of the work on *Dictyostelium* cells(Fig.A). There is no doubt that expression of StlB would be much easier in bacteria, if it could be achieved and gave a functional product, but I think my route is preferable because as far as I know, it is difficult to express whole enzyme in bacteria (Dr J. Noel personal communication). I have found that StlB can be C-terminally tagged to yield a fully active protein in *Dictyostelium* cells, and this was confirmed

by Cl labeling and also the phenotypic features of tag knocked-in mutants. This means that the inserted tag didn't interfere the activity of the StlB enzyme. Then I did pull-down experiment with tag that was inserted in the genome locus of *stlB* gene (Fig. A). The fusion protein retains full activity *in vitro* after affinity purification. I reconstituted the full activity of pulled down StlB protein with acetyl Co-A, malonyl Co-A and NADPH in the test tube and confirmed that this protein gave the right product (DIF-1 precursor) by TLC. At first it was difficult to reconstitute the activity and I got several products with pulled down StlB protein. Finally I found out that (perhaps) N-terminal proteolysis of the StlB protein occurred during purification steps and that caused the imperfect reconstitution of enzyme activity. The combination of strong protease inhibitors and reducing agent solved this problem. I also examined the time course of the tagged protein and found that the expression pattern was quite similar with the result by RT-PCR. Surprisingly, I found the smaller band in SDS-gel, that still has C-terminal tag, in the fruiting body stage when the product switch could be seen (Fig. B). The production of this smaller band depends on DIF-1 and it seems that they accumulate in stalk but not in spore cells.



Discussion & Summary

- Summary: For purification and identification of alternative products (CCDs) of StlB PKS, I found other strain, V12M2, is suitable producer. By the use of this stain, I optimized the conditions for purification. I created a *Dictyostelium* strain expressing TAP-tagged StlB from the endogenous locus. And I asked if these mutants can make DIF-1 and the CCDs by *in vivo* labelling with ^{36}Cl . I also examined the *in vitro* reconstitution of StlB from *Dictyostelium* slug-stage lysates, where DIF-1 is made and found full activity in the test tube.

2. Discussion: It is commonly said that the reconstitution experiment of the PKS enzyme activity is not easy. But by the combination of protease inhibitors and strong reducing agent solved this problem. I think it was a big step for this work. The appearance of smaller StlB protein (possibly by proteolysis) in the fruiting body stage is interesting because at this stage, the product-switch seemed to occur. In order to find out the relationship between these two events, I plan to pull down the StlB protein from slug stage and fruiting body stage and see the activity. The problem is the stalk cells are difficult to destroy and therefore it is difficult to pull down the StlB protein with reasonable yield. I plan to use detergent and/or other stain that has weaker stalk to solve this problem.

2) Medical Sciences
 2-1) Immune System

Molecular mechanism of immunological tolerance by cytokines

Akihiko Yoshimura

Medical Institute of Bioregulation, Kyushu University

yakihi@bioreg.kyushu-u.ac.jp

Introduction

Dendritic cells (DCs) induce immunity and immunological tolerance as antigen presenting cells. It has been shown that DCs secreting interleukin (IL)-10 induce IL-10⁺Tr1 type regulatory T cells, while Foxp3-positive regulatory T cells (Tregs) are expanded from native CD4⁺T cells by co-culturing with mature DCs. However, the regulatory mechanism of expansion of Foxp3⁺Tregs by DCs has not been clarified. Suppressor of cytokine signaling (SOCS) proteins regulate the strength of cytokine signals(1). Among these, SOCS3 is strongly induced by a variety of cytokines and other stimulators, including IL-6. In this study, we investigate the role of SOCS3 in dendritic cells by using SOCS3-deficient bone marrow-derived DCs (BMDCs).

Results

SOCS3-deficient mice die during embryonic development as a result of placental deficiency. Thus, to delete the SOCS3 gene in BMDCs, SOCS3-flo/flo mice were crossed with either Tie2-Cre mice or Lysozyme M (LysM)-Cre mice. SOCS3 gene has been deleted in all hematopoietic linages and monocytes/neutrophils, respectively. The SOCS3 gene was efficiently deleted in BMDCs from these mice. LPS upregulates class II MHC (I-A^b), CD40, co-stimulators (CD80 and CD86) and induces inflammatory cytokines, such as IFNg, IL-12 and IL-6 in wild type (SOCS3^{+/+}) DCs. However, SOCS3^{-/-}DCs expressed lower levels of class II MHC, CD40, CD86 and IL-12 than wild type (WT-) DCs, and showed constitutive activation of Signal transducer and activators of transcription-3 (STAT3)(2).

Allogeneic CD4⁺T cells were incubated with WT or SOCS3^{-/-}DCs for 4 days, then the same number of T cells was restimulated with anti-CD3 antibody. Anti-CD3 antibody-mediated proliferation of T cells expanded by SOCS3^{-/-}DCs was severely inhibited compared with after co-culture with WT-DCs, suggesting that T cells expanded by SOCS3^{-/-}DCs were anergic. Importantly, Foxp3⁻ effector T cells were predominantly expanded by the priming with WT-DCs, while Foxp3⁺Tregs were selectively expanded by SOCS3^{-/-}DCs. Approximately 50-70% of CD25⁺ T cells became Foxp3-positive after priming with SOCS3^{-/-}DCs, while Foxp3 positive CD25⁺T

cells were around 20-30% after priming with WT-DCs (Figure 1). We confirmed that T cells expanded by SOCS3-deficient DCs had suppression activity against naïve T cells. IL-10-DCs also hardly induced expansion of CD25⁺Foxp3⁻ effector T cells, however, CD25⁺Foxp3⁺T cells was not expanded by IL-10-DCs. Thus, SOCS3^{-/-}-DC was apparently different from IL-10-DC, and preferentially induced expansion of Foxp3⁺T cells.

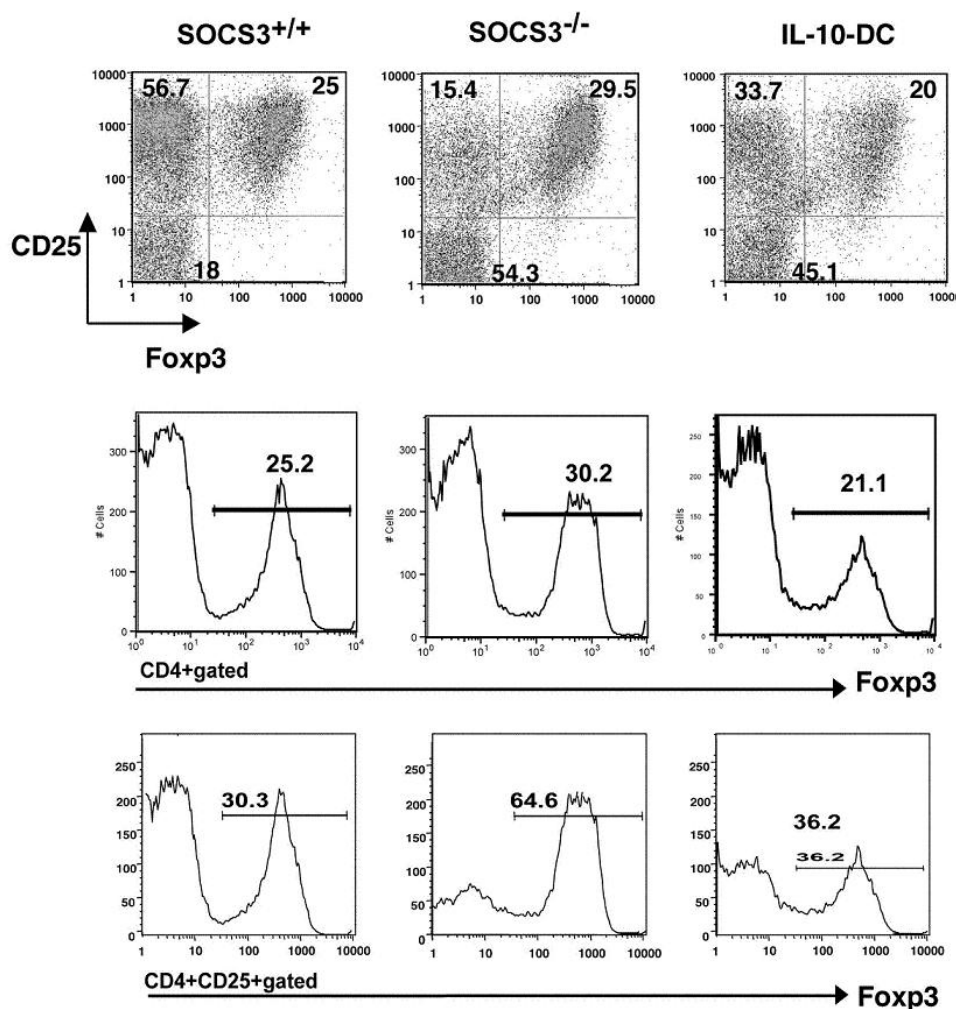


Figure 1. Predominant induction of Foxp3⁺ regulatory T cells primed by SOCS3^{-/-}-DCs. To generate IL-10-DCs, WT-BMDMs were cultured in the presence of IL-10 for 48h, then stimulated with LPS. CD4+T cells from BALB/c mice were co-cultured with SOCS3^{+/+}, SOCS3^{-/-}-DCs or IL-10-DCs for 4 days, then stained with anti-CD4, anti-CD25, and anti-Foxp3 antibodies. CD4+-gated cell populations are shown in upper panels. Foxp3-expression profiles gated on CD4+CD25+ cells or CD4+ are shown below.

Next, to assess the initiation of T cell responses *in vivo*, SOCS3^{+/+} and SOCS3^{-/-} DCs were pulsed with KLH and then injected into each footpad of the same mouse. Swelling of the popliteal lymph nodes (LNs) was observed on the side of the SOCS3^{+/+}DC-injected footpad, but little LN swelling was observed on the side of the SOCS3^{-/-}DC-injected footpad five days after injection. KLH-induced IFNg production from LN cells was lower in SOCS3^{-/-}DC-injected mice than WT-DC-injected mice, suggesting that SOCS3^{-/-}DC is less immunogenic than WT-DC.

To confirm a tolerogenic nature of SOCS3^{-/-}DCs *in vivo*, we performed adoptive transfer experiments. Then we investigated the *in vivo* immunnosuppressive effect of SOCS3^{-/-}DCs on experimental autoimmune encephalomyelitis (EAE). MOG-peptide-pulsed DCs were intravenously injected prior to immunization of the mice. Control mice receiving SOCS3^{+/+}DCs (WT-DCs) as well as untreated mice exhibited characteristic signs of EAE starting on day 8. In contrast, mice receiving SOCS3^{-/-}DCs developed significantly less severe EAE, indicating that SOCS3^{-/-}DC is immunosuppressive *in vivo* (Figure 2). These data indicate that SOCS3-deficeint DCs are tolerogenic rather than immunogenic.

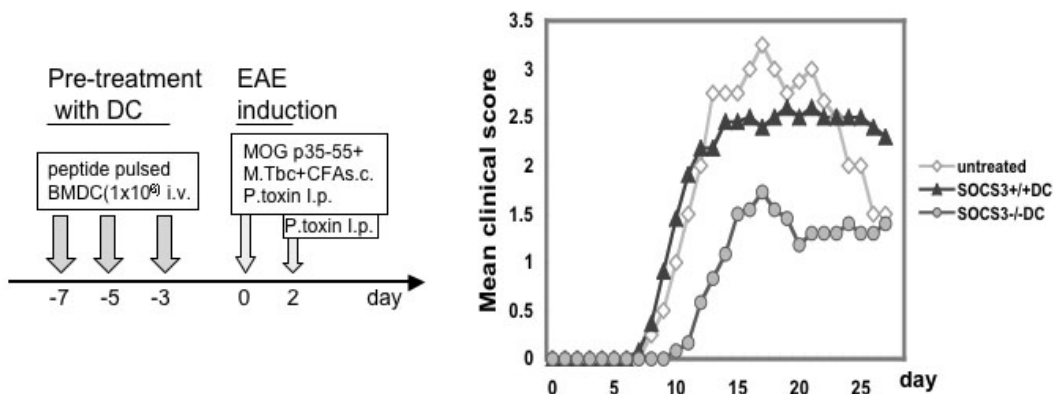


FIGURE 2. Tolerogenic nature of SOCS3-deficient DCs *in vivo*. EAE was induced in C57BL/6 mice (n=8-12 for each group) with MOG peptide and CFA, and DCs (1×10^6) were administrated 7, 5, and 3 days before peptide/CFA immunization. Asterisks indicate significant differences ($p < 0.05$) compared with SOCS3^{+/+}DCs using Mann-Whitney U test.

To define the molecular basis for Foxp3⁺Treg induction by SOCS3^{-/-}DCs, we examined the effect of antibodies against cytokines. Foxp3⁺T cell expansion was blocked by anti-TGF-beta antibody. Therefore we measured production of biologically active TGF-beta by using a reporter cell line, MFB-F11. SOCS3^{-/-}DCs produced higher levels of TGF-beta than WT-DCs. Upregulation of TGF-beta in SOCS3^{-/-}DCs was confirmed by RT-PCR. These data suggest that higher expression of TGF-beta in SOCS3^{-/-}DCs is one of an important mechanism for enhanced Foxp3⁺T cell expansion by SOCS3^{-/-} DCs.

Discussion & Summary

DCs have an important role in the control of the adaptive immune response. They simultaneously induce not only antigen specific effector T cells but also regulatory T cells. Here we demonstrated that suppressors of cytokine signaling (SOCS)-3 deficient DCs have a strong potential as Foxp3⁺T cell-inducing tolerogenic DCs. SOCS3^{-/-}DCs predominantly induce Foxp3⁺T cells and poorly induce Foxp3⁻ effector T cells. Probably, both the immature phenotype of DCs and the high levels of TGF-β1 are necessary for the predominant expansion of Foxp3⁺Tregs by SOCS3^{-/-}DCs. Our data indicate that the regulation of intracellular signaling pathways is extremely important for the decision of helper T cell fates. Our study also suggest an important role of SOCS3 in determining on immunity or tolerance by DCs

References

- (1) Yoshimura A, Naka T, Kubo M.
SOCS proteins, cytokine signalling and immune regulation.
Nat Rev Immunol. 2007 Jun;7(6):454-65
- (2) Matsumura Y, Kobayashi T, Ichiyama K, Yoshida R, Hashimoto M, Takimoto T, Tanaka K, Chinen T, Shichita T, Wyss-Coray T, Sato K, Yoshimura A.
Selective expansion of foxp3-positive regulatory T cells and immunosuppression by suppressors of cytokine signaling 3-deficient dendritic cells.
J Immunol. 2007 Aug 15;179(4):2170-9.

2) Medical Sciences
2-1) Immune System

Investigation on the role of CD100 in differentiation of Th17 cells

Atsushi Kumanogoh

Research Institute for Microbial Diseases, Osaka Univ.

kumanogo@ragtime.biken.osaka-u.ac.jp

Introduction

Semaphorins have been identified as axon guidance factors during neuronal development. Recently, it is emerging that several members of semaphorins are crucially involved in a variety of pathological immune responses. In particular, class IV semaphorins, Sema4D (CD100) and Sema4A have been shown to be implicated in pathogenesis by regulating helper T-cell differentiation. We here found recently that Sema4D is relevant to Th17-differentiation and Sema4D-deficient mice are resistant to development of experimental autoimmune encephalomyelitis. In addition, we present evidence that a class IV semaphorin Sema4A, an activator for T cell-mediated immunity, plays a key role in the progression of autoimmune myocarditis in which abnormal functions of Th17 are suggested. I here focus on the role of Sema4A in development of autoimmune myocarditis.

Results

Experimental autoimmune myocarditis can be induced by bone marrow derived dendritic cells (DCs) which are pulsed with a peptide derived from myosin heavy chain (MYHC). Here, we pulsed bone marrow-derived DCs with MYHC-derived peptides. The resulting DCs were then activated with LPS plus stimulatory antibodies to CD40 and then injected into BALB/c wild type (WT) mice or Sema4A-deficient mice. Myocarditis was scored at 10 days after first DC injection based on hematoxylin and eosin-stained sections of heart using grades from 0 to 4: 0, no inflammatory infiltrated; 1, small foci of inflammatory cells between myocytes; 2, larger foci of >100 inflammatory cells; 3, >10% of a cross section involved; 4, >30% of a cross section involved. As a result, WT recipient mice developed severe myocarditis, while Sema4A-deficient recipient mice were resistant to myocarditis. (Prevalence 100% v.s. 62%, Mean clinical score 3.55 v.s. 1.24; WT mice v.s. Sema4A-deficient mice) (Figure 1). The number of infiltrated

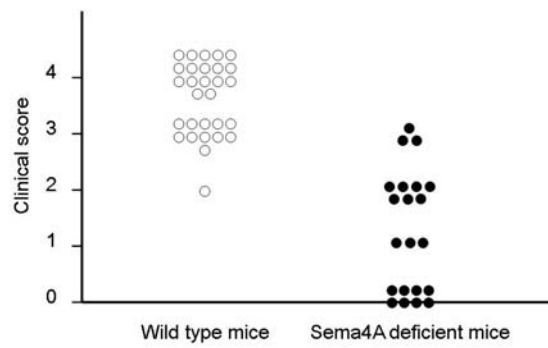


Figure 1

inflammatory cells, consisting of granulocytes and mononuclear cells, into the heart of WT recipient mice, was larger than that of Sema4A-deficient mice. CD4+ T cells prepared from the spleen of the Sema4A-deficient recipient mice produced less IL-17 but high amount of IL-4 and IL-10 compared to those from WT recipient mice. To investigate whether the abnormal differentiation of helper T cells was responsible for the resistance of myocarditis in Sema4A-deficient mice, we performed adoptive T cell transfer to severe combined immunodeficiency (SCID) mice. Splenocytes from immunized WT or Sema4A-deficient mice were re-stimulated in vitro for 72 h with MYHC-derived peptides and anti-CD28 antibodies. The resulting CD4+ T cells were purified and injected intraperitoneally into recipient SCID mice. CD4+ T cells from WT mice induced severe myocarditis. By contrast, CD4+ T cells from Sema4A-deficient mice could not induce myocarditis. Our results indicated that Sema4A is crucially involved in the progression of autoimmune myocarditis, regulating differentiation of CD4+ helper T cells.

Discussion & Summary

We have previously reported that Sema4A-deficient mice exhibited defective in vivo Th1 responses but rather enhanced in vivo Th2 responses. Similarly, we here found that CD4+ T cells from Sema4A-deficient mice immunized with MYHC-derived peptides exhibited enhanced production of Th2 cytokine, such as IL-4 and IL-10. Of note, Sema4A-deficient T-cells displayed impaired IL-17-production as it was found in Sema4D/CD100-deficient T-cells. This findings strongly suggest that class IV semaphorins are crucially relevant to helper T cell differentiation, including Th17. Our findings provide a novel therapeutic target for autoimmune disorders including myocarditis and dilated cardiomyopathy.

References

- Suzuki K, **Kumanogoh A**, Kikutani H. Semaphorins and their receptors in immune cell interactions. *Nat Immunol*. 9:17, 2008.

2) Medical Sciences
 2-1) Immune System

Mechanisms for Regulation of Inflammatory Responses via Inducible Transcriptional Regulatory Factors

Tatsushi Muta
 Tohoku University
 tmuta@biology.tohoku.ac.jp

Introduction

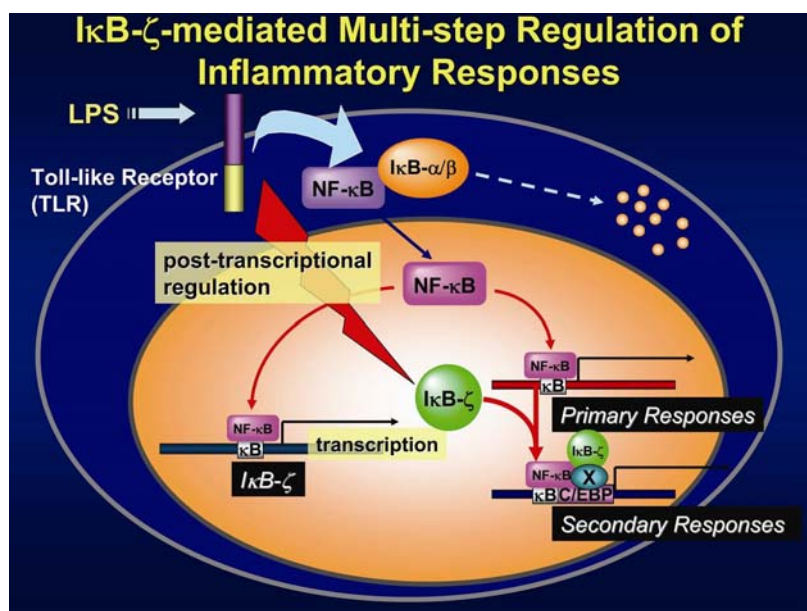
I κ B- ζ is a nuclear protein induced by various microbial components that stimulate the innate immune system. Our previous studies have revealed that I κ B- ζ is a critical regulator of inflammation, which plays an essential role for induction of secondary response genes such as interleukin (IL)-1 β and IL-12 and inhibits transcription of primary response genes represented by tumor necrosis factor (TNF)- α .

Results

In the present study, we analyzed mechanisms for the I κ B- ζ -mediated transcriptional activation. We found that both nuclear factor (NF)- κ B binding sites and CCAAT/enhancer-binding Protein (C/EBP) binding sites of the promoters of the human β -defensin 2 and neutrophil gelatinase-associated lipocalin genes were essential for the activation of I κ B- ζ -mediated transcriptional. On the other hand, I κ B- ζ inhibited transcription on a promoter harboring canonical NF- κ B binding sites. We further showed that I κ B- ζ induced on stimuli formed a complex with NF- κ B and the complex was recruited to the promoter containing NF- κ B and C/EBP binding sites. All of the NF- κ B p65 and p50 subunits and I κ B- ζ were essential for the transcriptional activation. Thus, it was strongly suggested that I κ B- ζ forms a stable transcriptional complex on the target genes by modifying the target sequences of NF- κ B via a conformation change of its DNA binding site. Expression of I κ B- ζ is induced by LPS and IL-1 β but not by another inflammatory cytokine TNF- α . We have shown previously that I κ B- ζ mRNA is specifically stabilized in response to LPS/IL-1 β . We analyzed here the post-transcriptional regulation mechanisms essential for the I κ B- ζ induction and found that a 165-nucleotide element in the 3'-untranslated region of I κ B- ζ mRNA is essential and sufficient for the post-transcriptional regulation that confers stimulus-specific induction of I κ B- ζ . Moreover, we found that I κ B- ζ is induced upon stimulation of B cell antigen receptor and that the induction was inhibited by co-crosslinking the inhibitory Fc receptor. It was, therefore, strongly suggested that I κ B- ζ also plays a critical role in the acquired immune system.

Discussion & Summary

It had been believed that in the inflammatory responses, an autonomously-controlled gene expression program is initiated by transcription factors such as NF- κ B and activator protein (AP)-1, which are rapidly activated upon stimulation. However, present study has shown that stimulus-specific inductions of genes are regulated by an inducible transcriptional regulator(s), which alters activity and targets of the transcription factor that controls the induction of primary response genes (Figure).



References

- Hijioka, K., Matsuo, S., Kimura-Eto, A., Takeshige, K., and Muta, T. (2007):
Induction of the Nuclear IκB Protein IκB-ζ upon Stimulation of B cell Antigen Receptor.
Biochem. Biophys. Res. Commun. 356 (2), 476-480.
- Watanabe, S., Takeshige, K., and Muta, T. (2007):
A Cis-element in the 3'-untranslated Region of IκB-ζ mRNA Governs its Stimulus-specific Expression. *Biochem. Biophys. Res. Commun.* 356 (3), 785-791.
- Matsuo, S., Yamazaki, S., Takeshige, K., and Muta, T. (2007):
Crucial Roles of Binding Sites for Nuclear Factor-κB (NF-κB) and CCAAT/enhancer-binding Proteins (C/EBPs) in IκB-ζ-mediated Transcriptional Activation. *Biochem. J.* 405 (3), 605-615.

2) Medical Sciences
 2-2) Central Nervous System

Analysis of genes specifically expressed in primate neocortical areas

Tetsuo Yamamori

National Institute for Basic Biology

yamamori@nibb.ac.jp

Introduction

The neocortex that is commonly observed in mammals and consists of six layer structure can be divided into so-called areas, which are distinguished by cyto architectonic and functions such as visual, auditory and motor areas etc. Our project has been to identify genes that are specifically expressed in particular areas in the primate neocortex to understand the molecular mechanisms underlying function and formation of neocortical areas.

Results

We aimed to isolate genes that are specifically expressed in particular areas of primate neocortex. In our first attempt to isolate such genes, we used differential display (DD) method and find a gene specifically expressed in the visual cortex (*occ1*). *occ1* expression is activity dependent and the visual area specificity is primate specific.. Another gene that shows association area specific expression is *RBP* (retinol binding protein) whose expression pattern is complementary to that of *occ1*.

In order to further analyze the significance of such gene expression patterns, we attempted a large scale screening the genes that are specifically expressed in primate neocortical areas using RLCS (restriction landmark cDNA scanning). We obtained several genes that showed significant area differences (more than five fold) among frontal, motor, temporal and primary visual areas.

We are currently examining the detailed expression pattern of each of the genes that shows significant area differences.

One of such genes, RLCS15, shows very similar properties of *occ1* expression in that it shows specific expression in the primary visual cortex but not in other mammals such as ferrets, rabbits and mice in an activity dependent manner.

Another gene, RLCS16, shows very similar expression pattern to that of *RBP* in that it is preferentially expressed in excitatory neurons in association areas of primate but not such a specific expression is observed in other mammals.

Discussion & Summary

Our study on the genes specifically expressed in the primate neocortex revealed that there are few genes that show marked difference among the neocortical areas. The overall percentage that shows such remarkable area difference among the entire genes is small, but can be divided into two groups: one group of genes is expressed in the primary sensory cortex, particularly in the primary visual cortex. The other group of genes is expressed in association areas. Since these two areas are particularly evolved during the course of primate evolution, we think that the distinguished area-specific expression of the two groups of the genes probably reflect such evolitional events in the primate neocortex. Therefore, studies of such genes will tell us how the primate brain and what is the specific features of such evolution.

Figures & Tables

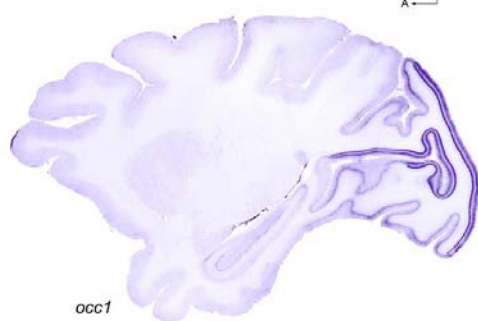
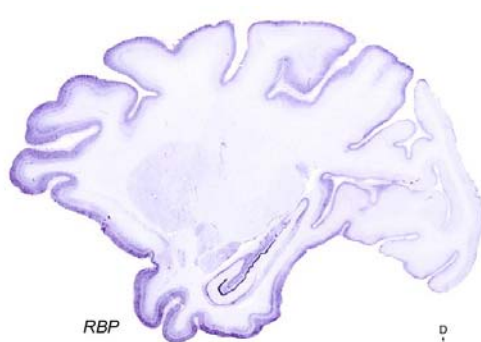


Figure 1

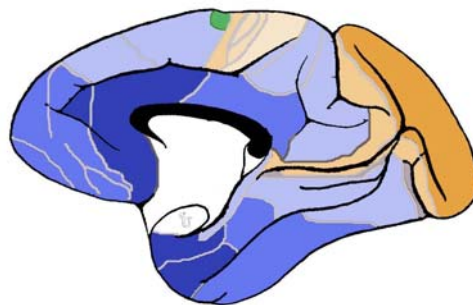
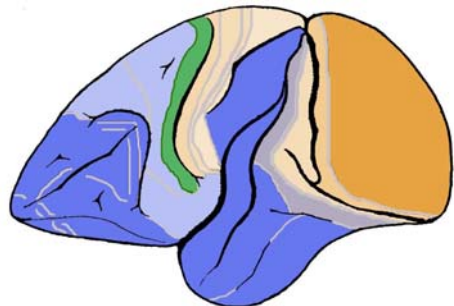


Figure 2

References

- Takahata T, Hashikawa T, Higo N, Tochitani S, Yamamori T. (2008) Difference in sensory dependence of occ1/Follistatin-related protein expression between macaques and mice. *J Chem Neuroanat.* 35, 146-157.
- Watakabe A, Ichinohe N, Ohsawa S, Hashikawa T, Komatsu Y, Rockland KS, Yamamori T. (2007) Comparative Analysis of Layer-Specific Genes in Mammalian Neocortex. *Cereb Cortex.* 17, 1918-1933.

2) Medical Sciences

2-5) Cardiovascular/Metabolic/Endocrine

Analysis of the molecular mechanisms of the development of non-alcoholic steatohepatitis (NASH)

Terauchi Yasuo

Department of Endocrinology and Metabolism, Yokohama City University Graduate School of Medicine
terauchi@yokohama-cu.ac.jp

Introduction

Nonalcoholic fatty liver disease (NAFLD) is the most common cause of chronic liver injury. The spectrum of NAFLD is broad, extending from simple steatosis through nonalcoholic steatohepatitis (NASH). Insulin resistance has been found to increase the risk of NASH, and obesity, and decreased levels of adiponectin are important factors in determining the severity of insulin resistance. We investigated the role of adiponectin and insulin resistance on the development of NASH.

Results

1. Impact of adiponectin and insulin resistance on the development of NASH in human subjects

We measured the plasma adiponectin and high-sensitive CRP (hs-CRP) concentrations, hepatic fat content based on the liver-to-spleen ratio (L/S ratio) according to computed tomography (CT) attenuation values, and the amount of visceral adipose tissue and subcutaneous adipose tissue by CT. Significant correlations were observed between the L/S ratios and aspartate aminotransferase, alanine aminotransferase, visceral adipose tissue, subcutaneous adipose tissue, and serum adiponectin values, and there was a highly significant inverse correlation between the visceral adipose tissue values and the serum adiponectin levels. There was a stepwise decrease in the serum adiponectin in parallel to the severity of hepatic fibrosis. As compared to that in cases with simple steatosis, hs-CRP was significantly elevated in cases of NASH. Furthermore, among the patients with NASH, hs-CRP was significantly elevated in cases with advanced fibrosis as compared with that in cases with mild fibrosis.

Serum gamma-glutamyltransferase (GGT) was significantly associated with the waist circumference, the waist/hip ratio and metabolic syndrome, however, it is still unknown whether the serum GGT is specifically associated with visceral or subcutaneous fat accumulation. We here investigated the association between the serum level of GGT and parameters of adiposity and lipid profile, including the serum triglyceride (TG), HDL-cholesterol (HDL-C) and LDL-cholesterol

(LDL-C) levels in Japanese patients with type 2 diabetes mellitus and non-diabetic subjects. Serum GGT was significantly correlated with the waist circumference, BMI, visceral fat area (VFA), L/S ratio and TG, but not with the subcutaneous fat area (SFA). The serum GGT was still correlated with the VFA and TG, but not with the SFA, after adjustment for the four variables of age, gender, serum HbA1c and the L/S ratio. Thus, serum GGT was specifically associated with the VFA, but not with the SFA.

2. Generation and analyses of IRS-2, adiponectin double knockout mice

We generated IRS-2, adiponectin double knockout mice by crossing adiponectin-knockout mice and IRS-2-knockout mice. The double knockout mice developed steatosis associated with fibrosis compared with wild-type mice on the same genetic background. As we have already demonstrated that telmisartan, an angiotensin II type 1 receptor blocker, controls progress of nonalcoholic steatohepatitis in rats, we will investigate the effect of ARB on the prevention from fat accumulation and fibrosis in the double-knockout mice.

3. Impact of inhibition of cholesterol absorption on the glucose and lipid metabolism in liver

On a high-fat diet, ezetimibe, a selective cholesterol absorption inhibitor, significantly lowered LDL-cholesterol, TG, cholesterol content in VLDL, TG content in VLDL, GGT and liver weight, significantly strengthened hypoglycemic effect of insulin during insulin tolerance test, and gave tendency of triglyceride content in liver to decrease with no significant changes in body weight and visceral fat accumulation. Euglycemic hyperinsulinemic clamp revealed that administration of ezetimibe improved glucose infusion rate and endogenous glucose production by liver, but not peripheral insulin sensitivity. Thus, ezetimibe improved dyslipidemia, hepatic steatosis and hepatic insulin resistance in high-fat diet-induced obese mice.

4. Effect of high-fat diet loading for 40 weeks on the development of NASH in mice

Histological analysis revealed that mice after 40 weeks on the high-fat diet developed fat droplet formation in the liver. Steatosis: any degree, mixed macro- and microvesicular, Ballooning: obvious and present in zone 3.

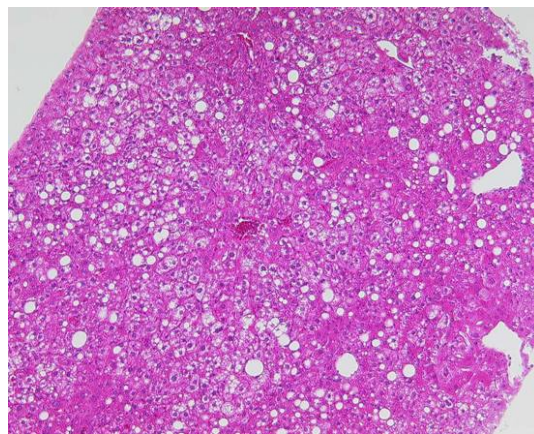
Discussion & Summary

We investigated the role of adiponectin and insulin resistance on the development of NASH in human subjects as well as mouse models. Increased insulin resistance and decreased levels of adiponectin and hs-CRP were important factors in determining the development of NASH and its severity. Serum GGT was specifically associated with the VFA, but not with the SFA, suggesting that the serum GGT may be useful as a convenient indicator of VFA in the clinical treatment of

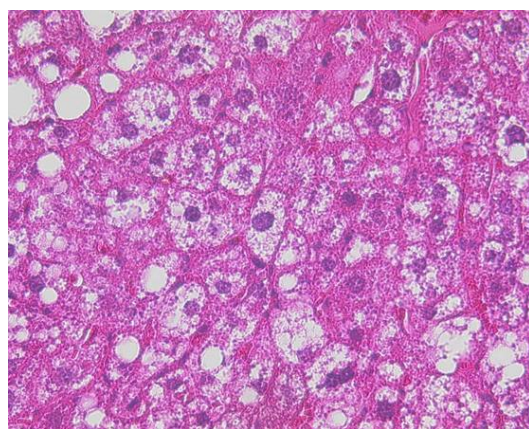
obesity. Ezetimibe improved dyslipidemia, hepatic steatosis and hepatic insulin resistance in high-fat diet-induced obese mice. Ezetimibe improved dyslipidemia, hepatic steatosis and hepatic insulin resistance in high-fat diet-induced obese mice. These results suggest a preferential effect of ezetimibe on liver steatosis in obese patients with dyslipidemia who favor high-fat diet.

Figures & Tables

Histological analysis of the liver derived from mice after 40 weeks on the high-fat diet



HE staining (x100)



HE staining (x400)

Steatosis: any degree, mixed macro- and microvesicular
Ballooning: obvious and present in zone 3

References

- Yoneda M, et al : Hypoadiponectinemia plays a crucial role in the development of nonalcoholic fatty liver disease (NAFLD) in patients with type 2 diabetes mellitus independently of visceral adipose tissue.
Alcohol Clin. Exp. Res. 31 (Suppl 1) : S15-S21, 2007.
- Yoneda M, et al: High-sensitivity C-reactive protein is an independent clinical feature of nonalcoholic steatohepatitis (NASH) and also of the severity of fibrosis in NASH.
J. Gastroenterol. 42 : 573-582, 2007.
- Iwasaki T, et al : Serum butyrylcholinesterase is strongly associated with adiposity, serum lipid profile, and insulin resistance.
Intern. Med. 46 : 1633-1639, 2007.
- Fujita K, et al : Telmisartan, an angiotensin II type 1 receptor blocker, controls progress of nonalcoholic steatohepatitis in rats.
Dig Dis Sci. 52 : 3455-3464, 2007.

2) Medical Sciences

2-5) Cardiovascular/Metabolic/Endocrine

Global functional analysis of microRNAs in cardiomyocyte differentiation

Jun K. Yamashita

Institute for Frontier Medical Sciences, Kyoto University

juny@frontier.kyoto-u.ac.jp

Introduction

Previously we have succeeded in generating a novel embryonic stem (ES) cell differentiation system that can reproduce the early process of cardiovascular cell differentiation and development in vitro. In the present study, to elucidate molecular mechanisms of cardiomyocyte differentiation, especially concerning the roles of microRNAs, we tried to examine global functional analysis of microRNAs during cardiomyocyte differentiation using our ES cell differentiation system.

Results

First, to prepare various cardiomyocyte populations for microRNA sources, we tried to induce various cardiomyocyte cell types, especially cardiac pacemaker cells and ventricular myocytes from mouse ES cells. We induced Flk1, a vascular endothelial growth factor receptor and a marker for lateral plate mesoderm cells, from undifferentiated ES cells. When Flk1⁺ cells were purified by fluorescent activated cell sorting (FACS) and re-cultured on OP9 mouse bone marrow-derived stroma cells, self-beating cardiomyocytes were successfully induced on 2-dimensional culture condition. These cardiomyocytes were induced as a mixture of various kinds of cardiomyocytes including pacemaker cells and ventricular cells. We evaluated ion channels that were responsible for the automaticity of cardiac pacemaker cells induced from ES cells, and found that hyperpolarization-activated, cyclic nucleotide-gated (HCN) channels (HCN1, 4) and T-type calcium channels (Cav3.1, 3.2) conferred pacemaker properties (Yanagi, Stem Cells, 2007). That is, Spontaneously beating colonies observed at day 9.5 of Flk1⁺ cell culture (Flk-d9.5) were significantly decreased at Flk-d23.5. Expressions of ion channels in pacemaker cells, HCN1, 4 and Cav3.1, 3.2 were significantly decreased in purified cardiomyocytes at Flk-d23.5 compared to at Flk-d9.5, whereas expression of an atrial and ventricular ion channel, Kir2.1, did not change. Blockade of HCNs and Cav ion channels significantly inhibited beating rates of cardiomyocyte colonies. Electrophysiological studies demonstrated that spontaneously beating cardiomyocytes at Flk-d9.5 showed almost similar features with those of the native mouse sino-atrial node except

relatively deep maximal diastolic potential and faster maximal upstroke velocity. Though ~60 % of myocytes at Flk-d23.5 revealed almost the same properties with those at Flk-d9.5, ~40 % myocytes showed loss of HCN and decreased Cav3 currents, and ceased spontaneous beating, with no remarkable increase of Kir2.1. Thus, HCN and Cav3 ion channels should be responsible for the maintenance of automaticity in ES cell-derived cardiomyocytes. Currently, we are examining specific induction and purification of cardiac pacemaker and ventricular cells.

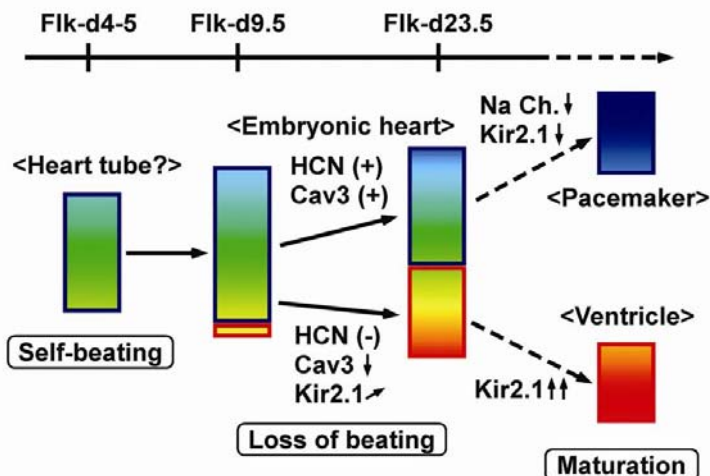
Recently, novel pluripotent stem cells were invented from mouse and human skin tissues, named induced pluripotent stem (iPS) cells (Takahashi, Cell, 2006; 2007). We applied our ES cell system to iPS cells and examined directional differentiation of mouse iPS cells to cardiovascular cells. Flk1⁺ mesoderm cells were induced from iPS cells after approximately 4days culture for differentiation. Purified Flk1⁺ cells gave rise to endothelial cells (ECs) and mural cells by addition of VEGF. Arterial, venous, and lymphatic ECs were also successfully induced. Self-beating cardiomyocytes could be induced from Flk1⁺ cells by cultured on OP9 stroma cells. Time course and efficiency of the differentiation are all comparable with those of mouse ES cells. Occasionally, re-expression of transgene mRNAs including c-myc was observed in long-term differentiation cultures. Currently, we are preparing microRNA sources of various cardiomyocytes and generating expression profiles of microRNAs during cardiomyocyte differentiation using both mouse ES and iPS cells.

Discussion & Summary

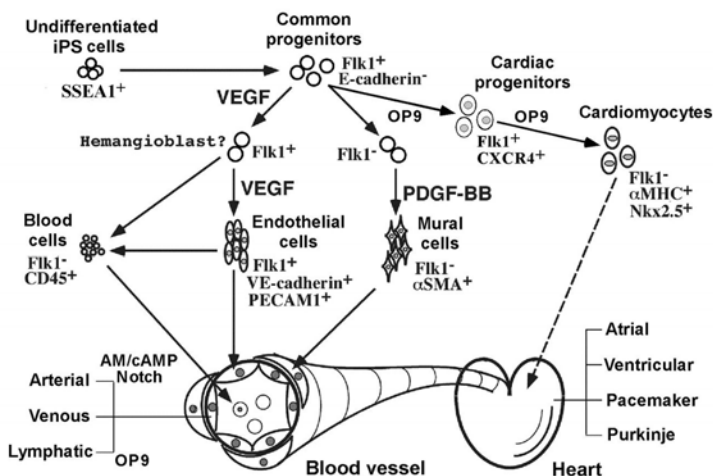
Balanced regulation of ion channel expressions, especially HCNs and Cav3s in cardiomyocytes should be important to constitute the spontaneously beating properties in ES cell-derived cardiomyocytes, and for the generation of complete biological pacemakers. Combined and coordinated regulation of multiple ion channels should be required to generate complete biological pacemakers and working cardiac muscles.

Various cardiovascular cells can be systematically induced from iPS cells. Differentiation properties of iPS cells are almost completely identical to those of ES cells. The iPS cell differentiation system would largely contribute to novel understanding for iPS cell biology and the development of novel cardiovascular regenerative medicine. Expression profiles and functional analysis of microRNAs during cardiomyocyte differentiation using these differentiation systems would largely contribute to elucidate novel molecular machinery for cardiomyocyte differentiation and regeneration.

Figures & Tables



Summary of differentiation and diversification process of cardiomyocytes. Blue to red color gradient represents MDP (or RMP) and dV/dt_{max} . Blue box: spontaneously beating cells. Red box: non-beating cells. Corresponding periods of ES cell differentiation are indicated. Na Ch.: Na^+ channel. (Ref. 1)



Systematic differentiation system of cardiovascular cells from iPS cells. Mouse iPS cell-derived Flk1⁺ cells give rise to ECs in the presence of VEGF. VEGF alone induces ephrinB2⁻ (EphB4⁺) venous ECs. When cAMP signaling is activated together with VEGF, ephrinB2⁺ arterial ECs are induced. For lymphatic EC differentiation, OP9 stroma cells are required. When Flk1⁺ cells are cultured on OP9 stroma cells for 4-5 days, cardiomyocytes are induced as a mixture of various cardiac cell types, atrial, ventricular, pacemaker, and purkinje cells. CD45⁺ blood cells are also induced from Flk1⁺ cells cultured on OP9 cells. Various cardiovascular cells are, thus, systematically induced from common progenitor, Flk1⁺ cells of mouse iPS cells. (Ref. 2)

References

1. Yanagi K, Takano M, Narazaki G, Uosaki H, Hoshino T, Ishii T, Misaki T, Yamashita JK*. Hyperpolarization-activated cyclic nucleotide-gated channels and T-type calcium channels confer automaticity of embryonic stem cell-derived cardiomyocytes. **Stem Cells**, 25: 2712-2719, 2007.
2. Narazaki G, Uosaki M, Teranishi M, Okita K, Kim B, Matsuoka S, Yamanaka S, Yamashita JK*. Directed and systematic differentiation of cardiovascular cells from mouse induced pluripotent stem cells. **Circulation, in press**
(*corresponding author)

2) Medical Sciences

2-5) Cardiovascular/Metabolic/Endocrine

Genetic analysis of zebrafish cardiac regeneration

Shinji Makino

Department of Regenerative Medicine and Advanced Cardiac Therapeutics Keio University

School of Medicine

koshinji@sc.itc.keio.ac.jp

Introduction

Teleost fish and urodele amphibians have remarkable regenerative capabilities. Zebrafish acutely regenerate heart, fins, optic nerve, scales and spinal cord. To identify the molecular mechanisms of regeneration, we performed a genetic screen for mutant zebrafish with defects in fin and cardiac regeneration. As a result, we have begun to identify regenerative genes at specific stages of regeneration.

Results

To identify mutants that failed to regenerate, we treated male zebrafish with *N*-ethyl-*N*-nitrosourea and generated mutagenized families by early pressure parthenogenesis.

We identified a zebrafish mutant with an early fin regeneration defect. Fin regeneration failed in mutant fish due to defective blastema formation. The regeneration phenotype was inherited as a recessive trait and was identified in a family in which 4 of 17 members displayed regenerative defects. Mutant fish regenerates did not form new bone and failed to grow beyond the amputation plane after 7 days at 33° C.

Mutant fish also failed to regenerate hearts. We surgically removed 20% of the ventricular myocardium from 1-year-old adults and examined hearts histologically. WT fish formed fibrin clots by 7 days postamputation, and cardiac myofibers penetrated the clot and constructed a new muscle around the wound by 17 days. The restoration of cardiac muscle resulted from cardiomyocyte proliferation. In contrast, mutant fish could not initiate cardiac regeneration. Mutant fish failed to fill in the wound area with fibrin clots or collagen scar. BrdUrd studies showed no evidence of myocyte or nonmyocyte proliferation around the wound at 12 days postamputation.

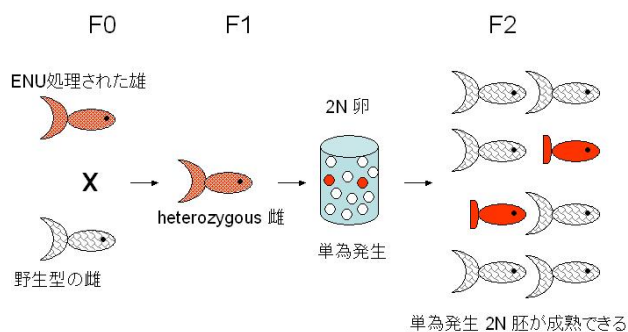
Positional cloning and mutational analyses revealed that mutation is linked to chromosome 9. Sequence of 4 genes in critical region is ongoing.

Discussion & Summary

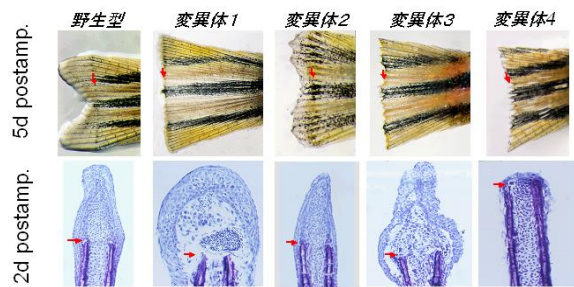
The study of regeneration holds great promise for the emerging field of regenerative medicine, but to realize this promise, regenerative phenomena must be understood in molecular terms. Genetic analysis of regeneration in zebrafish provides a unique instrument for achieving this goal. Zebrafish are the only genetic model system that reliably regenerates complex tissue. Accumulating technological advances in zebrafish genetics, including the genome sequencing initiative, stand to substantially advance discoveries through regeneration genetics. From our genetic screen for fin regeneration mutants, we expected to find disruptions in wound healing, tissue dedifferentiation, blastema formation and proliferation, and organ patterning. While the our mutant represents a defect in blastemal formation, mutants in other stages of regeneration have also been found and should shed light on these events. In future experiments, we will focus on the early events that initiate fin regeneration, and also extend our studies to additional organ systems that have not yet been examined for regenerative potential, such as the heart.

Figures & Tables

再生変異体のスクリーニング



スクリーニングより発見された再生変異体



- スクリーニングより約500家系をつくった
- 7 家系において再生の異常を認めた
- 2 家系につきpositional cloningを行っている

References

- Makino S, Whitehead GG, Lien CL, Kim S, Jhawar P, Kono A, Kawata Y, Keating MT. Heat-shock protein 60 is required for blastema formation and maintenance during regeneration. **Proc Natl Acad Sci U S A.** 2005;102:14599-604.
- Whitehead GG, Makino S, Lien CL, Keating MT. Fgf20 is essential for initiating zebrafish fin regeneration. **Science.** 2005; 310: 1957-60.
- Lien CL, Schebesta M, Makino S, Keating MT. Gene expression analysis of zebrafish heart regeneration. **PLoS Biol** 2006; 4: e260

2) Medical Sciences
2-6) Gastro-intestinal

Gene expression profiling and comparative analysis of normal esophagus stem/progenitor cells and esophagus cancer-derived cells

Atsushi Suzuki
Kyushu University
suzukicks@bioreg.kyushu-u.ac.jp

Introduction

The esophageal epithelium is exposed to everything taken from the mouth and the nose: for example, food, alcohol, and smoke of cigarettes. To maintain the esophageal epithelial tissue in such condition, esophageal stem cells should exist and continuously produce functional epithelial cells that form the multi-layers of esophageal epithelium. Although it is important to understand where stem cells are and how stem cells proliferate and differentiate in the normal and malignant esophageal epithelia, the stem cell biology of esophagus is still not established well. Here, we sought to identify the position of esophageal stem cells, the mechanism of differentiation and proliferation of these cells, and the relationship between stem cells and tumor cells in esophagus.

Results

Esophageal stem cells could be thought as cells with highly proliferative potential. To identify where these cells are, we performed immunohistochemical analysis of Ki67, a marker of proliferating cells, for the epithelial tissues of the mouse esophagus. Then, we prepared mRNA samples from proliferating esophageal stem cells and non-proliferating esophageal epithelial cells, which reside in the esophageal epithelial layers, following isolation of each cell population using a laser microdissection. After the microarray analysis with those mRNA samples, we identified several interesting genes that expressed differentially in esophageal stem cells or differentiated esophageal epithelial cells. Moreover, immunohistochemical analysis for the protein products of these genes showed similar expression patterns in the esophagus. Therefore, we are further examining the role of these genes in the esophagus.

Also, in order to determine the relationship between stem cells and tumor cells in the esophagus, we obtained esophageal tumor-derived cell lines and analyzed the gene expression profiles of these cell lines. In the result of comparing gene expression patterns among tumor-derived cells, stem cells, and differentiated cells in the esophagus, there were many genes expressing equivalently in esophageal tumor-derived cells and esophageal stem cells, or in esophageal tumor-derived cells and

differentiated esophageal epithelial cells. Thus, we are now analyzing the function of these genes in the esophageal tumor-derived cell lines to determine whether there is a common mechanism underlying the proliferation of esophageal tumor cells and normal esophageal stem cells.

Discussion & Summary

The esophagus is one of the regenerative organs, including skin and intestine. However, compared to other regenerative organs, the mechanism of proliferation and differentiation of esophageal stem cells is still poorly understood. Also, in the esophagus, a tumor is often generated, because of the genetic background or continuous exposure to unhealthy substances, while the mechanism of tumor formation in the esophageal epithelium remained unclear. In this study, the gene expression analyses of stem cells, differentiated cells, and tumor-derived cells in the mouse esophagus identified specific gene expression patterns that may regulate proliferation and differentiation of normal esophageal stem cells and may represent a common mechanism of proliferation of esophageal tumor cells and esophageal stem cells. Further examination of the role of these genes may eventually enable the therapeutic approaches for the esophagus failures by inducing stem cell-mediated regeneration and for the esophagus cancer by negatively regulating the proliferation of esophageal cancer stem cells.

2) Medical Sciences
2-6) Gastro-intestinal

Roles of host immune responses in the development of *Helicobacter*-induced gastritis

Norihiko Watanabe
Kyoto University
norihiko@kuhp.kyoto-u.ac.jp

Introduction

Helicobacter bacteria colonize in the stomach and induce strong, specific local and systemic humoral and cell-mediated immunity. *Helicobacter* binds to the host epithelial cells, directly triggering the recruitment of neutrophils. Local inflammatory processes in the gastric mucosa are followed by extensive immune-cell infiltration, resulting in chronic active gastritis. One type of *Helicobacter*-induced chronic gastritis is characterized by a marked infiltration of Th1 cytokine-producing CD4⁺ T cells. The other type of *Helicobacter*-induced chronic gastritis is follicular gastritis, in which development Th2 cells appear to play an important role. However, the mechanisms underlying the development of Th1 and/or Th2 cytokine-mediated chronic gastritis are not fully understood.

Results

(1) Peyer's patches (PPs) are the major inductive sites for mucosal immunity in the gut system. We generated PP-null mice that normally develop well-organized lymphoid organs except for PPs and intragastrically infected the resulting PP-null mice with *Helicobacter*. PP deficiency severely impaired both the development of Th1 cell-mediated gastritis induced by *Helicobacter* and the production of anti-*Helicobacter* antibodies despite marked bacterial colonization of the gastric mucosa. Although PP deficiency did not impair the differentiation of *Helicobacter*-specific CD4⁺ T cells into IFN- γ -producing Th1 cells, *Helicobacter*-specific IFN- γ -producing CD4⁺ T cells in PP-null mice lacked the ability to migrate into *Helicobacter*-colonized gastric mucosa.

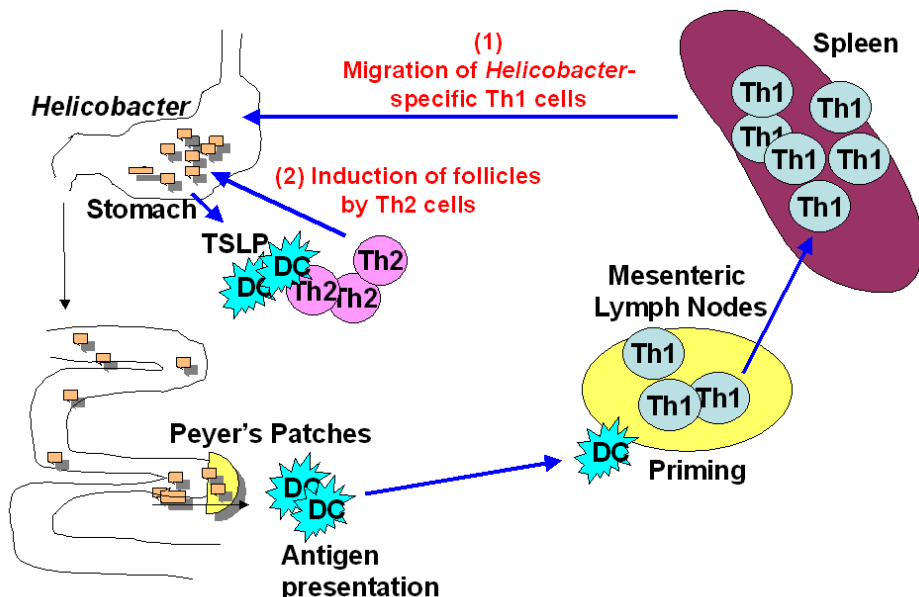
(2) Thymic stromal lymphopoietin (TSLP), an epithelial cell-derived cytokine that strongly activate dendritic cells (DCs), induces DC-mediated inflammatory Th2 responses. We showed that *Helicobacter* triggered gastric epithelial cells to produce TSLP and a DC-attracting chemokine, MIP-3 α . The gastric epithelial cell-conditioned DCs expressed high levels of costimulatory molecules and triggered naïve CD4 T cells to produce high levels of the Th2 cytokines, IL-4 and IL-13 and of TNF- α .

Discussion & Summary

PPs have an essential role in the host immune response to *Helicobacter* infection, including the development of Th1 cytokine-mediated atrophic gastritis. In contrast, TSLP produced by *Helicobacter*-infected gastric epithelial cells may play an important role in the development of Th2 cytokine-mediated follicular gastritis.

Figures & Tables

Host immune responses to *Helicobacter* infection



Figure

(1) PPs have an essential role in the development of Th1 cytokine-mediated atrophic gastritis. (2) TSLP produced by *Helicobacter*-infected gastric epithelial cells may play an important role in the development of Th2 cytokine-mediated follicular gastritis.

References

1. Watanabe N, Kiriya K, Chiba T. Small intestine Peyer's patches are major induction sites of the *Helicobacter*-induced host immune responses. **Gastroenterology** 134 : 642-643 : 2008.
2. Kiriya K, Watanabe N, Nishio A, Okazaki K, Kido M, Saga K, Tanaka J, Akamatsu T, Ohashi S, Asada M, Fukui T, Chiba T. Essential role of Peyer's patches in the development of *Helicobacter*-induced gastritis. **Int Immunol.** 19 : 435-446 : 2007.

2) Medical Sciences

2-12) Hematology

Regulation of self-renewal capacity of leukemic stem cells by hematopoietic transcription factors

Hideaki Nakajima

Keio University School of Medicine

hnakajim@sc.itc.keio.ac.jp

Introduction

C/EBP α and PU.1 are lineage-specific transcription factors critical for myeloid differentiation. Recent study revealed that C/EBP α and PU.1 are expressed in hematopoietic stem cells (HSCs) at low levels, implicating that these factors play a role in HSC functions.

Results

To gain further insight into the HSC regulation by C/EBP α or PU.1, we used transgenic (Tg) mice expressing conditional form of these transcription factors to examine if their activation alone is sufficient for modulating HSC functions. The activation of C/EBP α or PU.1 in HSCs *in vitro* or *in vivo* led to their suppression of growth, decreased mixed colony formation, and impaired competitive repopulating activities due to their defective self-renewal. These effects are more prominently observed when C/EBP α was activated, and the differentiation capacity to megakaryocytic lineage was selectively impaired upon C/EBP α activation. Unexpectedly, the expression of Bmi-1 and HoxB4, well-known regulators for self-renewal of HSCs, was not affected by the activation of C/EBP α or PU.1, suggesting that they regulate HSC function through an as yet unknown mechanism.

Discussion & Summary

These data suggest that the activation of C/EBP α or PU.1 is sufficient to repress stem cell capacities in HSCs, and their fine-tuned regulation is critical for HSC homeostasis.

3) Chemical Sciences
 3-1) Organic Chemistry

Preparation of Chiral Boron Reagents for Efficient Synthesis of Biologically Active Substances

Toshimichi Ohmura
 Graduate School of Engineering, Kyoto University
 ohmura@sbchem.kyoto-u.ac.jp

Introduction

It is highly desirable to develop new chiral organometallic reagents that achieve efficient construction of chiral molecular structures that include in biologically active substances. Chiral organoboron compounds are attractive because they are stable to handle but can activate under a certain conditions. However, asymmetric synthetic method of chiral organoboron reagents has not been fully explored. In this study, we developed a new route to enantioenriched alkenylboron compounds via silaborative asymmetric desymmetrization of *meso*-methylenecyclopropanes using a chiral palladium catalyst.¹

Results

We have developed palladium-catalyzed silaborative C–C bond cleavage of methylenecyclopropanes, in which proximal C–C bond cleavage is accompanied by regioselective introduction of a silyl and a boryl groups at the cleaved C–C bond.² The original palladium catalyst bearing an isocyanide ligand seemed unfavorable for the asymmetric induction, because of the requirement for a relatively high reaction temperature (110 °C) and less flexibility in the design of chiral isocyanides. We found that the palladium-phosphine catalyst showed high catalyst activity in the reaction of (dimethylphenylsilyl)pinacolborane with 7-methylenebicyclo[4.1.0]heptane; the reaction proceeded even at 50 °C in the presence of Pd(dbu)₂ (2.0 mol %) with PPh₃ (2.4 mol %), giving 2-(1-borylethenyl)-1-silylcyclohexane in 64% yield after 24 h. The catalyst activity was found to be highly dependent upon the Pd/P ratio. The reaction slowed down significantly in the absence of the phosphine ligand or in the presence of increased amounts of the ligand (Pd/P ratio of 1/2.4) (4% and 0% yield, respectively, under otherwise identical reaction conditions).

In the presence of a palladium catalyst bearing an optically active monodentate phosphorus ligand (Pd/P = 1/1.2), the reaction of *meso*-methylenecyclopropanes with silylboranes was carried out in toluene at 50 °C. The reaction proceeded with cleavage of one of the two enantiotopic C–C bonds of cyclopropane ring to give chiral 2-boryl-4-silyl-1-butenes in high yields.

Enantioselectivity of the products depended on the structure of chiral phosphorus ligand and silylborane. We found that the palladium catalyst having (*R*)-2-bis(3,5-dimethylphenyl)phosphino-1,1'-binaphthyl [(*R*)-3] gave the highest enantioselectivity in the reactions with (methyldiphenylsilyl)pinacolborane (**1**). It is interesting to note that the optimized reaction conditions using silylborane **1** and Pd/(*R*)-3 catalyst are identical to those for the enantioselective silaboration of allenes reported recently,³ indicating mechanistic similarity in the asymmetric induction step.

Various *meso*-methylene cyclopropanes were subjected to asymmetric silaborative C–C cleavage under the optimized conditions using **1** and Pd/(*R*)-3 catalyst (Table 1). The reaction of bicyclic methylenecyclopropanes that have fused five-, six-, seven-, and eight-membered carbocycles gave the corresponding **3** in high yields with high enantioselectivities (90–91% ee, entries 1–4). On the other hand, non-fused methylenecyclopropane afforded the product with lower ee (81% ee, entry 5). We also carried out the reaction of the methylenecyclopropane with fused cyclic acetal, giving the alkenylboron compound with 89% ee, although the yield was modest (entry 6).

Table 1. Synthesis of Enantioenriched **4** via Asymmetric Desymmetrization of *meso*-Methylenecyclopropanes

entry	methylene cyclopropane	product	yield (%)	ee (%)
1			n = 1 72	90
2			n = 2 87	90
3			n = 3 95	91
4			n = 4 85	90
5			72	81
6			50	89

Synthetic utility of the enantioenriched silaboration products obtained was demonstrated by a diastereoselective homologation-allylboration sequence (Table 2). The reaction of **4a** with ClCH₂Li followed by treatment with EtCHO gave homoallylic alcohol **5a** in 78% yield with high diastereomeric ratio (94:6, entry 1). High diastereoselectivities were observed not only in the reaction of **4a** with *i*-PrCHO and PhCHO (entries 2 and 3), but also in the reactions of **4b–4d** with

PhCHO (entries 4-6). These reactions indicate that the stereochemistry of the *b*-substituent on allylic boronates efficiently controls the diastereoface selection in the six-membered cyclic transition state. As expected, enantioenriched **4c** afforded **7** without a drop in ee (entry 5).

Table 2. Diastereoselective Synthesis of Homoallylic Alcohols

entry	boron reagent	R ³ CHO	product	yield (%)	dr	
1		EtCHO		5a (R = Et)	78	94:6
2		i-PrCHO		5b (R = i-Pr)	80	94:6
3		PhCHO		5c (R = Ph)	70	97:3
4		PhCHO		6	63	93:7
5		PhCHO		7	69	97:3 (91% ee)
6		PhCHO		8	71	93:7

Discussion & Summary

In conclusion, we developed palladium-catalyzed asymmetric silaborative C–C cleavage of *meso*-methylenecyclopropanes, affording enantioenriched 2-boryl-4-silyl-1-butene derivatives in high yield with up to 91% ee. The chiral organoboron compounds were applied to diastereoselective synthesis of homoallylic alcohols having relatively complex structures. This new synthetic method using optically active organoboron reagents is expected to be attractive alternative for preparation of biologically active substances.

References

1. Ohmura, T.; Taniguchi, H.; Kondo, Y.; Suginome, M. *J. Am. Chem. Soc.* **2007**, *129*, 3518-3519.
2. Suginome, M.; Matsuda, T.; Ito, Y. *J. Am. Chem. Soc.* **2000**, *122*, 11015-11016.
3. Ohmura, T.; Taniguchi, H.; Suginome, M. *J. Am. Chem. Soc.* **2006**, *128*, 13682-13683.

3) Chemical Sciences

3-1) Organic Chemistry

Development of the Novel Artificial Nucleoside Derivatives for the Control of the Gene Expression in Cells

Fumi Nagatsugi

Institute of Multidisciplinary Research for Advanced Materials Tohoku University

nagatugi@tagen.tohoku.ac.jp

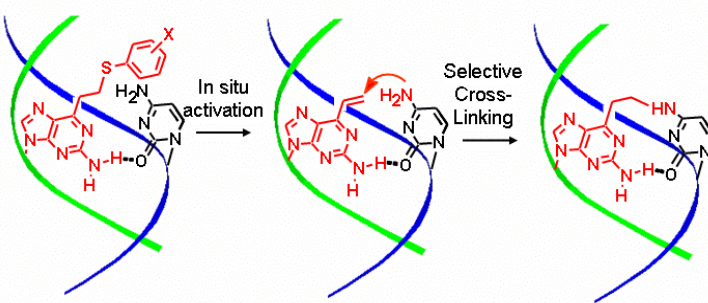
Introduction

The exploitation of chemical agents capable of sequence-specific DNA modification has provided a wide potential for the gene knockdown and gene repair technologies. Especially, synthetic oligodeoxynucleotides (ODNs) having chemically reactive appendages have been widely investigated to create new functions based on the specific reaction toward the corresponding target gene. In this research, we propose a plan for the development of recognition methods of duplex DNA for regulation of gene expression.

Results

We have developed the 2-amino-6-vinylpurine nucleoside analog (**1**) as the new cross-linking agent.¹ Its sulfide derivatives as stable precursors are automatically activated without need of UV-irradiation or chemical activation in the hybrids to form the cross-link selectively to cytosine (Fig. 1). We have planned to apply these strategies for targeting duplex DNA. For this purpose, we synthesized peptide nucleic acid (PNA) containing 2-amino-6-vinylpurine. PNAs can bind to single strands of DNA and RNA with high affinity, and more interestingly, they disrupt the double stranded DNA to form a DNA-PNA strand-invasion complex.²

Figure 1 In Situ Activation Synchronous to Hybridization

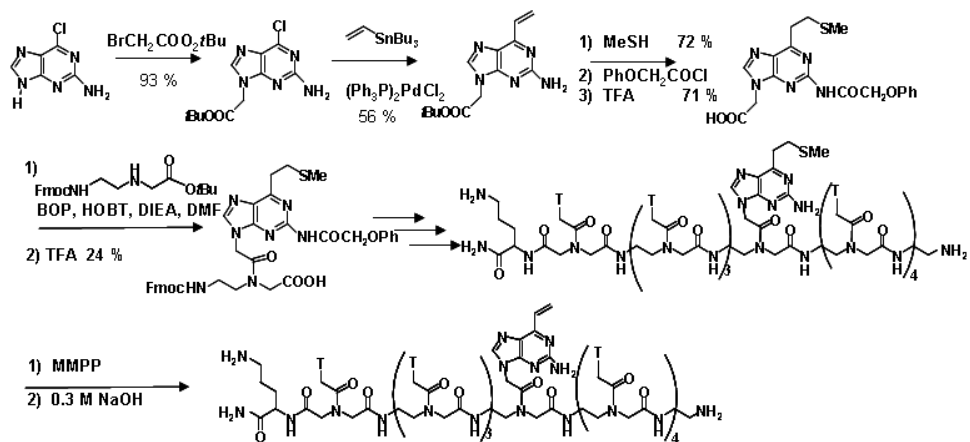


The synthesis of PNA monomer

(**2**) containing the stable precursor of 2-amino-6-vinylpurine is summarized in Scheme 1. The solid-phase synthesis of the PNA oligomer was performed manually on NovaSin TG resin by the Fmoc strategies. The PNA containing **2** was cleaved from the resin under TFA-*m*-cresol (4:1) and purified by reverse phase HPLC, followed by treatment with 28 % ammonia to give the desired PNA

(3). The sulfide-protected PNA (**3**) was smoothly converted to **4** by oxidation with magnesium monoperphthalate (MMPP) following elimination of the resulting sulfoxide derivative under an alkaline condition. The structure of **4** was confirmed by MALDI-TOF mass measurements. The presence of the vinyl group of **4** was further proven by the fact that **4** returned to **3** cleanly by the treatment with an aqueous NaSMe solution. Thus, this study has demonstrated successful synthesis of the PNA (**3**) incorporating the methylsulfide derivative of the 2-amino-6-vinylpurine as well as its easy transformation to **4** with the vinyl functional group. In the preliminary studies, cross-linking reaction by using PNA containing 2-amino-6-vinylpurine took place with single strand DNA and RNA. Interestingly we found that 2-carboxyphenyl sulfide derivative, which was a stable precursor of 2-amino-6-vinylpurine, exhibited cross-linking more effectively than vinyl derivative.

Scheme 1 Synthesis of PNA Containing 2-Amino-6-vinylpurine



Discussion & Summary

In this research, we have achieved the synthesis of PNA containing the reactive artificial nucleic acid efficiently by using the stable precursor of 2-amino-6-vinylpurine. Preliminary results showed that the reactive PNA reacted with single strand DNA and RNA. It should be noted that the 2-carboxyphenyl sulfide derivative, which was a stable precursor of 2-amino-6-vinylpurine produced the adduct in higher yield than reactive vinyl derivatives. These results suggested that 2-carboxyphenyl sulfide derivative might be activated in the duplex between PNA and DNA to re-generate 2-amino-6-vinylpurine, resulted in efficient cross-linking reaction. We expect that PNA containing 2-carboxyphenyl sulfide derivative can invade to duplex DNA effectively and react to cytidine with high selectivity.

References

1. a) Ali M. M., Oishi M., Nagatsugi F., Mori K., Nagasaki Y., Kataoka K., Sasaki S., *Angew. Chem. Int. Ed.* **2006**, *45*, 3136-3140, b) Kawasaki T., Nagatsugi F., Ali, M.M., Maeda M., Sugiyama K., Hori K., Sasaki S., *J. Org. Chem.* **2005**, *70*, 14-23, c) Nagatsugi F., Kawasaki T., Usui D., Maeda M., Sasaki S., *J. Am. Chem. Soc.* **1999**, *121*, 6753-6754.
2. a) Kim K.H., Fan X. J., Nielsen P.E. *Bioconj. Chem.* **2007**, *18*, 567-572, b) , Zhilina ZV. Ziembra AJ. Nielsen PE. Ebbinghaus SW. *Bioconj. Chem.* **2006**, *17*, 214-222.

3) Chemical Sciences
 3-1) Organic Chemistry

**Design of nano-foldamer having chiral centers at the helical surface
 and its application to chiral molecular recognition**

Masakazu Tanaka

Graduate School of Pharmaceutical Sciences, Kyushu University
 mtanaka@phar.kyushu-u.ac.jp

Introduction

α,α -Disubstituted amino acids are α -amino acids in which the hydrogen atom at the α -position of the amino acid is replaced with an alkyl substituent. We have designed and synthesized chiral cyclic α,α -disubstituted amino acids in which the α -carbon atom is not the chiral center but chiral centers exist at the side-chain cycloalkane. The oligomers composed of the cyclic amino acid are nano-foldamers having chiral centers at the helical surface.

Results

As a chiral cyclic α,α -disubstituted amino acid, we designed a seven-membered ring amino acid; $(4R,5R)$ -1-amino-4,5-di(methoxy)cycloheptanecarboxylic acid $\{(R,R)\text{-Ac}_7\text{c}^{\text{dOM}}\}$ in which the α -carbon atom is not a chiral center, and developed a chemoenzymatic strategy for the synthesis of optically active $(R,R)\text{-Ac}_7\text{c}^{\text{dOM}}$.

We prepared racemic *trans*-4,5-dihydroxy-1,1-bis(methoxycarbonyl)cycloheptane (**3**) starting from dimethyl malonate. That is to say, dialkylation of dimethyl malonate with 4-bromo-1-butene gave diene (**1**). Olefin metathesis of **1** with Grubbs catalyst afforded cycloheptane (**2**) in 98% yield. Epoxidation of **2** with MCPBA, followed by acidic hydrolysis produced racemic cyclic *trans*-1,2-diol **3** having a diester moiety in 80% yield. Kinetic resolution of the racemic diol (\pm)-**3** by transesterification with lipase Amano AK in vinyl acetate afforded (+)-monoacetate (**4**) of 95% ee in 51% yield and the recovered (-)-diol **3** of >99% ee in 43% yield. To determine the absolute configuration of the optically active diol, the unreacted diol (-)-**3** was converted into the corresponding dibenzoate. The CD spectrum of dibenzoate indicated that the first Cotton effect (236 nm) was negative and the second Cotton effect (223 nm) was positive (negative chirality). According to the dibenzoate chirality rule, the configuration of the unreacted diol (-)-**3** is *R,R*. The assignment of the absolute configuration is opposite to that of the reported data, in which the lipase-catalyzed kinetic resolutions of racemic plain cycloalkane-1,2-diols were described. To explain the lipase-catalyzed enantiomer selectivity, computer modeling of lipase-substrate

complexes was performed. The modeling suggested the existence of hydrogen bond between the carbonyl function of the diester (substrate) and the hydroxyl function of the amino acid residue (Thr 18). The hydrogen bond may be crucial for the reversal of the enantiomeric selectivity.

Methylation of the diol function in $(-)\text{-}3$ with MeI and Ag_2O gave a dimethoxy compound $\{(-)\text{-}5\}$ in 99% yield. Monohydrolysis of the diester under basic conditions, followed by Curtius rearrangement and workup with benzyl alcohol afforded the cyclic amino acid $\text{Cbz}\text{-}\{(4R,5R)\text{-Ac}_5\text{c}^{\text{dOM}}\}\text{-OMe}$ in 92% yield. (Fig. 1)

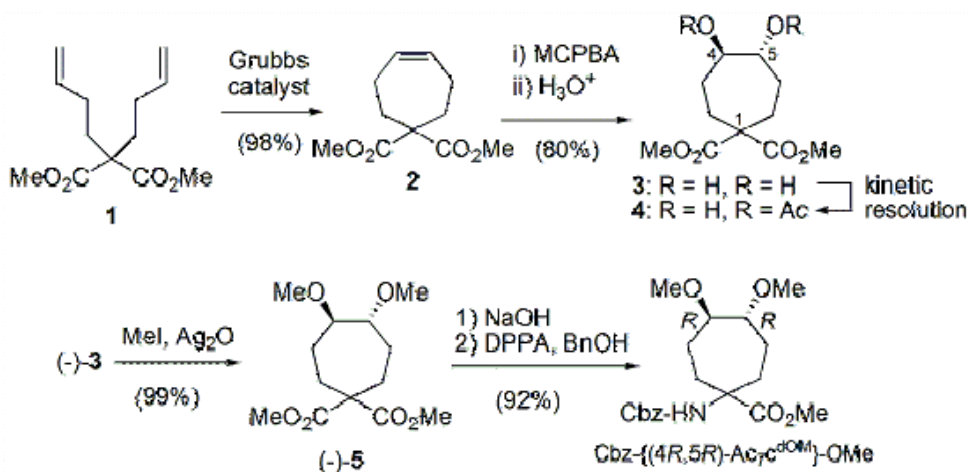


Figure 1

Oligomers $\text{Cbz}\text{-}(L\text{-Leu-L-Leu-dAA})_n\text{-OMe}$ having cyclic amino acid; (S,S) - or (R,R) - $\text{Ac}_5\text{c}^{\text{dOM}}$, and dimethylglycine (Aib) in L-Leu sequences have been designed and prepared by solution-phase methods. At first, we analyzed the preferred secondary structure of these oligomers. The IR spectra of oligomers showed a weak band at 3430 cm^{-1} [free (solvated peptide NH group), and a strong band at 3340 cm^{-1} [intramolecularly H-bonded peptide NH groups]. The ROESY or NOESY ^1H NMR spectra did not clearly show the complete series of sequential d_{NN} cross-peaks of NOEs, which are characteristic of helical structures. The CD spectra of oligomers in 2,2,2-trifluoroethanol solution showed negative maxima at 222-228 nm and 204-208 nm and a positive maximum at 191-193 nm, which are characteristic of a right-handed (*P*) helical structure. The L-Leu residues in the oligomers would control the helical-screw direction to the right-handedness. The crystal structures of Aib hexamer $\text{Cbz}\text{-}(L\text{-Leu-L-Leu-Aib})_2\text{-OMe}$ and (S,S) - $\text{Ac}_5\text{c}^{\text{dOM}}$ hexamer $\text{Cbz}\text{-}[L\text{-Leu-L-Leu-}\{(S,S)\text{-Ac}_5\text{c}^{\text{dOM}}\}]_2\text{-OMe}$ were determined by the X-ray crystallographic analysis. The Aib hexamer showed right-handed 3_{10} -helix, forming three consecutive hydrogen bonds of the $i \leftarrow i+3$ type in the crystal state, while the (S,S) - $\text{Ac}_5\text{c}^{\text{dOM}}$ hexamer showed right-handed α -helix, in which two consecutive intramolecular hydrogen bonds of the $i \leftarrow i+4$ type were observed.

Furthermore, we studied an asymmetric epoxidation of chalcone using the α -helical oligomers containing the cyclic amino acids as a chiral catalyst. The asymmetric epoxidation catalyzed by hexamer afforded an epoxide product of low ee, but that by α -helical nonamer gave the epoxide of >80% ee in 95% yield. (Fig. 2)

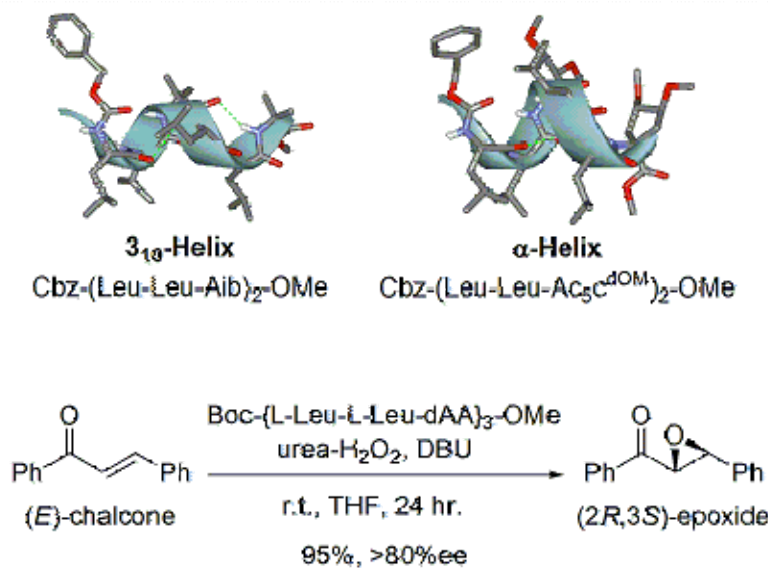


Figure 2

Discussion & Summary

We designed chiral cyclic α,α -disubstituted α -amino acids, in which the α -carbon atom is not a chiral center but chiral centers existing at the side chain. Optically active cyclic amino acid (*R,R*)-Ac₇C^{DOM} was synthesized by using lipase-catalyzed kinetic resolution of racemic *trans*-1,2-diol as a key step.

Oligomers Cbz-(L-Leu-L-Leu-dAA)_n-OMe having cyclic amino acid; (*S,S*)- or (*R,R*)-Ac₅C^{DOM}, and Aib in L-Leu sequences have been prepared by solution-phase methods, and their preferred secondary structures were analyzed by the IR, ¹H NMR, CD spectra, and X-ray crystallographic analysis. The L-Leu-based peptide having Aib preferentially formed right-handed 3_{10} -helix, while that containing (*S,S*)-Ac₅C^{DOM} assumed right-handed α -helix.

The α -helical oligomers containing the cyclic amino acids were used as asymmetric catalysts for epoxidation. The asymmetric epoxidation of chalcone by using α -helical nonamer gave the epoxide of >80% ee in 95% yield.

These results revealed that the α -helical secondary structures as nano-foldamers are useful for the chiral molecular recognition.

References

- 1) M. Tanaka, *Chem. Pharm. Bull.*, **55**, 349-358 (2007).
- 2) M. Tanaka, Y. Demizu, M. Nagano, M. Hama, Y. Yoshida, M. Kurihara, H. Suemune, *J. Org. Chem.*, **72**, 7750-7756 (2007).
- 3) Y. Demizu, M. Tanaka, M. Nagano, M. Kurihara, M. Doi, T. Maruyama, H. Suemune, *Chem. Pharm. Bull.*, **55**, 840-842 (2007).
- 4) In preparation.

3) Chemical Sciences
 3-1) Organic Chemistry

Development of Effective Synthetic Method for Oxindoles based on a Claisen Rearrangement

Atsuo Nakazaki

Tokyo University of Science

nakazaki@rs.noda.tus.ac.jp

Introduction

Oxindoles incorporating a quaternary stereogenic center at the C3 position are attractive targets in organic synthesis because of their significant biological activities as well as wide ranging utility as synthetic intermediates for alkaloids, and drug candidates and clinical pharmaceuticals. In this research, we have developed an efficient and convenient method for the synthesis of spirocyclic oxindoles from haloindoless by means of a one-pot procedure.

Results

Based on the previous results,^[1] we envisioned that a Claisen rearrangement of alkenyl pyranoindoless **2** would produce spirocyclic oxindoles **3**, which are potential synthetic intermediates for indole alkaloids (Scheme 1). Pyranoindoless **2** might in turn be prepared by an intramolecular Ullmann coupling (IUC) of haloindoless **1** bearing an allylic alcohol unit. Among the conditions examined using **1a**, the Hauptman protocol (CuCl/2-aminopyridine, NaOMe)^[2] with slight modifications was found to provide **2a** in 91% yield. The IUC of **1a** proceeded rapidly and was completed within 10 minutes. Interestingly, neither dehaogenated product **A**, nor the product of cross-coupling with NaOMe, **B**, was obtained. Finally, the isolated product **2a** underwent Claisen rearrangement to afford the desired oxindole **3a** by heating in 1,2-dimethoxyethane (DME) at 150 °C, as expected.

As **2a** was found to be relatively unstable, especially under acidic conditions, we next attempted a one-pot synthesis of **3a**. When the reaction mixture was heated to 100 °C for 24 h, **3a** was obtained in 53% yield. On the other hand, on raising the reaction temperature to 150 °C after complete formation of **2a** (100 °C, 10 min), the rearrangement of **2a** went cleanly to afford **3a** in 84% yield.

To study the effect of substituents on the Claisen rearrangement, compounds **1** with a variety of substituents at the allylic alcohol unit were next explored. It is noteworthy that all of the indoles with *trans*-oriented substituents on the allylic double bond afforded the corresponding oxindoles as a single isomer, irrespective of substituents. The stereochemistry of these products indicates that the

Claisen rearrangement proceeds through a boat-like transition state analogous to previous results.^[3]

Since the Claisen rearrangement is stereospecific in most cases, this methodology would also be applicable to the enantioselective synthesis of spirocyclic oxindoles. Indeed, the one-pot IUC/Claisen protocol of enantioenriched 2-iodoindole **4** afforded corresponding spirocyclic oxindole **5** without loss of stereochemical integrity (Scheme 2)

The resulting spirocyclic derivatives are considered to be useful intermediates for the synthesis of pyrrolidinoindoline alkaloids as oxidative cleavage of the cyclohexene ring would provide a C-3a substituted oxindole skeleton. We next applied to the synthesis of (–)-debromoflustramine B using spirocyclic oxindole **5** (Scheme 2). Thus, oxidative cleavage of the carbon-carbon double bond of **5** with OsO₄-NaIO₄ gave ketoaldehyde **6**, which was further oxidized with NaClO₂ to obtain a ketoacid **7**. The ketoacid **7** was then converted into *exo*-methylene **8** by Wittig olefination in 73% yield from **5**. Treatment of *exo*-methylene **8** with conc. H₂SO₄ in the presence of MgSO₄ resulted in the desired isomerization to an internal olefin. Carboxylic acid was transformed to an amide **9**, by the mixed anhydride method using ethyl chloroformate and MeNH₂, in 90% yield from carboxylic acid **8**. Finally, reduction of amide **9** using AlH₃·EtNMe₂ complex followed by deprotection-prenylation sequence afforded a biologically active alkaloid, (–)-debromoflustramine B.

Discussion & Summary

In conclusion, we have developed a convenient and efficient method for the preparation of spirocyclic oxindoles, with vicinal stereogenic centers, from the corresponding 2-haloindoles by a one-pot IUC and Claisen rearrangement. The IUC is a simple and low cost method for the preparation of the rearrangement precursors, alkenyl pyranoindoles. The Claisen rearrangement of the pyranoindoles proceeds smoothly to give the desired oxindoles in good yield and high diastereoselectivities. We also achieved to the total synthesis of biologically active alkaloid, (–)-debromoflustramine B, which demonstrated the utility of spirocyclic oxindole as a synthetic intermediate of alkaloids bearing a prenyl group at C-3a.

References

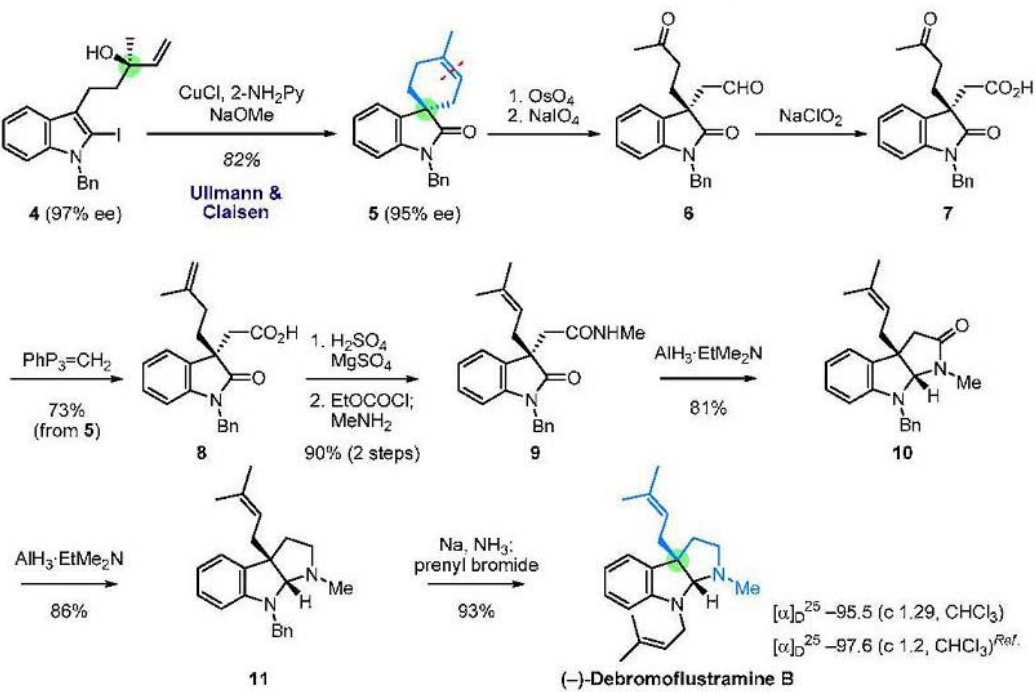
- [1] A. Nakazaki, S. Kobayashi *Journal of Synthetic Organic Chemistry* **2008**, 66, 124, and references therein.
- [2] E. Hauptman *et al.* *J. Am. Chem. Soc.* **2000**, 122, 5043.
- [3] G. Büch *et al.* *J. Am. Chem. Soc.* **1970**, 92, 3126.

Figures for Research Report

Scheme 1. One-pot Intramolecular Ullmann Coupling / Claisen Rearrangement



Scheme 2. Total Synthesis of (–)-Debromoflustramine B Using One-Pot Procedure



Ref. M. S. Morales-Ríos et al. *Tetrahedron: Asymmetry* 2005, 16, 2493.

3) Chemical Sciences

3-1) Organic Chemistry

Synthesis of polycyclic natural products including heteroatom

Kan Toshiyuki

School of Pharmaceutical Sciences, University of Shizuoka

kant@u-shizuoka-ken.ac.jp

Introduction

Heteroatom-containing compounds are important chemical entities, many of which show unique bioactivity. In view of this their efficient synthesis is an important issue in the development of pharmaceutically active molecule. However it limits the scope of reaction conditions to which these compounds may be submitted. Thus the development of novel synthetic method for natural products was strongly needed.

Results

In this research, synthetic investigation of polycyclic natural products serotobenine (**1**), altemicidin (**2**), lemomycin (**3**), epigallocatechin gallate (EGCG) (**4**) were demonstrated.

Total synthesis of serotobenine (**1**) was commenced with indole derivative, which was readily synthesized by according to Leimgruber-Batcho protocol. After regioselective Claisen rearrangement, the diazoester was subjected to the C-H insertion reaction to afford dihydrobenzofuran in higher diastereoselectivity. After construction of 8-membered lactam ring and the deprotection, total synthesis of **1** has been accomplished.

Stereoselective synthesis of the key intermediate for altemicidin (**2**) has been accomplished. The synthesis commenced with a bicyclo[3.3.0] framework, which was readily obtained via an intramolecular C-H insertion reaction. A Curtius rearrangement was employed as a key step to stereoselectively construct the β -hydroxyl α -disubstituted- α -amino acid structure. Synthesis of vinylogous urea was achieved using hydrolysis of nitrile intermediate.

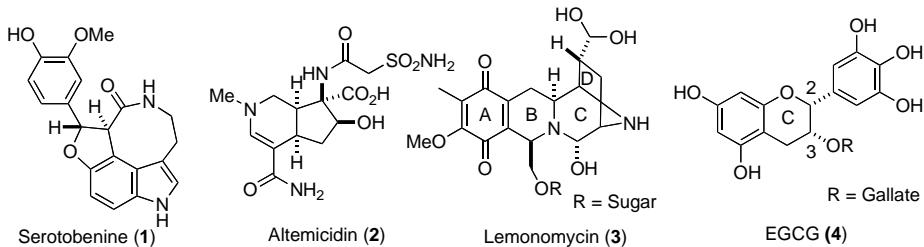
Stereoselective synthesis of the pentacyclic key intermediate for (-)-lemonycin (**3**) has been accomplished using the Ugi 4-CC reaction with our novel isonitrile. During the course of our synthetic study on EGCG (**4**), we found dideoxy-EGCG possessed the same level of biologically activity as well as natural product.¹ Since the hydroxy group of the A-ring did not affect the activity, we envisioned the incorporation of probe-units at A-ring incorporation of EGCG would be possible. We accomplished the synthesis of the EGCG proe precursor which possessed the alkyl linker and amino group.

Discussion & Summary

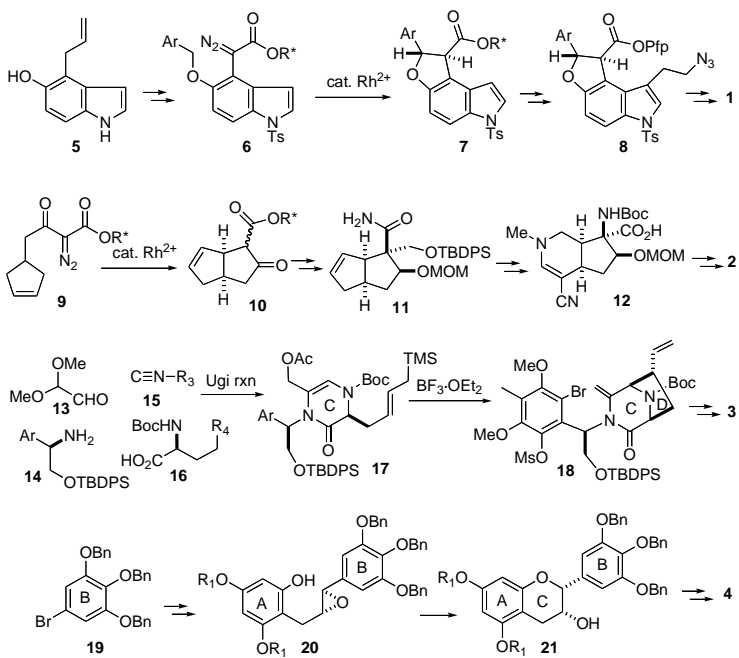
Synthetic study of serotobenine (**1**) and altemicidin (**2**) was carried out by employment with Rh-carbenoid mediated C-H insertion reaction as a key step. In this reaction, an Optically active cyclopentane ring was synthesized by an intramolecular C-H insertion reaction with diazo-ester which has a chiral diazoester. The highest diastereoselectivity was attained by combining Rh-catalyst and auxiliary, which derived from mandelic amide derivatives.

Figures & Tables

Figure 1. Structure of polycyclic natural products



Scheme 1. Synthetic investigation of **1 – 4**



References

- 1) Synthetic Studies on Altemicidin: Stereocontrolled Construction of the Core Framework., T. Kan, Y. Kawamoto, T. Asakawa, T. Furuta and T. Fukuyama, *Org. Lett.*, **10**, 169-171(2008).
- 2) Concise synthesis of dideoxy-epigallocatechin gallate (DO-EGCG) and evaluation of its anti-influenza virus activities., T. Furuta, Y. Hirooka, A. Abe, Y. Sugata, M. Ueda, K. Murakami, T. Suzuki, K. Tanaka and T. Kan, *Bioorg. Med. Chem. Lett.*, **17**, 3095-3098 (2007).

Part II

Reports from the Recipients of Garants
for International Meetings
(Fiscal Year 2006)

The 2007 Molecular Biology Society of Japan (MBSJ) Spring
Symposium
on “Biology -Old Codes and New Molecules-“
(The 7th the MBSJ spring symposium)

1. Representative

Haruhiko Siomi, the chairman of the organizing committee

2. Opening period and Place

April 23 - April 24, 2007 at the Awaji Yumebutai International Conference Center in Awaji Island

3. Number of participants

137 persons including 5 invited speakers from the US and the United Kingdom

4. The total cost

5,680,000 yen

5. Main use of the subsidy

Support for travel expense of invited speakers

6. Results and Impression

The MBSJ Spring Symposium was the 7th in the MBSJ spring conference series, and was being organized in collaboration with the Institute for Genome Research University of Tokushima in Tokushima. Like the first six meetings, this conference was focused on an emerging intersection between disciplines, and brought together scientists working on various aspects of biology to stimulate discussion and found common themes among the questions facing the field.

Topics in this symposium included small RNAs and development, non-Mendelian inheritance and epigenetics, germ line stem cells and hubs, and cell cycle and chromosome segregation cycle. This two-day symposium was divided into eight oral sessions and a poster session. In oral sessions, 25 speakers including 5 invited speakers from overseas presented recent progress in their research. 50 young researchers including graduated students presented their research in the poster session.

On the whole, we got the impression that many people had good interactions with many others during the symposium.

7. Additional description

As part of the 7th the Molecular Biology Society of Japan spring conference, a special lecture titled ‘Mechanisms of Planarian Regeneration’ was given by Professor Kiyokazu Agata (Kyoto University) at the Nagai Memorial Lecture Hall of the University of Tokushima. This lecture encouraged many young people (from elementary school students to high school students) to get interested in biology.

The 5th International Symposium on Molecular Breeding of Forage and Turf (MBFT2007)

1. Representative

Toshihiko Yamada, the Chairman of Local Organizing Committee of International Symposium on Molecular Breeding of Forage and Turf

2. Opening period and Place

July 1 – July 6, 2007

Sapporo Convention Center

3. Number of participants

147 (80 persons from foreign countries)

4. The total cost

Thirteen million yen

5. Main use of the subsidy

Support for hall fee, rental fee of equipments, wage (students part-time), and stationeries

6. Result and Impression

The International Symposium on Molecular Breeding of Forage and Turf (MBFT) is held every 2 or 3 years under the control of international organizing committee of MBFT. Previous MBFT Symposia were held in Japan in 1998, Australia in 2000, the USA in 2003 and the UK in 2005. On this occasion the 5th MBFT was held in Sapporo, in 2007.

For the present symposium, 9 societies and association in Japan have approved. There were the financial aids by donation from 13 enterprises and the subsidies supported by 8 foundations.

The objective of this symposium was to deliberate on issues relating to molecular breeding technologies of forage and turf, including assessment of genetic diversity, discovery of novel genes involved in target traits, application of genetic mapping, establishment of molecular marker assisted selection, and other topics, such as comparative genomics, bioinformatics, transgenics, and risk assessment.

The symposium was started from two keynote speakers. Prof. J. Bouton summarized the current statues of molecular breeding of forages. He mentioned the future problems to be overcome by our efforts. Bio-energy is a major global concern. Renewable biomass energy

is increasingly being accepted as a possible alternative to fossil fuels and some forages are promising for energy crops. He emphasized that all biofuel industries will be local with their own cropping systems and that the initial feedstock traits to be improved are increased biomass yield, reduced input costs, and reduced chemical recalcitrance. Prof. K. Yamaguchi-Shinozaki highlighted that a cis-acting element DRE/CRT/LTRE plays an important role in regulating gene expression in response to environmental stresses such as cold, drought and high salinity. *DREB1/CBF* and *DREB2* have been isolated and overexpression analysis have been carried out. Regulon biotechnology is the control of signal transduction networks, a manipulation which in turn is expected to improve stress tolerance in plants. *DREBs* are quite useful for improvement of tolerance to environmental stresses in various kinds of plants such as forage and turf.

The symposium contained 10 plenary papers and 30 short oral presentations as well as 104 posters presentations. These presentations covered wide range of molecular breeding: comparative genomics using model legume crops, efficient and rapid characterization of genetic diversity using DNA markers, functional genomics and bioinformatics, mapping and marker assisted selection, transgenic, endophyte, turf grass molecular breeding including East Asian native species, *Zoysia*. Special lectures on biomass conversion were presented. Dr. S. Thomas highlighted energy crops, overall goals for energy crop breeders and descriptions of various biomass conversion processes. Prof. A. Kondo highlighted developed novel yeast strains for production of biofuels from biomass using cell surface display technology.

In the previous symposia, there is little presentation on bio-energy subject. However, in the present symposium, many participants felt a great interest in new research activity of biomass conversion. Cellulose biomass like forage grasses would be promising for bio-energy supply in the future. Therefore genetic improvement of energy crops could be one of the important factors for development of bio-energy system to establish sustainable society.

We have helped 10 foreign young scientists the travel expense as young scientist awards. Three young scientists were selected as winners of best poster awards.

It was decided that the next MBFT is held at Buenos Aires (Argentina) in 2010. The academic result of this international symposium will be published the proceedings of the molecular breeding of forage and turf by publisher of Springer in spring 2008.

7. Additional description

7.1 Number of participating countries: 19 countries.

Number of students participants: 13 persons

7.2 Approvals:

National Agricultural Research Center for Hokkaido Region, National Institute of Livestock and Grassland Science, Sustainability Governance Project, Hokkaido University, Japan Grassland Agriculture and Forage Seed Association Japan, Livestock Technology Association, Green Techno Bank, Japanese Society of Grassland Science, Japanese Society of Plant Breeding, Japanese Society of Turf Science



International Congress on Plant Mitochondrial Biology (ICPMB2007)

1. Representative

Hirokazu HANNA, the chair of organizing committee

2. Opening period and Place

June 25-29, 2007. Nara Women's University and Hotel Nikko Nara, Nara, Japan

3. Number of participants

154 persons (87 persons from foreign countries)

4. The total cost

Eight million Japanese yen

5. Main use of the subsidy

Mainly support for accommodation costs of invited speakers, and also partly costs for the congress venue and personnel expenses

6. Results and Impression

This congress is the only international scientific congress featuring plant mitochondria as a main target, and is held every 2 or 3 years under auspices of association of volunteer in the country nominated as host country for next meeting. Its purpose is exchange of the recent information and discussion of the current result for basic and applied researches on mitochondria in plant species.

Since the first meeting was held in Marseilles, France in 1978, there were already twelve meetings to be held at several places in the world. However the present congress was held in Japan, also in Asia for the first time.

In view of the importance of this scientific field, National Institute of Agrobiological Sciences, one of the biggest plant molecular biology research stations in Japan, have approved to become co-organizer of the present congress. On the other hand, there were the financial aids by donation from 10 enterprises and the subsidies supported by 6 foundations.

Mitochondria has been thought to be an energy-producing factory in the eukaryotic cells, but recent studies revealed mitochondria have more wide and important roles for the differentiation and the function of the cell not only for supplying an energy. Plant mitochondria have a lot of unique features compared to those of other organisms like animals

and fungi. The object of this congress further widened scientific information about plant mitochondria from all possible aspects, physiologically, genetically, biochemically, evolutionary, etc. Also the congress promoted the collaboration among many specialists of various fields for plant mitochondria for the future basic and applied research of plant mitochondria.

In this congress three plenary lectures were presented as follows: "My life with plant mitochondria from '70 to '07" by C.J. Leaver, "Chloroplast photorelocation movement: its photoperception and moving mechanisms" by M. Wada, and "The mode of mitochondrial DNA transmission in mice" by H. Shitara. Eight symposia and one pre-symposium were opened. They were as follows: I, Genomics & Genetics; II, Organellar Proteins; III, Stress & Environments; IV, Gene Expression; V, Organelle Crosstalk; VI, Dynamics & Biogenesis; VII, Evolution; VIII, Respiration; and Pre-Symposium, "From the dawn of plant mitochondrial research to the present". The congress invited 8 keynote speakers for each symposium, and also selected 24 peoples as an oral presentation. 94 poster presentations, which were classified to these eight themes, were displayed during the congress. In addition to oral presentations, the congress offered student participants the chance to present the contents of their posters as "Short Talks from Student Posters". In total there were 44 short talks by student participants. The congress selected three best posters from all presented posters and conferred the poster prizes by the supports of *Physiologia Plantarum*, the international journal of plant physiology, and the UK Biochemical Society.

In the previous three congresses (Sweden in 1998, Australia in 2002, and France in 2005), the entire genomic sequences of several plant mitochondrial genomes were reported. And also nuclear genome sequencing has been completed in the model plants, *Arabidopsis* and rice. Nowadays based on these genomic data for nuclear and mitochondrial genomes the post genomic studies are remarkably developing. This congress covered such post genomic studies to find novel functions of mitochondrial genes and mitochondria in plant cells.

In this congress, we had 51 student participants in total, which is corresponding to 1/3 of total participants. Especially 60% of student participants were from foreign countries. We think that this is very important for our scientific field, and we expect that they will contribute to the development of plant mitochondrial research and future collaborations between Japan and other countries.

It was decided that North American researchers would organize the next congress in 2009. We do not have a plan to publish the proceedings of this congress, but the *Mitochondrion*, an international journal for mitochondrial research by Elsevier, will publish the special issue for plant mitochondria at the end of 2007 at this opportunity (H. Handa, chair of ICPMB2007, is one of editors for this special issue).

7. Additional description

7.1 Number of participating countries: 14 countries and 1 area

7.2 Approval:

National Institute of Agrobiological Sciences is former governmental institute and now independent administrative agency. It is one of biggest research institute on the filed of basic and applied plant molecular biology.

The 5th International Symposium on Receptor Mechanisms, Signal
Transduction and Drug Effects
-Development of Novel Therapy to Specific Diseases in Organ-

1. Representative

Shizuo Yamada, the chairperson of organizing committee

2. Opening period and Place

May 10 (Thu) – 11 (Fri), 2007

GRANSHIP (Shizuoka Convention & Arts Center), Shizuoka, Japan

3. Number of participants

350 persons (30 persons from foreign countries)

4. The total cost

Fifteen million yen

5. Main use of the subsidy

Support for travel expenses of invited speakers and printed matters

6. Results and Impression

This symposium is held every 3 or 4 years around Japan. The first international receptor symposium (IRS) was opened in Niigata in 1995, and thereafter, held in Sapporo (1997), Tokyo (2000), Fukui (2003). The purposes is to explore recent achievements in detail and to integrate them by interdisciplinary discussion involving receptor mechanism, signal transduction, diseases, new analysis of drug action, and novel drug discovery and development.

For the present symposium, 5 academic societies and association in Japan have approved. There were the financial aids by donation from 89 enterprises and the subsidies supported by 6 foundations.

Receptors play pivotal roles not only in various physiological and pathophysiological functions, but also as promising drug targets. Currently, there is remarkable progress in the basic and clinical research in a number of receptors based on the recent progress of molecular biology and genomics. The aim of this symposium was to provide the opportunity for the integration and fruitful discussion of current accumulating results which were related to the receptor mechanism such as signal transduction, diseases, novel technology in evaluating the

receptor function and novel drug discovery.

A special lecture “Membrane transporters and drug response” was presented by Prof. Yuichi Sugiyama (University of Tokyo) and facilitated interdisciplinary discussions. Two luncheon seminar were presented as follow: ”Therapeutic receptor targets for lower urinary tract dysfunction” by Dr Naoki Yoshimura (University of Pittsburgh) and “At the frontline of Alzheimer’s disease treatment: γ -secretase inhibitor/modulator mechanism” by Dr Taisuke Tomita (University of Tokyo). The major contents in 5th IRS Symposia were six comprehensive symposia of the following titles: (1) Brain receptors-Basic to clinical research on function, disease and drug targets, (2) Lower urinary tract receptors-Basic to clinical research on function, disease and drug targets, (3) GPCR as a novel drug discovery target, (4) Cardiovascular receptors-Basic to clinical research on function, disease and drug targets, (5) Analysis of pharmacokinetics and pharmacodynamics, and novel technology in determining receptor function, and (6) Current topics. Twenty-six invited speakers lectured on these symposia, and also 63 posters were displayed.

In the previous four symposia, the subjects were inclined to basic researches on receptor mechanisms, signal transduction and drug effects. As additional themes, in the present symposium, we were focusing on receptors in major regulatory systems in the body. This symposium covered the central nervous system, cardiovascular system, urological system, GPSR as a novel drug discovery target and current other topics as shown in the above special lectures and symposium titles. Further, the sessions for the analysis of pharmacokinetics and pharmacodynamics and for the novel technology in determining receptor function lapped up the aspects relating drug discovery and development. We are convinced that this symposium could propose not only new direction and prospective for future receptor research, but promote mutual exchange between researchers in Japan and overseas and also that stimulating discussions in this meeting must lead to many new breakthroughs and promote mutual exchanges between researchers.

Have done travel expense help to not only 16 specialists (invited speakers) from 7 countries and 1 area, but also 5 young researchers and students from two University in Thailand, which are friendship schools of University of Shizuoka. Owing to many foundations and contributors including the Novartis Foundation, suppressing the registration fee for the young researcher to low amount (15,000 yen and 5,000 yen for student) became possible. In connection with this fact, 63 posters by young researchers and students were presented and about 120 graduate students attended this symposium. They possibly pursue the second revolution in the research for receptors.

Organizing committee will decide the time and place for the next symposium in a few months. The academic outcome of 5th IRS will be published as a special issue of Naunyn

Schmiedebergs Archives of Pharmacology in Germany (Chief Editor: Martin C. Michel) in 2007.

7. Additional description

7.1 Number of participating countries: 12 countries and 1 area

7.2 Approvals: For the present symposium, 5 academic societies and association in Japan have approved.

7.3 Photos



Hall panorama (Special Lecture)



Hall panorama



Hall panorama (Luncheon Seminar)



Invited speakers and organizing committee